Structural analysis and tectonic interpretation of the Thabazimbi Kumba Iron Mine region, using the Operational Land Imager (OLI), Landsat 8 satellite imagery

Thesis

by

NKHUPETSENG MOHLAHLANA (BSc Hons)

Supervisor

Prof W. Altermann

Co-supervisor

Prof A.J. Bumby & Prof T. Woldai

Submitted in partial fulfillment of the requirements of the degree

MAGISTER SCIENTIAE (GEOLOGY)

In the

In the Faculty of Natural and Agricultural Science

UNIVERSITEIT VAN PRETORIA
UNIVERSITY OF PRETORIA
YUNIBESITHI YA PRETORIA
Denkleiers • Leading Minds • Dikgopolo tša Dihlalefi

January 2019

DECLARATION

I, Nkhupetseng Mohlahlana, declare that this thesis which is hereby submitted for the award of Magister Scientiae (MSc), is my own work. It has not been previously submitted for the ward of a degree at this or any other tertiary institution. All the sources I have used or quoted have been indicated and acknowledged by means of complete references.

…………………………….   ……………………..

Signature   Date

N Mohlahlana [Mr]

2019

University of Pretoria,

South Africa

Abstract:

The tectonic framework of the Neoarchaean - Mesoproterozoic (2.58 to 1.87 Ga) supracrustal rocks exposed in the Thabazimbi region and Kumba Fe-Mine, Transvaal Supergroup, South Africa, has been studied using remote sensing (RS) techniques (based on Landsat 8 Operational Land Imager (OLI) and in the field. This highly deformed and structurally controlled mining region boarders the northern flank of the Rustenburg Layered Suite (RLS) of the Bushveld Igneous Province (Complex), which intruded into the Transvaal Supergroup rocks and thus, played a significant role in the deformation and mineralization processes. Detailed RS mapping and structural field investigations reveals three deformational phases (D_1, D_2, D_3) that demonstrate the tectonic history of the Thabazimbi region and its ore deposits.

A pre- to syn-Bushveld compressional deformation event (D_1) caused the development of thrusts, folds and reverse faults that have an overall NW–SE to N–vergence. This compressional event resulted in the ENE–WSW and/or E–W striking Bobbejaanwater Thrust Fault (BTF) and Belt-of-Hill Thrust Fault (BHTF), which may be connected to a basal sole thrust. Thrusting of the Thabazimbi region is evident by duplication and in parts, triplication of the stratigraphy, along parallel east-west trending mountain ranges (Northern, Southern and Middle ranges). The Middle Range developed only locally between the BTF and BHTF in the Thabazimbi Thrust and Fold Belt. The BTF and BHTF are located south of the ENE-trending Thabazimbi-Murchison Lineament (TML), which they parallel in the Thabazimbi region, and are regarded as parallel thrusts that formed as a result of sporadic reactivation of the TML. A post-Bushveld extensional event (D_2), which followed shortly after D_1, is characterized by ENE–WSW to E–W striking, steeply S dipping normal faults in the Thabazimbi Range and E–W trending lineaments in the Rosseauspoort Range. This extensional event likely occurred during cooling and sagging of the 2.05 Ga RLS and led to steepening of the Transvaal Supergroup strata, fold axes and thrusts in the Thabazimbi Ranges, which now dip with ca. 70 degrees south.

The D_3 extensional event, is defined by two major lineament trend directions, the NW–SE to NNW–SSE (D_{3a}) and cross-cutting NE–SW orientated lineaments (D_{3b}). These lineaments also crosscut the Rustenburg Granophyre Suite and the granitic rocks of the Bushveld Complex ($\leq$ 2.055 Ga), and the $\leq$1.87 Ga Waterberg Group (upper Waterberg unconformity-bounded sequence, WUBS-II). The age of D_3 is widely bracketed between post-Waterberg basin development and perhaps pre- to syn-Karoo basalts ($\geq$ 0.18 Ga) or even later events. It is however unlikely that it has occurred in the Phanerozoic, but rather is related to the occasional deformation of unknown age visible in the Waterberg Group itself and in older rocks across the central Transvaal basin. The enrichment of the Thabazimbi BIF iron- oxides (> 15% weight percent (wt%) FeO) to high-grade haematite Fe-ores (>60 weight percent (wt%) FeO) is likely to have occurred during D_1 to D_2 events.

DEDICATION

This work is dedicated to my family and most importantly to my wife Nozizwe Aletta Mohlahlana. Thank you ma-sweet-choco lumoi for your ever-constant love and support. You inspire me and I look forward to a future of discovery with you.

ACKNOWLEDGEMENTS

[…*To God be the Glory*…]

Table of Contents

List of Tables

Chapter 1

1. Introduction

1.1. Rationale

Banded iron formation high-grade (>60 weight percent (wt%) Fe) haematite iron ore deposits of South Africa are hosted exclusively in the Transvaal Supergroup (TSG) of the Kaapvaal craton, in the Griqualand West and the Transvaal sub-basins. The deposits of the Griqualand West basin are exploited at Sishen, Khumani, Beeshoek, Welgevonden and Kolomela Mine. The Transvaal basin deposit, which occurs in the Thabazimbi region, was mined at five of the Thabazimbi Kumba Fe-Mine pits, namely: the Kwaggashoek East, the Donkerpoort West, the Donkerpoort Nek, the Buffelshoek West and the Bobejaanswater. The banded iron formation (BIF)-hosted high-grade haematite iron ore deposits are among the largest metallic deposits on earth, not only in volume but also in value. Globally, in 2016 their reserves were estimated to exceed 3.1 billion tonnes world-wide and supply ninety percent of Fe to the total iron ore mined in the world (Dalstra, et al., 2003; Smith and Beukes, 2016). In addition to South African deposits, their production largely occurs in Brazil, Australia, and India. The deposits in United States, Canada, and Ukraine are nearly mined out (Dalstra and Guedes, 2004).

Given their world economic importance, BIF-hosted high-grade haematite iron ore deposits have been extensively studied. They occur in sedimentary environments, often with hydrothermal and magmatic overprint in Archaean and Proterozoic Banded Iron Formations (BIFs). The BIFs are chemical sedimentary rocks which are laminated and/or banded and contain anomalous amounts of Fe as iron-rich oxides (> 15%), carbonates and silicates.

The primary Fe content in the BIFs is not of economic significance due to relatively high Si contents. BIFs hosting economic Fe deposits are enriched through processes that increase Fe content mainly by the removal or leaching of silica from the iron formation host rock. The mode of enrichment is, however, a matter of contention, with some scholars favouring the supergene process and hydrothermal model, while others adjudicate a supergene modified hydrothermal origin, under oxidizing conditions (Smith and Beukes, 2016). Despite this cognizance, many aspects of BIF origin remain controversial and are subject of universal debate to this day. With reference to the origin of the BIF-hosted high-grade haematite iron ore deposits of South Africa the metallogenesis and tectonic framework of the Griqualand West basin deposit is well investigated. The origin of this deposit is envisaged to be of supergene origin and related to a 2.2 to 2.0 Ga pre-Gamagara-Mapedi erosional unconformity in the TSG (Van Schalkwyk and Beukes, 1986). The ores are derived from the leaching of chert from the BIF during supergene alteration (Smith and Beukes, 2016). Though the Griqualand West basin high-grade haematite BIF-hosted Fe-ore deposits are well documented, the genesis and tectonic framework of the counterpart deposit, Thabazimbi region of the Transvaal basin, is still a matter of geo-scientific investigation.

It is of a concern that after a long history of Fe-mining in the Thabazimbi region, this deposit is poorly documented. To this day, few studies have addressed the tectonic framework of this deposit and its temporal and spatial relationship to metallogenesis (Fe-ore formation). Apart from the structural studies done by Du Preez (1944), Strauss (1964), Du Plessis and Clendenin (1988), Netshioswi, (2002), and the recent work of Basson and Koegelenberg (2017), very little has ever been published on the regional tectonic framework of the Thabazimbi deposit. Nonetheless, several authors (Wagner, 1921; De Villiers, 1944; Du Preez, 1944; Boardman, 1948; Strauss, 1964; Van Deventer, 1986; Du Plessis and Clendenin, 1988; and Netshiozwi, 2002) have attempted to address the origin of the Thabazimbi Fe-mineralisation, and the ores are thought to be hydrothermal in origin.

Currently, the Fe-mining in the Thabazimbi region has ceased. This is due to 1.) the assumption that the high-grade haematite BIF-hosted iron ore deposit of this region is largely depleted, 2.) the cost of mining this deposit is colossal due to technical challenges encountered during operation, and 3.) the gigantic open pit slope-failure which occurred in 2016. This research study is however of the view that the Thabazimbi region has a high potential for Fe-mining and should thus, not be given up on. Based on Netshiozwi (2002), tectonic structures and/or host rocks have controlled the Fe mineralisation of this region. However, the lack of up-to-date tectonic and geological maps and well-documented mineral potential maps of this region hinders most of the mining investments and development activities of the area. Understanding of the tectonic framework of the Thabazimbi high-grade haematite BIF-hosted iron ore deposit is essential for mining-related targets and preservation of this mineral resource. For example, in the case of unconformity-bounded supergene ores, the stratigraphic setting and lateral continuity of the unconformity may be most important (Netshiozwi, 2002), whereas in hydrothermal deposits, understanding local and regional structural controls on the migration of ore-forming fluids is more important for successful exploration.

The understanding of the structural setting of the Fe ores in this mining area has always been incomplete and thus hindering prospecting activities. It has therefore been aimed to improve this understanding by a combination of detailed geological field data collection and a remote sensing approach to this structurally complicated area. Most of the tectonic features of this area are not fully exposed on the land-surface and/or documented on the published 1:250000 scale geological map of the Thabazimbi region, formerly the Geological Survey of South Africa, now Council for Geoscience (Series 2426 Thabazimbi, 1974). To better document the tectonic framework of the Thabazimbi region, it was thus decided to undertake a detailed structural geology study of the Thabazimbi region and Kumba Fe-Mine using remote sensing (RS) techniques.

Remote sensing (RS) technology is a powerful tool, which has been used in the disciplines of field geological mapping and mineral exploration, which have advanced tremendously through the application of this technique. In geological mapping, remote sensing (RS) technology has been used largely for discriminating the different lithologic units, trace the major structures and to detect alteration zones (Karnieli et al., 1996; Abdulla et al., 2013). Similarly, in mineral exploration, RS technology is mostly used to delineate areas with potentially economic mineral deposits (geology, major structures and alteration zones). Authors such as Sabins (1999), Masoud and Koike (2006), Abdullah et al. (2013), and Gannoumi and Gabtni (2015), have shown that the integration of remotely sensed datasets and geoscience datasets, together with image analysis software (i.e. Geographic Information Systems (GIS) and ENVI) can help delineate surface tectonic structures that are covered by soil and vegetation, for structurally controlled mineralization like that of the Thabazimbi region.

The advantage given by the RS technique is that it provides the opportunity for the desk-top study of the surface structural features of regions from elevated, aerial viewpoint. This method can benefit exploration programs and geological investigations of mineralised zones such as the Thabazimbi Kumba Fe-Mine, by providing improved and detailed knowledge of e.g. the lineament and alteration framework of such deposit. The structural geology of the Thabazimbi region has been studied by Du Preez (1944), Strauss (1964), Du Plessis and Clendenin (1988) and Basson and Koegelenberg (2017) in selected, areas of the Kumba Fe-mine and through conventional methods (geological mapping, drilling, gravity and magnetic methods). With the innovative technology driven world we live in today, most exploration programs are moving away from conventional methods to more flexible, dynamic, 3-D modelling using advanced technology software that integrates large numbers of datasets (Basson and Kogelenberg, 2017).

This research, therefore, employs the RS techniques to study the structural geology of Thabazimbi region and derive a tectonic framework model of the Thabazimbi stratigraphic units, which sit along the Thabazimbi-Murchison Lineament (TML) and the margins of the western limb of the Bushveld Large Igneous Province (BLIP).

1.2. Research aims and objectives

The main objectives of this research are to unravel:

1. The tectonic history of the Neoarchaean - Mesoproterozoic (2.58 to 1.87, Ga) supracrustal rocks exposed in the Thabazimbi region and Kumba Fe-Mine;
2. To investigate the structural relationship (temporal and spatial) to metallogenesis (Fe-ore formation) in the region.

By utilizing remotely sensed datasets, in particular, Landsat 8 OLI - Operational Land Imager, this investigation shall lead to the development of an overall model for the tectonic framework of the Thabazimbi Kumba Fe-Mine and the broader region. The research has, therefore, undertaken studies such as:

1) Analysis and interpretation of the structural geology of the Thabazimbi region and mining area using Remote Sensing (RS) data and software packages such as GIS, ENVI and Global Mapper, aided by Google Earth Imagery where necessary.
2) Integration of RS datasets and auxiliary geoscientific datasets (1:250000 scale geological map of Thabazimbi region, Series 2426 Thabazimbi, 1974) in order to combine these data to one tectonic map of the Thabazimbi region.
3) Include own field geological structure investigations and analysis.

4) Interpret the above combination of the RS data and interpretation results with the published previous investigation results and discuss the possible dependence of mineralization from tectonic structures interpreted and observed.

Geological datasets collected in and around the Thabazimbi region by previous investigators such as Strauss, (1964), Du Plessis and Clendenin, (1988), Netshiozwi, (2002), Mahlayeye M., honours project, (2013) and Basson and Koegelenberg, (2017), were consulted during the course of this investigation.

1.3. Location and physiology of the study area

The Thabazimbi mine area is situated in the south-western part of the Limpopo Province of the Republic of South Africa. It lies approximately 200 km north-northwest of Pretoria and 129 km north of Rustenburg, in the North West Province. The topography of the area is characterized by alluvial plains, rugged and steep mountain ranges that strike E-W and N-S (**Figure 1.1**).

Figure 1.1: Satellite image showing the Thabazimbi region landscape. The topography is mostly defined by Rosseauspoort and the Thabazimbi (Northern, Southern and Middle) Ranges. The Crocodile River is the main drainage system of the region (Image sourced from Google, 2016).

The E-W striking mountain range is known as the Thabazimbi Range, while the N-S striking mountain is locally known as the Rosseauspoort Range. The Thabazimbi Range is further subdivided into three mountain ridges, locally referred to as Southern, Northern, and a minor range located between the Northern and Southern range, known as the Middle range. The region is covered by a widespread grassland biome that defines the bush savannah vegetation of the area (Reynolds, 2004). Thabazimbi area is classified as arid, dry sub-tropical mountains (Reynolds, 2004). The night and day temperatures are recorded at an average of 15˚C to 30˚C in summer, 10˚C to 26˚C in autumn and 10˚C to 18˚C in winter (South African Info, 2013). Summer seasons are generally hot and wet, while winter is cold and dry with occasional early morning frosts. The average annual rainfall is recorded at 625 mm of which 500 mm fall in summer (Reynolds, 2004). Rain is most common in November, December, and January, but generally, the area can experience some rain throughout the year. Rare floods caused by heavy rains occur in the area. The main drainage channel is the Crocodile River, which flows towards the Northwest of the Thabazimbi region (South African Info, 2013).

Chapter 2

2. **Geological and structural setting of the deposits**

2.1. **General geology of the Thabazimbi region**

The stratigraphic framework of the Thabazimbi region, as indicated by **Figure 2.1**, consists of the Neoarchaean – Mesoproterozoic supracrustal rocks that encompass the 2.58 to 2.06 Ga Transvaal Supergroup (TSG) of the Transvaal basin (Eriksson et al., 1995; Altermann, 1996; Altermann and Nelson 1998), the 2.061 Ga Bushveld Igneous Province (Walraven et al., 1990; Zeh et al., 2016), and the 2.054 to 1.87 Ga Waterberg Group (Du Plessis and Clendenin, 1988; Netshiozwi, 2002, Dorland et al., 2006).
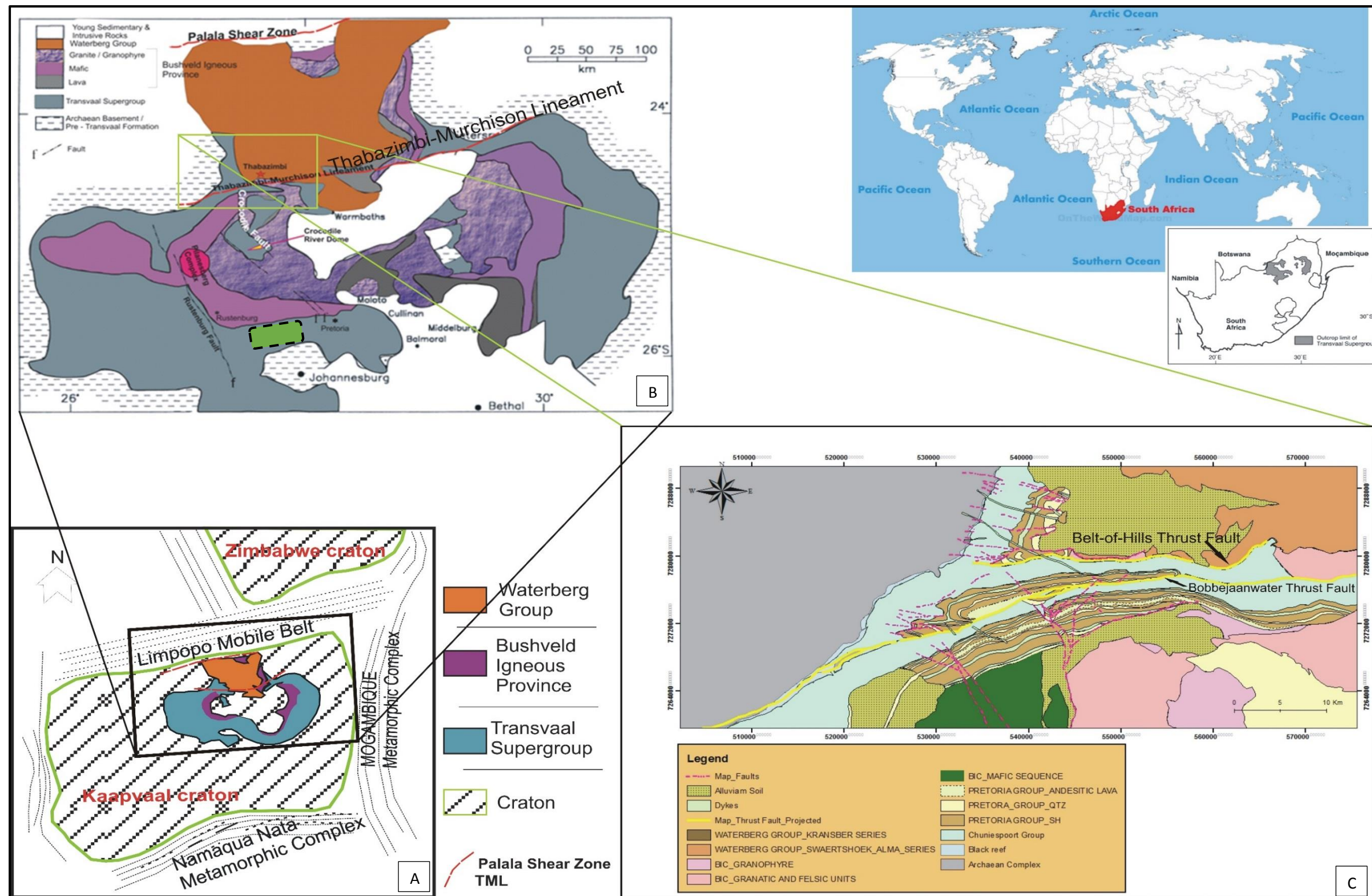
Figure 2.1: (A) Composite diagram, illustrating the relationship between the Transvaal Supergroup, Bushveld Igneous Province and Waterberg Group with the Kaapvaal craton and the Limpopo Mobile Belt. Modified after Eriksson et al. (1995). (B) Simplified geological map showing the outlined stratigraphic sequence of the Thabazimbi region, which encompasses Transvaal Supergroup, Bushveld Igneous Province, and Waterberg Group. The Thabazimbi-Murchison Lineament (TML), the Palala Shear Zone (PSZ), Rustenburg Fault, Crocodile River Dome are shown. The green dashed rounded rectangle in B shows the study area of Alexandre et al. (2006). Modified after Cawthorn and Webb, (2001). (C) Digitized geological map showing the lithological units of the Kumba Fe-Mine and the structural elements in the study area. The Belt-of-Hills Thrust Fault, Bobbejaanwater Thrust Fault and mapped Faults are shown. This map is digitized from the 1: 250000 scale geological map of the Thabazimbi region (Series 2426 Thabazimbi, 1974).

The stratigraphic sequence of the Transvaal Supergroup preserved in the region of Thabazimbi consists of the 2642.2 ± 2.3 Ma (U-Pb zircon ages; Walraven and Martini, 1995) Black Reef Formation, the 2587 ± 49 Ma Chuniespoort Group, and the 2.35 to 2.06 Ga Pretoria Group (Walraven and Martini, 1995; Eriksson and Reczko, 1995; Zeh et al., 2016). The Pretoria Group is deformed by the igneous rocks of the Bushveld Igneous Province, with an age estimated at 2.061 Ga (Dorland et al., 2006). The 2.054 – 1.87 Ga (U – Pb dating on zircons from the porphyritic lava of the Rust de Winter and Lower Swaershoek Formation, Waterberg unconformity-bounded sequence (WUBS I): Dorland et al., 2006) Waterberg Group sedimentary rocks rest unconformably on the Transvaal strata, the Bushveld igneous rocks and 3.0 to 2.8 Ga Archaean gneisses and granites of the Kaapvaal craton (Zeh et al., 2016). The deposition of the Waterberg Group marks a pivotal period of the Earth evolution, upon which free atmospheric oxygen became available to produce widespread terrestrial red beds for the first time in Earth history (Bumby, 2000; Barker et al., 2006; Corcoran et al., 2013). This thesis will, however, not discuss the inferred depositional conditions of the strata of the Thabazimbi region, but will, outline their general geologic setting in order to elucidate the structural framework of the Thabazimbi region.

2.1.1. The Transvaal Supergroup (TSG)

2.1.1.1. Black Reef Formation

The ≥2588 ± 6 Ma (SHRIMP on zircons: Altermann, 1996; Altermann and Nelson 1998) Black Reef Formation rests unconformably on the Protobasinal rocks of the Transvaal basin and the Archaean rocks of the Kaapvaal craton (Eriksson and Reczko, 1995). The formation is preserved around the margins of the Transvaal basin and is well-exposed in the Crocodile River, Dennilton, and Marble Hall fragments, where isolated occurrences of Transvaal lithologies are enveloped by Bushveld igneous rocks (Eriksson et al., 1995).

The Black Reef Formation consists of mature quartz arenites with lesser conglomerates and subordinate mudrocks. The formation is characterised by a thin veneer of arenaceous rocks that comprise poorly sorted lenticular clast- and matrix-supported conglomerates, trough and planar cross-bedded sandstones and carbonaceous mudrocks unconformably overlying older successions. The sandstones vary in thickness between ±30 m and ±60 m across the formation, with anomalous thicknesses (up to 210 m) observed in some parts of the Marble Hall, Dennilton and Crocodile River outcrops (Eriksson and Reczko, 1995; Eriksson et al., 1998).

2.1.1.2. The Chuniespoort Group

Conformably resting on the Black Reef Formation are the 2587 ± 49 Ma chemical facies of the Chuniespoort Group (Walraven and Martini, 1995; Martin et al., 1998; Altermann and Nelson 1998). The group consists of carbonate rocks of the Malmani Subgroup, the 2480 ± 6 Ma Banded Iron Formation (BIFs) of the Penge Formation (Walraven and Martini, 1995) and the siliciclastic rocks of the Duitschland Formation (Eriksson et al., 2001; Bumby et al., 2012; Möller et al., 2014). The Malmani Subgroup is characterized by stromatolitic carbonates with high chert content in places. Based on chert content and stromatolite morphology the Malmani Subgroup is divided into five formations namely, the Oaktree Formation, the Monte Christo Formation, the Lyttelton Formation, Eccles Formation, and the Frisco Formation (Eriksson and Altermann, 1998). The carbonate facies of the Malmani Subgroup are considered to signify part of a much larger carbonate platform preserved in the Transvaal structural basin of the Kaapvaal craton. Overlying the Malmani Subgroup is the Penge iron formation with a conformable gradational contact, which is locally faulted (Eriksson et al., 2001; Frauenstein et al., 2009). The BIF of the Penge Formation comprises of rhythmically banded iron oxide (hematite, magnetite, goethite), iron-silicates like stilpnomelane, minnesotaite and siderite, all in a chert matrix, and with shale layers in variable proportions (Möller et al., 2014).

Unconformably overlying the Penge Formation is the Duitschland Formation, with a bounding angular unconformity (Eriksson et al., 2001). The Duitschland Formation is regionally restricted and consists of an unconformity bound wedge of thick sequence of siliciclastic rocks (mudrocks with ferruginous argillites and thin quartzite inter-beds) sandwiched below the Pretoria Group and older rocks. The Pretoria Group and older rocks are metamorphosed to greenschist facies and in parts by the Bushveld intrusion and the ca. 1.1 Ga volcanic event of the Pilanesberg alkaline complex (Eriksson et al., 1993).

2.1.1.3. The Pretoria Group

Prior to the onset of deposition of the Pretoria Group, there is an 130 myr gap of localized erosion between the chemical deposition of the Chuniespoort and Pretoria Groups, which is marked by a regional angular unconformity and the development of a palaeokarst surface (Eriksson et al., 1991; 1995). Palaeokarst features are well developed in the upper Malmani carbonates, where the Penge Formation is locally nearly or completely eroded before the deposition of the Pretoria Group (Martini et al., 1995). The 2.35 Ga Rooihoogte Formation defines the basal unit and the onset deposition of the siliciclastic and volcanic strata of the Pretoria Group (Möller et al., 2014). The Pretoria Group is broadly characterised by an alternation of shale, sandstone, subordinate conglomerates, diamictites and carbonate beds, with two interbedded volcanic horizons within the successions of the group which make up a significant portion of the stratigraphy (Schreiber et al., 1990; Eriksson et al., 1993; Catuneanu and Eriksson, 1999).

The Pretoria Group consists of fourteen formations namely, the lowermost Rooihoogte Formation, succeeded by Timeball Hill, Boshoek, Hekpoort, Dwaalheuwel, Strubenkop, Daspoort, Silverton, Magaliesberg, Rayton, Vermont, Lakenvlei, Steenkampsberg, and uppermost Houtenbek Formation (Eriksson et al., 1991).

In the Thabazimbi region, the Rooihoogte Formation cuts erosionally across the Penge Banded Iron Formation, down into the dolomites, producing a pronounced unconformity marked by the chert pebble to cobble basal conglomerate of the Bevet Member of the Rooihoogte Formation.

2.1.2. The Bushveld Igneous Province

The 2.061 Ga Bushveld Igneous Province represents the tectono-magmatic events within the structural setting of the TSG and the Kaapvaal craton (Kinnaird, 2006). The Bushveld Igneous Province abruptly terminated deposition and basin fill of the TSG. As a result of the intrusion, the Transvaal strata proximal to the Bushveld complex have undergone contact metamorphism, mostly producing hornfelses, garnet-bearing assemblages and quartzites from clastic protoliths and asbestos deposits from BIFs (Eriksson et al., 2001). Overall, the province comprises five limbs namely, the Eastern, Western, Northern/Potgietersrus, South-eastern and Far Western compartments. The magmatic activity of the province was relatively short-lived (~1-3 myr), beginning with the extrusion of the Rooiberg Group 2061.8 ± 5.5 Ma (Cawthorn and Walrav1998; Cawthorn and Webb, 2013; Zeh et al., 2015). This was followed by the intrusion of the mafic and/or ultramafic Rustenburg Layered Suite (RLS) at 2058 ± 0.8 Ma (U-Pb zircon; Scoates and Friedman 2008), the Lebowa Granite Suite at 2054 ± 3 Ma (Gleason et al., 2011) and lastly, the Rashoop Granophyre Suite at 2053 ± 12 Ma (U-Pb zircon; Walraven 1997).

2.1.3. The Waterberg Group

The fault-bounded Waterberg basin rests unconformably on rocks of the TSG, the granites and mafic rocks of the Bushveld Igneous Province, and the Archaean gneisses and granites of the Kaapvaal craton (Barker et al., 2006).

The basin rocks are truncated by two major cratonic faults striking approximately ENE–WSW and subparallel to each other, namely: the Palala Shear Zone (PSZ) in the north and the Thabazimbi-Murchison Lineament (TML) in the south, (**Figure 2.1)** (Eriksson et al., 1997). The basin is made up of three subgroups, Nylstroom, Matlabas and Kransberg Subgroup, which are collectively subdivided into seven unconformity-bounded formations. These are the Swaershoek and Alma formations of the Nylstroom Subgroup, the Skilpadkop-Setlaole and Aasvoëlkop-Makgabeng formations of Matlabas Subgroup and Sandriviersberg-Mogalakwena, the Cleremont and Vaalwater formations of the Kransberg Subgroup (Van der Neut et al., 1991; Bumby, 2000; Barker et al., 2006). The fault-bounded Waterberg basin is characterized by siliciclastic red beds and minor volcanic rocks (Möller et al., 2014). The red colour of the siliciclastic rocks is interpreted as an artifact of hematite grain coatings, which appear to be early diagenetic in origin, and therefore suggests an oxidizing environment during the deposition of the Waterberg Group (Bumby, 2000).

2.2. The tectonic setting of the Thabazimbi Region

Different tectonic events have been recognized within the supracrustal rocks of the Thabazimbi region. These include the tectonic events related to the TML, the tectonic events of the TSG (post-Pretoria Group deposition and/or pre-Bushveld Igneous Province (≥ 2.06, Ga)), the tectonic event concomitant to the Bushveld Igneous Province (~2.06, Ga), and the tectonic events related to the Waterberg basin (2.054 – 1.87 Ga). Notably, the 2.06 Ga Rooiberg Group and 1.1 to 1.3 Ga Pilanesberg Complex are in the periphery of the Thabazimbi region and are also thought to have reactivated some of the tectonic structures adjacent to the Thabazimbi region and Kumba Fe-Mine. The tectonic events relating to the Rooiberg Group and Pilanesberg Complex will, however, not be examined here, but if necessary, some aspects of it may be mentioned in order to give an explanation to the structural framework of the region and mine.

Of tectonic interest to this research study is the Thabazimbi-Murchison Lineament (TML). The TML is an ENE–WSW trending major tectonic fault of the Kaapvaal craton, with a recorded tectonic history of more than 2500 million years (Good and De Wit, 1997). This lineament has been reactivated several times in its long-lived tectonic history and shows normal, strike-slip and reverse movement (Du Plessis, 1990). Furthermore, the lineament is noted to exhibit structural variations in style over time, from a ductile-dominated regime to a brittle-dominated regime that indicates varying stress fields, possibly as a result of variable P–T conditions and strain partitioning along the zone (Du Plessis and Walraven, 1990, Good and De Wit, 1997). The lineament has influenced the tectonic setting of the northern margin of the Transvaal basin, the Bushveld Igneous Province and the southern margin of the Waterberg basin (Good and De Wit, 1997). In its trajectory, the TML traverse through the Thabazimbi region and the iron mine. Du Plessis and Walraven (1990) and Good and De Wit (1997) documented pre- and post-Bushveld intrusion strike-slip (wrench) faulting showing sinistral and dextral tectonics, strike-slip duplexes and flower structures in the Thabazimbi region, which they tie to the reactivation of the TML. These deformational structures are also described by Good and De Wit (1997) as relay thrust structure features of the TML. The stratigraphic units of the Thabazimbi region and Kumba Fe-Mine are folded, faulted, thrusted and duplicated parallel the ENE–WSW trending TML fault line (Netshiozwi, 2002; Basson and Koegelenberg, 2017). The structural geology of the region and mine is, therefore, defined by duplication of the stratigraphy along this strike line.

Beside the TML, structural deformations discussed by Du Plessis and Walraven (1990), Hartzer (1995), Bumby et al. (1998) and Alexandre et al. (2006) are considered important for the holistic interpretations of the tectonic framework of the Thabazimbi region. Du Plessis and Walraven (1990) studied the tectonic setting of the Bushveld Igneous Province in Southern Africa, with special attention to the structural deformation and distribution of the Bushveld Igneous Complex.

Du Plessis and Walraven (1990) documented open folds with approximately NW trending axes in the Western compartment of the Bushveld Igneous Province. The folding is interpreted to have resulted from NE–SW compressive forces during the interval from the emplacement of the magnetite gabbro until after intrusion of the Nebo Granite. Furthermore, these authors suggest that the Bushveld Igneous Province or event has reactivated the TML and this has resulted in strike-slip movement (indicated by sinistral as well as dextral movements) in the Thabazimbi-Warmbaths (Bela-Bela) regions, producing strike-slip duplexes, flower structures, and pull-apart basins. Hartzer (1995) studied the tectonic development of the Transvaal Supergroup inliers and their relationship with the Bushveld Igneous Province. Of a tectonic interest to the here presented study is the Crocodile River Dome, situated ~35 km south of the Thabazimbi Kumba Fe-Mine (**Figure 2.1B**). According to Hartzer (1995), the Crocodile River dome formed as a result of interference folding, by means of initial NW–SE trending F_1 fold that was refolded along an F_2 axis with an ENE–WSW strike. The petrographic study by Hartzer (1995) indicates that deformation preceded the metamorphism caused by the intrusion of the Bushveld complex. The model proposed by Hartzer (1995) makes provision for pre-Bushveld regional deformation due to lithospheric stresses that prevailed since the Archaean and proceeded in pulses thereafter.

On the other hand, Bumby et al. (1998) studied the compressive deformation in the floor rocks to the Bushveld Complex, with a specific focus on the Rustenburg Fault Zone (RFZ). The Rustenburg Fault Zone is in the south western side of the Thabazimbi Kumba Fe-Mine, in proximity (~50 km) to the field study (**Figure 2.1B**). The fault was classified by Bumby et al. (1998) as a dextral strike-slip fault, with the σ_1 for the strike-slip movement at a 30˚ direction from the trend (330˚) of the fault. This orientates the shortening direction of the RFZ in the N-S direction. Bumby et al. (1998) revealed that in post-Pretoria Group or pre-Bushveld time (at 2050 Ma), the area surrounding the RFZ was subjected to two compressive deformational events (D_1 and D_2).

D_1, with a shortening direction in the NE–SW, which produced SE–NW trending F_1 fold and a D_2, with a shortening direction directed at NNW–SSE, which produced the strike-slip movement along the Rustenburg Fault and the ENE–WSW trending F_2 fold. According to Bumby et al. (1998), the F_2 fold is cut by the Rustenburg Fault, suggesting that F_2 fold formed as an early response to a NNW–SSE directed compressional stress that culminated in strike-slip displacement of the Rustenburg Fault. They argued that the NNW–SSE shortening direction corresponds with NNW–SSE principal trend which developed during early deformation of the Kaapvaal craton that resulted in two principal trend directions, ENE–WSW and NNW–SSE. Alexandre et al. (2006) studied low-grade regional metamorphism synchronous with brittle-ductile deformation that formed small-to medium-scale folds, cleavages, monoclines and thrusts in the dolomite, slates, and phyllite of the Palaeoproterozoic Transvaal Supergroup (i.e. the Black Reef Formation, Chuniespoort and Pretoria Groups), see **Figure 2.1B**. $^{40}Ar/^{39}Ar$ dating of synkinematic white mica from the phyllite gave well-defined ages of 2.15 Ga and ⁓2.042 Ga for the tectonic deformation observed in the Transvaal Supergroup. The 2.15 Ga age closely follows the end of sedimentation of the Pretoria Group. According to Alexandre et al. (2006), this age might be considered inherited from an earlier, pre-Bushveld dynamo-thermal event. The ⁓2042.1 ± 2.9 Ma age represents and/or corresponds to a dynamo-thermal episode of mica growth under tectonic conditions favourable for the development of regionally extensive cleavage and the age closely follows the Bushveld emplacement (2.05 Ga).

2.3. The general geology of the Thabazimbi Kumba Fe-Mine

The stratigraphic units defining the geology of the Thabazimbi Kumba Fe-Mine encompass rocks of the upper sequence of the Chuniespoort Group, the Eccles and Frisco formations of the Malmani Subgroup, which form the basal strata of the Fe-mine.

These formations consist of chert-poor dolomites with localized carbonaceous shale bands (Strauss, 1964), and are in faulted contact with the overlying BIFs of the Penge Formation (Du Plessis and Clendenin, 1988). The Penge BIFs form the major component of the stratigraphic column of the Thabazimbi mine. The basal unit of the Penge BIFs is defined by chert-rich shale, which is frequently brecciated due to the solution (karstic collapse) of the underlying dolomites. The Fe-orebodies occur in this basal unit of the BIFs and are up to ±80 m thick, but also as fill of the karst in the dolomites. The ore itself is defined as having over 60 wt% of iron oxide and less than 15 wt% silica (Netshiozwi, 2002). The Penge Formation is unconformably overlain by the siliciclastic sedimentary rocks and volcanic rocks of the Pretoria Group, which are best observed in the Buffelshoek and Wachteenbietjies Draai farms (Van Deventer et al., 1986).

2.4. The structural geology of the Thabazimbi Kumba Fe-Mine

2.4.1. Previous work on the structural geology of the Thabazimbi mine area

The most detailed published works directly concerning the structural geology of the herein study area were done by Du Preez (1944), Strauss (1964), Du Plessis and Clendenin (1988) and Basson and Koegelenberg (2017), who studied the structural architecture of the Thabazimbi region.

2.4.1.1. Summary of the work of Du Preez (1944)

The study by Du Preez (1944) was the first to provide structural geology of the Thabazimbi region and associated mineralization map. After in-depth lithological and physiographic study of the Thabazimbi region, he reported folds, overturned folding, and thrust faulting in this region, between the Northern and Southern ranges of the Thabazimbi Range.

According to Du Preez (1944), an anticline develops in the Malmani dolomite and disappears beneath the Penge BIF, while the syncline occurs in the Penge BIF. Several thrusts faults, namely, the Gatkop Thrust, now named the Belt-of-Hills Thrust Fault (BHTF), the Southern Thrust, now named the Bobbejaanwater Thrust Fault (BWTF) and the Intermediate thrusts (**Figure 2.1)** were documented. The BWTF was further subdivided by Du Preez (1944) into the Daspoort, the Sandrivierspoort, and the Weltevreden thrusts. The BHTF exceeds all the other thrusts in regional extent and in the amount of horizontal stratigraphic displacement. The timing of this thrust postdates the Waterberg deposition, as the Transvaal strata are thrusted over the lower Waterberg Group strata deposited between 1.97 and 2.01 Ga. Du Preez (1944) however, could not conclusively determine the relative ages of the major and minor thrusts of this region and assumed that they are all initiated during the same time, with the BHTF commencing first and the minor thrusts instigated after the end of movement of the BHTF-plane. Furthermore, Du Preez (1944) suggested that at the time when deformation occurred, the Transvaal strata had not been tilted with a southerly inclination as observed now and proposed that the southerly inclination is probably due to overloading and consequent sagging caused by the Bushveld intrusion.

2.4.1.2. **Summary of the work of Strauss (1964)**

Strauss (1964) described the Thabazimbi region as a fault dominated area, exhibiting all three senses of faulting (i.e. normal, strike-slip and reverse). He recognized that the outcropping rocks of the Rousseauspoort and Thabazimbi Ranges are intensely faulted, and the major components are low-angle strike-slip faults and thrust faulting. According to Strauss (1964), the thrust faults have duplicated and/or triplicated the rocks of the Malmani dolomite and Pretoria Group in the area and have caused the BIF to now stand out as prominent parallel east-west trending mountain ranges (Northern, Southern and Middle ranges).

2.4.1.3. Summary of the work of Du Plessis and Clendenin (1988)

Du Plessis and Clendenin (1988) mapped the Bobbejaanwater Thrust Fault system (BWTF) and provided a structural analysis of the fault. They recognized that the BWTF exhibits complex fault patterns. It splays into three sub-parallel faults. They also described the complex fault patterns of the NE–SW to NW–SE trending faults south of Thabazimbi, as a flower structure related to left-lateral wrench fault movement along BWTF. According to Du Plessis and Clendenin (1988), the existence of the tectonic flower structures in Thabazimbi region is a reflection of convergence and the configuration of the underlying basement blocks and the probability of reactivation of the pre-existing zones of weakness in the basement during periods of tectonic activity. Du Plessis and Clendenin (1988), agreed with Du Preez (1944) that the timing for the Thabazimbi thrusting could be ± 2.0 Ga, as thrusting occurred after the ~2.01 Ga deposition of the 2nd Waterberg Group Unconformity-Bounded Sequence (WUBS II) (Cheney and Twist, 1986).

2.4.1.4. Summary of the work of Basson and Koegelenberg (2017)

The study by Basson and Koegelenberg (2017) is the most recent published work providing a structural analysis of the Thabazimbi mine. These authors investigated the structural controls on the Fe - mineralization at five of the Thabazimbi Mine pits. These are Kwaggashoek East pit, the Donkerpoort Nek pit, the Kumba-Donkerpoort West pit, the Buffelshoek West pit, and the East Mine pit (**Figure 2.1**). Thrust, reverse and normal faults in the five mine pits of the Thabazimbi iron ore mine were documented, which have an overall vergence to the north. The tectonic structures observed in the Thabazimbi Fe-Mine pits were interpreted as produced through a compressional deformation event, which resulted in folding accompanied by interconnected structural features such as bedding-parallel and low- to high-angle stepping thrusts or reverse faults that are spatially controlled by progressive stages of folding.

Basson and Koegelenberg (2017), suggested that the principal shortening direction (σ_1) liable for structural deformations observed in the Thabazimbi Fe-Mine pits is N–S to NNE–SSW. Furthermore, they advocate for the compressional deformational phase that is tectonically associated with the TML, over a protracted period of 2.04 – 2.0 Ga. This is because in their view, the folding and thrusting must have occurred after the emplacement of several ca. 2046 ± 3.4 Ma Bushveld Complex sills (U–Pb ages after Rajesh et al., 2013) and before the ca. >1927 Ma deposition of lower Waterberg Group conglomerates.

2.5.   Economic geology of the Thabazimbi Region and Kumba Fe-Mine

The high-grade iron ore deposit of the Thabazimbi region is hosted by the Penge Iron Formation of the Chuniespoort Group, Transvaal Supergroup. The Fe-ores mainly crop out in the Northern and Southern ranges, and to a lesser extent emerging in the so-called Middle range (Van Deventer, 1985). In the Northern range, orebodies are well developed, and they are extracted at the Donkerpoort-West, Donkerpoort, van der Bijl, East and Kwaggashoek East pits (**Figure 2.1)**. In the Southern range, two orebodies crop out, the Buffelshoek East and the Buffelshoek West deposits (**Figure 2.1)**. In the Middle range, only, the Bobbejaanwater orebody occurs. The Thabazimbi BIF-hosted high-grade iron ores occur as strata-bound bodies of variable size and are subdivided into three different types of orebodies according to their lithostratigraphic setting. These are the basal, the upper and the lenticular orebodies (Strauss, 1964). The basal Fe-ores constitute the main type of deposit at Thabazimbi Fe-Mine. These orebodies are situated in the lowermost parts of the Penge Formation along the contact with the underlying shale covering the dolomites (Du Preez, 1944; Strauss, 1964). Generally, this type of ore develops as tabular bodies elongated along the strike of the iron-formation to shale contact. They pinch out laterally in the succession. They can however also occur in karst structures.

The upper orebodies are tabular and stratabound and develop along the strike of the Penge iron-formation. Such Fe-ores are mined at the Donkerpoort West and Buffelshoek pits. Finally, the lenticular orebodies, which are generally represented by small irregular lenses of iron ore enveloped in the hosting Penge iron- formation (Netshiozwi, 2002). These orebodies occur at different stratigraphic levels, in the lower or central part of the Penge Formation, but never high up in the succession. The orebodies in the different ranges are generally similar in composition, however, each range has its own geological features. Most of the orebodies are brecciated, with primary haematite fragments set within a secondary hematite matrix. The iron ore is separated from thick underlying dolomites by a thin shale unit (Netshiozwi, 2002). The ore zones have moderately steep dips (30˚ – 50˚), and the shape of the ore lenses is controlled by karst topography in the underlying dolomites (Strauss, 1964). Faults at Thabazimbi region have caused duplication or triplication of the orebodies (Dalstra et al., 2003).

2.5.1. Proposed models for the mineralization of the Thabazimbi Fe-deposit

Although the process responsible for transforming the Thabazimbi deposit into an orebody that contains more than 60 wt% Fe from ca. 20 wt% Fe of the Penge Iron Formation seems to be well documented, is, however, still debated. As such, different models have been proposed for this high-grade iron ore deposit whereby the different occurrences described above probably may at least in part represent different genetic models.

2.5.1.1. Supergene Model

The supergene origin model was proposed and argued by Wagner (1921), Boardman (1948) and Van Deventer (1985). According to Wagner (1921), the banded ironstones originated as banded sideritic cherts. The concentration of Fe was enriched by descending oxygenated waters which dissolved silica out of the sideritic cherts and deposited haematite in its place.

The contacts of the cherts with the overlying and underlying formations, were presumably the most favourable plane for the movement of the solutions and the largest orebodies are thus located along these horizons. Wagner further suggested that the iron oxide was probably deposited as soft, earthy limonite or hydrated hematite. These minerals were subsequently dehydrated and compacted by contact metamorphism of the Bushveld Igneous Province. In general, the model proposed by Wagner (1921), Boardman (1948) and Van Deventer (1985), involves the movement of descending oxygenated meteoric water along fractures. This meteoric water is held responsible for both introduction of iron and leaching of silica from protore iron-formation. Boardman (1948) further suggested that the high-grade iron ore formed by supergene enrichment during folding and brecciation of the strata.

2.5.1.2. **Magmatic Model**

The magmatic model was proposed and argued by De Villiers (1944), who did not accept the concept of the Fe-ore mineralization of the Thabazimbi region to have formed from the replacement of Penge Formation. He was of the view that the haematite was not deposited as hydrated iron oxides, which later dehydrated and compacted and that it is unlikely that the metal was leached out of the banded ironstones. De Villiers (1944) argued that ferruginisation of the banded ironstones took place after fracturing and brecciation and not before, as stated by Wagner (1921). He thought that this deposit post-dated the Transvaal but pre-dated the Waterberg age. As such, he argued that the Fe-deposit may be genetically connected with the Bushveld Igneous Province, because the physical characteristics of the Thabazimbi ores, the presence of high-temperature manganese minerals and the chemical properties of the mineralizing solutions, all indicate that the ores were formed along similar planes of slippage and fracturing. Such planes would afford suitable channels for the movement of solutions whether they are descending or ascending.

De Villiers (1944) proposed that the Fe is of magmatic origin, related to the intrusion of the Bushveld Igneous Province and therefore, the precipitation of iron took place when ascending Fe-rich magmatic waters mixed with oxygenated meteoric water.

2.5.1.3. **Metasomatic and Supergene Model**

The model of metasomatic and supergene ore formation was first proposed by Du Preez (1944), supported by Strauss (1964) and Van Deventer (1985). According to Du Preez (1944), the solutions that formed the orebodies were derived from the dolomites of the Malmani Subgroup, underlying the iron ore. Du Preez (1944) suggested that prior to Fe mineralization, meteoric waters saturated with calcium and magnesium from reaction with the carbonates were trapped in the dolomites. These meteoric waters ascended into the overlying iron-formation during burial, silica was leached out from the iron proto-ore, while at the same time, iron was deposited as specularite. The movement of the meteoric waters up into the overlying BIF was prompted by and propagated through thrusting and faulting. Du Preez (1944) suggested that the Fe was derived mainly from the limonitic iron in the BIF.

Building from the model of Du Preez (1944), Strauss (1964) proposed that the first process to occur was the formation of haematite-dolomite ore, through a complete replacement of chert and chemical reaction of the chert with dolomite to form talc. This process was followed by decomposition and leaching of iron-bearing talc and the formation of high-grade haematite ore. According to Strauss (1964), dolomite is leached and replaced by calcite through supergene processes. Van Deventer (1985), on the other hand, suggests that the Thabazimbi ore genesis took place subsequent to the metamorphic overprint of the BIF, caused by the intrusion of the Bushveld Igneous Province and the tectonism associated with the deposition of the Waterberg sedimentary rocks, which controlled metasomatic alteration of both dolomite and BIF, and the generation of the carbonates and talc-rich haematite rocks.

2.5.1.4. **Hydrothermal Model**

Following a comprehensive review of the geology and metallogenesis of the Thabazimbi high-grade iron ore, Netshiozwi (2002) proposed and argued a hydrothermal model for the Fe mineralization. Based on the nature of the Thabazimbi deposit, Netshiozwi suggested two different stages of the hydrothermal model.

The first stage:

A hydrothermal alteration marked by oxidation of all ferrous (Fe^{2+}) minerals (carbonate and grunerite) and their replacement by haematite. This oxidation process is associated with only minor leaching of chert and resulted in the formation of a typical "oxidized" Penge Formation. In this "oxidized iron-formation", former magnetite is altered first to kenomagnetite and finally to martite.

The second stage:

A hydrothermal alteration characterized by efficient leaching of chert in the banded iron-formation to form high-grade haematite ores or carbonate-hematite ore followed the Bushveld intrusion. The chert was replaced by porous masses of microplaty haematite, resulting in the formation of massive or laminated haematite ore.

2.6. **Summary on the reviewed tectonic setting of the Thabazimbi region and Kumba Fe-Mine**

After the above literature review (Du Preez, 1944; Strauss, 1964; Du Plessis and Clendenin, 1988; Netshiozwi 2002 and Basson and Koegelenberg, 2017), it is suspected herein that the described structural deformation around and in the Thabazimbi Kumba Fe-Mine is related to broad-scale regional tectonic deformational events that are not yet fully documented.

The consensus amongst these authors is that the stratigraphic units of the Thabazimbi region and Kumba Fe-Mine have experienced extensive, complicated, broad-scale fold-and-thrust events. The folds and thrust faults of this region have an overall vergence to the north and a general ENE–WSW and/or E–W strike direction parallel to the TML. The timing for the folding and thrusting remains controversial, with some authors suggesting ± 2.0 Ga age as the Transvaal strata are thrusted over the lower Waterberg Group strata deposited between 1.97 and 2.01 Ga. Whilst others agues for a protracted period of 2.04 – 2.0 Ga that is tectonically associated with the TML, after the ~2.01 Ga deposition of the 2nd Waterberg Group Unconformity-Bounded Sequence (WUBS II). Moreover, it is not clearly documented if thrusting occurs as a result of folding or *vice-versa*, folding develops as a result of thrusting. The controversy around the age of the deformation of the Thabazimbi Kumba Fe-Mine region, also brings to question the mode and age of the Fe-mineralization at the Kumba Fe-Mine. However, with the imprecise tectonic framework of the region and mine, this has left geoscientific researchers with nothing but educated speculations.

The exposed Neoarchaean - Mesoproterozoic supracrustal rocks of the Thabazimbi region provide an opportunity to properly study, analyse, interpret and constrain the regional tectonic framework of Thabazimbi. In addition, the structural interpretation provided here may give new insights into the Fe-ore mineralisation of the Thabazimbi Kumba Fe-Mine and additional understanding of previously proposed genetic models of the Thabazimbi BIF-hosted high-grade iron ore mineralisation.

__Chapter 3__

3. **Methodology**

Two methods are integrated in order to obtain a meaningful and comprehensive analysis of the tectonic framework of the exposed Neoarchaean – Mesoproterozoic supracrustal rocks of the Thabazimbi region and Kumba Fe-Mine. The first method employed is the remote sensing (RS). In this approach, Landsat 8 data together with image analysis software such as, ENVI, Global Mapper and Geographic Information Systems (GIS) are used to investigate, analyse and interpret the surface expressions of geological structures and lithology of the Thabazimbi region and Kumba Fe-Mine. The second method employed is the field structural investigation. This approach allows to verify satellite data interpretation with interpretation of the structural geology of the area around the Thabazimbi Kumba Fe-Mine, for which access could be granted. Because of the difficulty of accessing some of Kumba Fe-Mine premises and the private game farms that surround the mine site, the field investigation results obtained are used as supporting evidence rather than fully validating the RS analysis and interpretations. Therefore, the tectonic interpretations are strongly based on the analysis of the remote sensing dataset from satellite images.

3.1. **Remote Sensing (RS) studies**

Remote sensing is the study of the electromagnetic energy reflected, scattered and emitted from the Earth's surface, the atmosphere and the oceans by means of aerial sensor and spaceborne technologies (Sabins, 1999). RS is therefore defined as the practice of acquiring, processing and interpreting images and related data acquired from aircraft and satellites that record the interaction between matter (earth objects) and electromagnetic energy (Sabins, 1999).

The approach underlying remote sensing is that electromagnetic energy recorded by sensors mounted on aircraft or satellite is used to uniquely identify earth objects. Accordingly, RS technology is applied to obtain surface structural data for regional tectonic investigations of the Thabazimbi region and the Fe-Mine. The method of applying RS for geoscientific research investigations is an effective tool that offers an opportunity to examine the geological characteristics of the earth surface without the need to access the area on the ground (Price, 1994; Abdullah et al., 2013; Laake, 2011). Furthermore, it is able to provide a synoptic overview of the regional geology and can directly assess the characteristics of geological structural features extending over large areas. Since the unveiling of the Landsat Missions by NASA, Landsat instruments have acquired valuable remote sensing data for a wide range of applications (Sabins, 1999, Di Tommaso and Rubinstein, 2007, Mekonnen, 2008). The datasets produced by Landsat sensors are of high quality in detail, coverage and value (Sabins, 1999). The first generation is termed Landsat 1, 2 and 3, and operated from 1972 to 1985. This was replaced by the second generation called Landsat 4, 5, 7 and 8, which began operation in 1982 and continues to the present (Kamel et al., 2015).

Landsat 8 is the latest advanced scientific technology of the Landsat satellite family. This satellite was launched in 2013. Operationally, Landsat 8 consists of two main sensors, namely, the Operational Land Imager (OLI) and the Thermal Infrared Sensor (TIRS). OLI is a push-broom sensor that collects images in nine spectral bands (of visible, near-infrared and shortwave) to observe a 185 km across-track ground swath of the Earth with 15 to 30 meters resolution (USGS, 2016). While TIRS is as a push-broom sensor that collects image data using a focal plane with long arrays of photosensitive detectors to measure longwave thermal infrared (LTIR) energy emitted by the Earth surface (USGS, 2016). The Landsat 8 data consist of four visible energy bands (band 1, 2, 3, and 4) and the three reflected infrared bands (band 5, 6, and 7) that are complemented by one panchromatic high resolution bands, band 8 (0.503 – 0.676 μm) with 15 meter spatial resolution (Kamel, et al., 2015).

Band 10 (10.60 – 11.19 μm) and band 11 (11.50 – 12.51 μm) of the Landsat 8 satellite images records in the thermal infrared (TIR) at a spatial resolution of 100m. The Landsat 8 (path_171 and row_077) dataset, ID: LC81710772015138LGN00 (1) used here was acquired on the 13 of August 2015 (day-time acquisition) from the U.S. Geological Survey Earth Resources Observation and Science Center (USGS). Landsat 8 datasets are processed according to the geoscientific application.

3.1.1. **The first step:**

Since the focus of this investigation is mostly structural analysis and interpretations, preprocessing of Landsat 8 dataset is limited to atmospheric and geometric correction, band combination and spectral enhancement. The acquired Landsat 8 dataset was preprocessed for atmospheric corrections that include radiometric calibration and geometric corrections in ENVI platform following Harris Geospatial Solution, (2017) to improve image interpretation. Various band combinations based on three Landsat bands were tested to generate red-green-blue (RGB) composites in ENVI software platform to enhance the interpretation of geomorphology and geology of the Thabazimbi region (**Figure 3.1)**. From the different RGB composite images that were generated, the combination of 5-4-3 was preferred (**Figure 3.1**), because it stands out to be the best for visual interpretation of lineaments and geological structures of the region and mine. To further enhance interpretation of structures, the chosen image underwent pan-sharpening in ENVI software platform. As most of the major lithological units of the region are well known, further image processing (e.g. rationing or classification) were not performed.
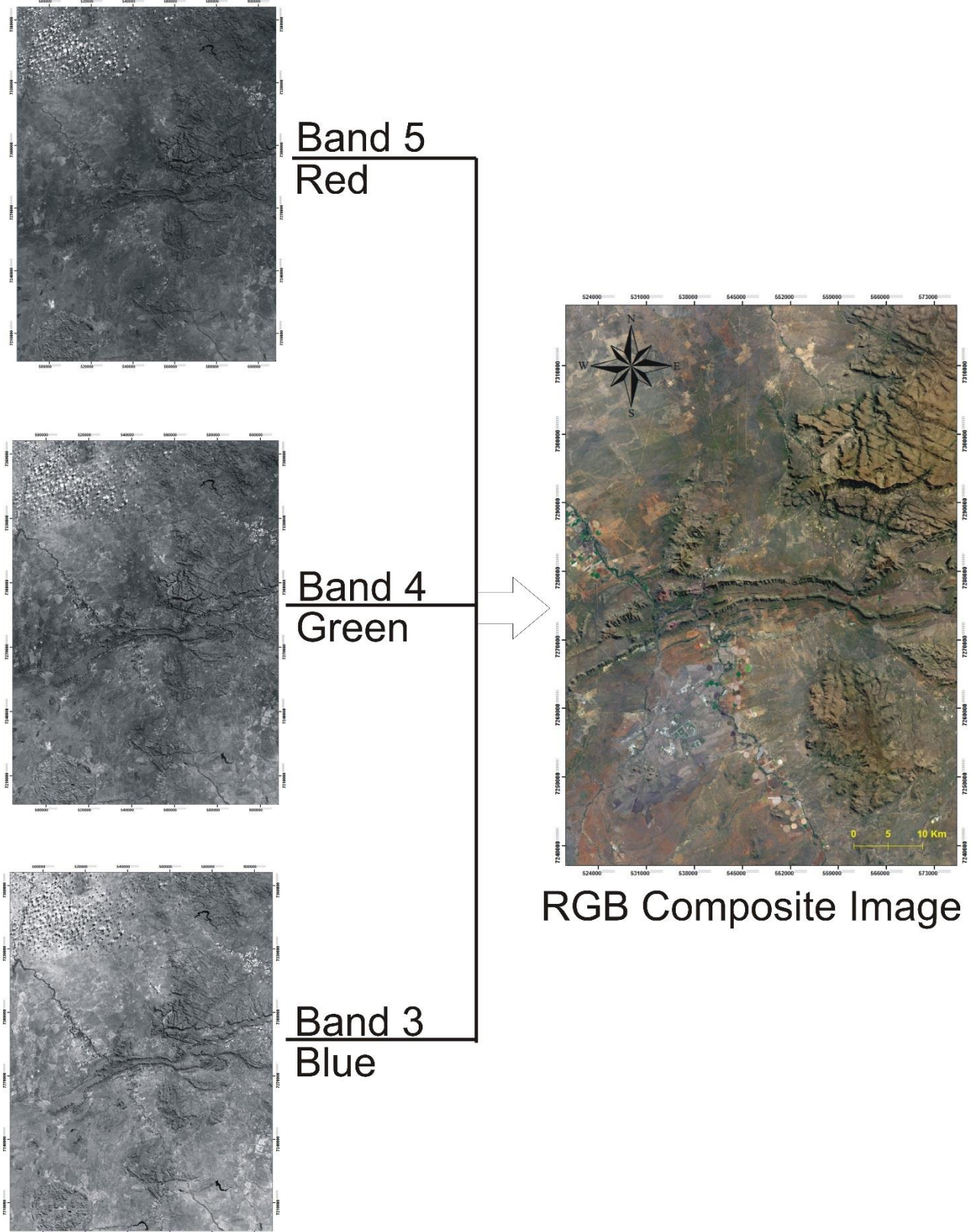
Figure 3.1: Band combination procedure as followed in ENVI software platform in generating red-green-blue (RGB) composites image, here labelled RGB composite image 5-4-3.

3.1.2. **The second step:**

This step evolves the scanning and georeferencing of the geological structures and lithological units of the Thabazimbi region and Kumba Fe-Mine from the 1: 250 000 geological map (see **Figure 3.2)**. The scanned 1: 250 000 geological map was georeferenced into World Geodetic System (WGS 84) and its associated Universal Transverse Mercator projection (UTM 24S) and used as a layer in GIS software. The scanned and georeferenced 1: 250 000 geological map of the Thabazimbi region were used as an auxiliary dataset in order to compare the remote sensing results with the previously mapped tectonic lineaments, geological structures and the major lithological units of the Thabazimbi region and Kumba Fe-Mine.

3.1.3. **The third step:**

This step involved the integration of step 1 and 2 in GIS software program (ArcMap), for better analysis and interpretation of the structural geology of the Thabazimbi region and Kumba Fe-Mine. In this step, the RGB composite image (see **Figure 3.1**) and the georeferenced, digital 1: 250000 scale geological map of the Thabazimbi region (see, **Figure 3.2** below) are integrated in ArcMap platform as two autonomous layers. From the RGB satellite image, lineaments were mapped in ArcMap platform (see **Figure 4.1a** in **chapter 4**).
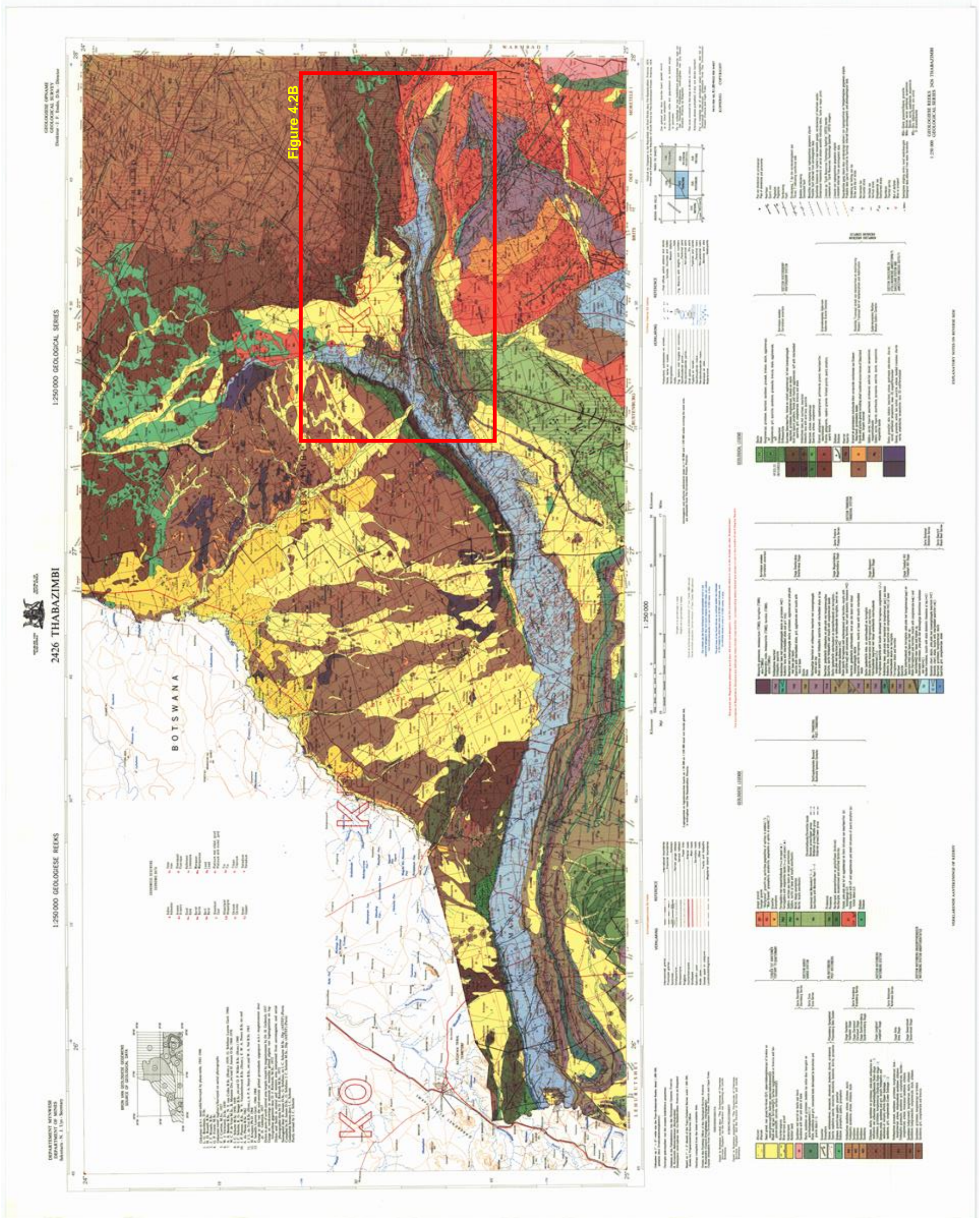
Figure 3.2: 1:250000 scale geological map of the Thabazimbi region digitized and georeferenced for ArcMap purposes (Series 2426 Thabazimbi, 1974). The solid red rectangle represent the limit–extension of the zoomed in area, superimposed on the lineaments mapped from the RGB image in order to test whether the mapped lineaments were previously documented (in the 1:250000 scale geological map of the Thabazimbi region) or not (see **Figure 4.2B** in **chapter 4**).

3.1.4. **The fourth step:**

This step encompasses mapping of the recognized lineaments of the Thabazimbi region and Kumba Fe-Mine. Lineaments were defined after Solomon and Ghebreab (2006) and Abdullah et al. (2013) as an extensive mappable linear feature of a surface whose parts are aligned in a rectilinear or slightly curvilinear relationship that can be observed on the satellite imageries and presumably reflect geological structure features such as faults, joints, folds, dykes, crustal fracturing, and/or lithological contacts. Geomorphological features such as river passages, straight drainage channel segments, and valleys can shadow geologically controlled structures such as fault line and/or dykes. Therefore, analysis and interpretation lineaments using remote sensing imageries is depended on 1.) the reflected surface expression of the geological structure feature, 2.) the manifest of the geological structure feature in the image and 3.) the expertise and scientific skill to interpret the expressed structure features as being of tectonic origin (Heddi et al., 1999). Visual mapping of lineaments was here done based on geological experience and the ability to interpret tectonic features (i.e. fault, dyke, and/or joints).

Lineaments were mapped from RGB image and grouped after the major geomorphological terrain of their occurrences namely: the Rosseauspoort and Thabazimbi (Northern, Southern and Middle) Ranges (see, **Figure 4.1** in **chapter 4**). Accordingly, different layers of the mapped lineaments (i.e. Rosseauspoort Range and Thabazimbi Range lineaments) were created in the ArcMap platform as separated layers and subsequently superimposed on the scanned and georeferenced 1:250000 scale geological map of the Thabazimbi region (see, **Figure 3.2**) in order to establish the geological setting of the extracted lineaments. Based on this map of the Thabazimbi region, the geological setting underlying the lineaments of the Rosseauspoort and Thabazimbi Ranges is the Transvaal Supergroup of the Transvaal basin.

To better analyze and interpret the tectonic regime of the lineaments mapped from the RGB composite image, the lineaments were plotted using frequency rose diagram in order to classify, compare and determine their dominant trends and length. A layer of faults traced from the geological map of the region, here called "Geological Map Fault" (see, **Figure 4.2** in **Chapter 4**) was then created in ArcMap, and superimposed on the lineaments mapped from the RGB image, in order to test whether the mapped lineaments were previously documented (in the 1:250000 scale geological map of the Thabazimbi region) or not.

3.1.5. **The fifth step:**

After thorough mapping of the lineaments from RGB composite image, geological structural features (i.e. anticlinal and/or synclinal folds) were also mapped. Portrayal of geological structure features for visual illustration was done using Corel-DRAW software program. For better analysis of the mapped lineaments and geological structure features from RGB image, Global mapper 16 (64-bit) software platform was utilized. 30m SRTM-DEM data of the Thabazimbi region and Kumba Fe-Mine was downloaded from the U.S. Geological Survey Earth Resources Observation and Science Center (USGS). This DEM was used as additional datasets for better visibility and interpretation of the mapped lineaments and geological structures (see, **Figure 4.1b** in **chapter 4**).

3.2. **Fieldwork studies**

This research undertook field structural measurements of the tectonic structures that include thrust faults, normal and reverse faulting and folding in order to understand the kinematics and dynamic history of the Thabazimbi region and Kumba Fe-Mine. The structural field data presented in this research were collected from three areas of the Thabazimbi Ranges (Northern, Southern and Middle ranges), see **Figure 3.3** below.
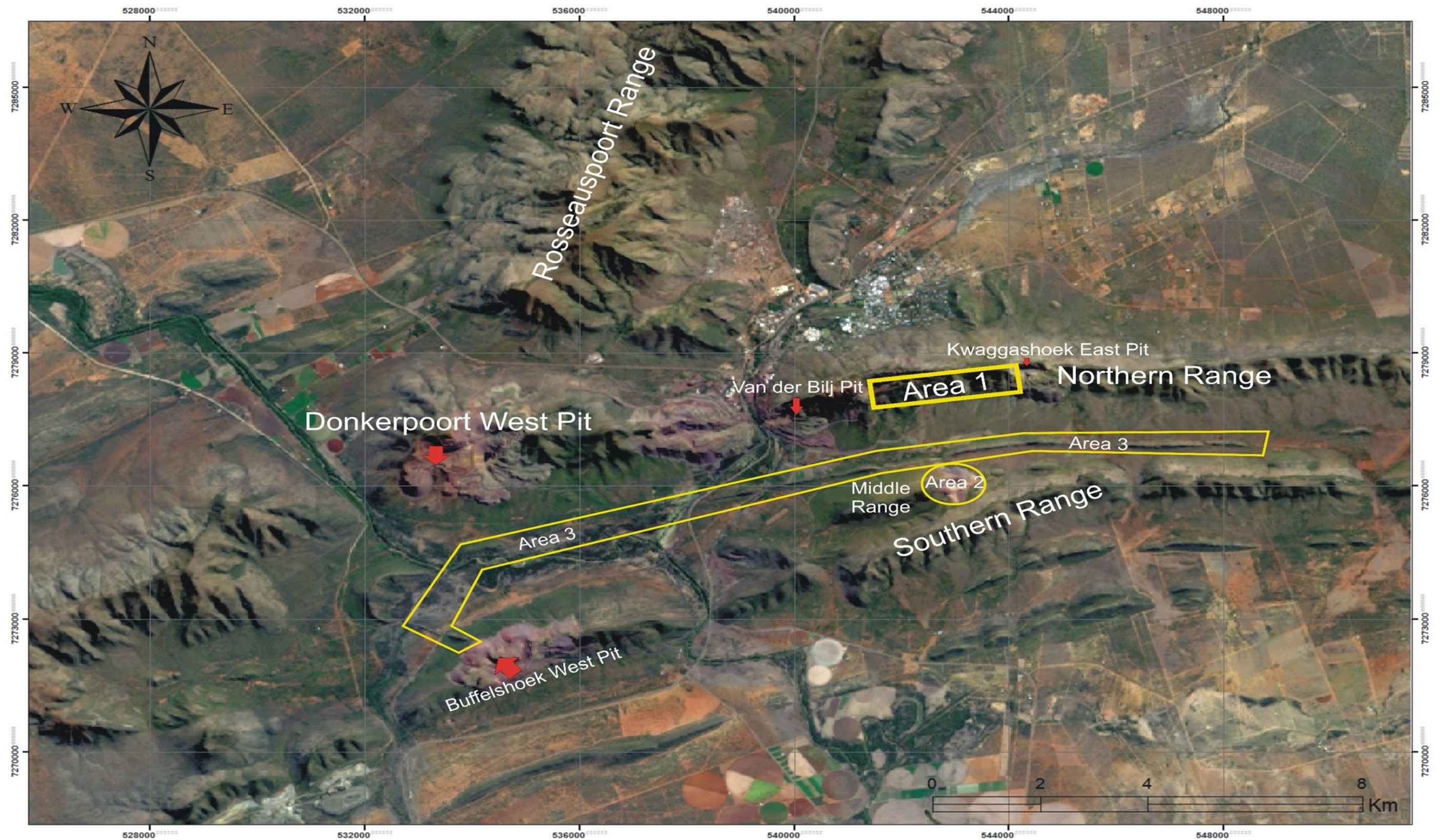
Figure 3.3: RGB composite image (image 5-4-3) of the Landsat 8 OLI (path_171 and row_077), showing the location of the study areas, Area 1, 2 and 3. Area 1 indicated by yellow rectangle. This area is situated between Van der Bijl and Kwaggashoek East Mine. Area 2 indicated by yellow circle, located in the Bobbejaanwater pit mine. Area 3 encompass of the outcrops between the Northern and Southern range of the Thabazimbi Range, as highlighted by the yellow solid line.

Area 1 encompasses the field structural investigations area along the Northern rage (**Figure 3.3**). This area is divided into four locations, where structural data were collected. Area 2 encompasses the structural investigations from the Middle range, Bobbejaanwater Mine Pit (see **Figure 3.3**). Structural data collected from area 2 are few, but fundamental for the kinematic history of the region. Area 3 encompasses the field structural investigations between the Northern and Southern range (**Figure 3.3**). Area 3 was mainly investigated for verification of a geological structures mapped on the remote sensing satellite imageries.

Fieldwork was carried out in the months of May 2016, August 2016 and May 2018. The field areas were mainly mapped on foot, and geological data were recorded in a notebook and plotted on field base maps. Navigation in the field was generally accomplished using a G.P.S. (Global Positioning System) receiver. General geological data collected during the course of the fieldwork comprised mostly tectonic structural features. Dip angles and dip directions were recorded for directional and orientations of tectonic structures. Where present, the orientation of the kinematic indicators along the fault zone and folded areas (i.e. slickenside lineations and hinge lines) were recorded. The orientation (e.g. strike, dip angle and dip direction) of tectonic structures were measured using geological compass-clinometers. Furthermore, the stereographic projection was performed in order to identify any dominant tectonic trends analyzed (see, **Figure 4.7** and **4.8** in **chapter 4**).

Analyses of stereographic data were done using SpheriStat software (Stereonet 7 and Fabric 8). Each stereographic projection presented in this research is in a lower hemisphere projection on a Schmidt (equal area) net. This was done in order to classify and compare different fold structures and to aid with the determination of the orientation of the fold axial plane.

__Chapter 4__

4. Remote Sensing and Fieldwork Results

4.1. Remote Sensing (Image analysis) results

4.1.1. Lineament Mapping

Figure 4.1a is RGB composite image that displays band 5 on the red channel, band 4 on the green channel and band 3 on the blue channel, as described in chapter 3. In this composite image (**Figure 4.1a**), topographic landmarks such as Thabazimbi Range (i.e. Northern, Middle and Southern Ranges) and Rosseauspoort Range and prominent geological and tectonic features (i.e. Bushveld Igneous Province and the Waterberg basin) are clearly distinguished. The Northern and Southern ranges of the Thabazimbi Range are visible, as long curvilinear ridges that trend E–W. The Rosseauspoort Range trends N–S, seemingly splay from E–W striking Thabazimbi Range, forming an "Y" shape topographic feature with the Thabazimbi Range (see, **Figure 4.1a** below). From **Figure 4.1a**, the observable flatirons indicate southwards dip directions for the Thabazimbi Range lithological units and an eastwards dip direction for the Rosseauspoort Range strata. Of structural importance, the image exposes extensive mappable linear features of a surface whose parts are aligned in a rectilinear or slightly curvilinear. Some of the mappable linear features are long, extensive and curvilinear while most are short and straight (**Figure 4.1a**). Furthermore, some of these mappable linear features appear naturally modified by surface erosional processes and are accentuated by valleys, ridges and other topographic features. **Figure 4.1b** is an SRTM-DEM image that shows deep vertical extent and/or how penetrative the observed mappable linear features are. In addition to **Figure 4.1a**, **Figure 4.1b** shows that the geological units have a different physical response to erosion and weathering, based upon their physical properties.
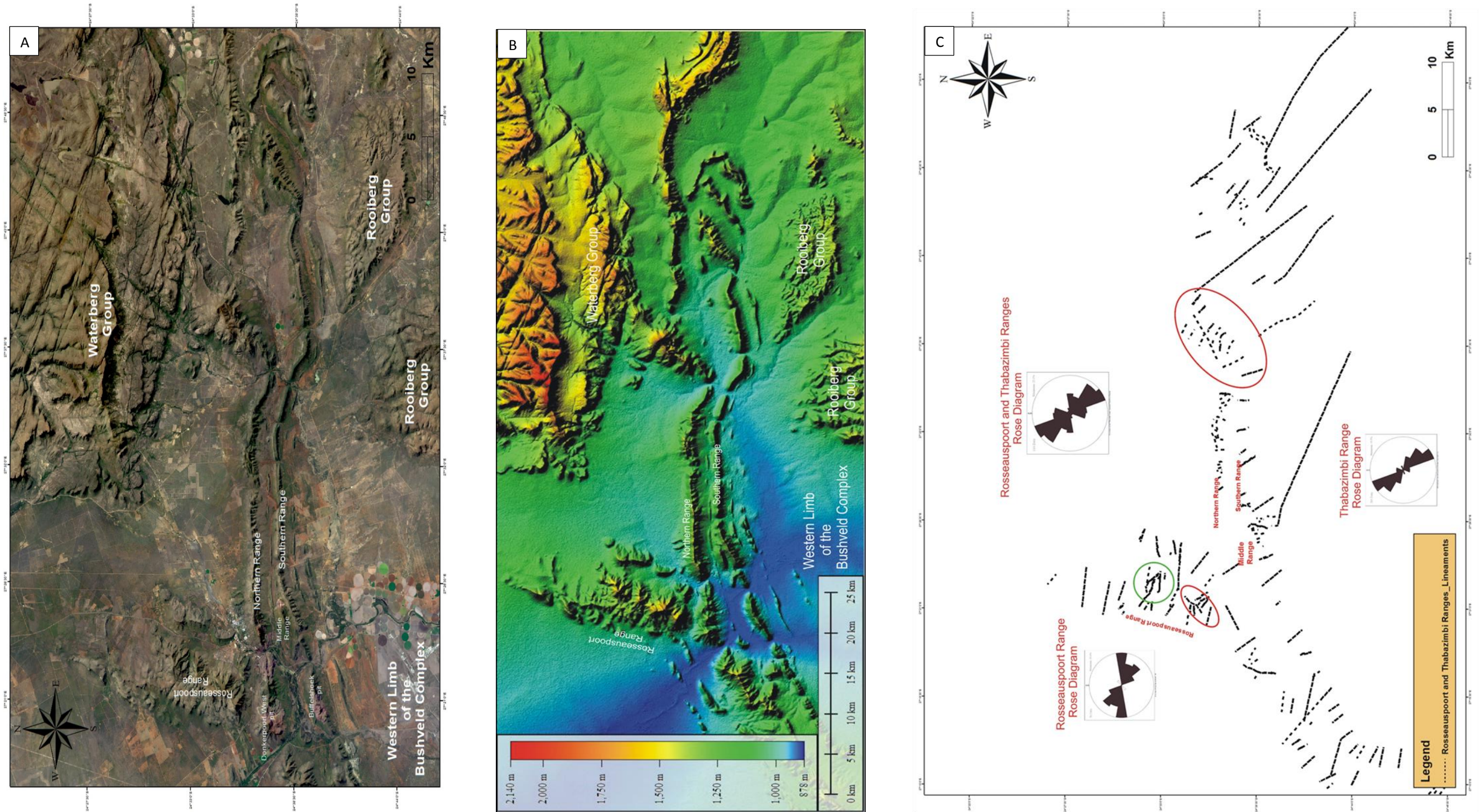
Figure 4.1: (a) Generated RGB composite colour image 5-4-3 of Landsat 8 OLI. The major lithological boundaries are identified by topography difference (i.e. the Bushveld Igneous Province indicated by low relief, south-western part; the Rooiberg Group indicated by high relief, south-eastern part and the Waterberg Group indicated by high relief, north-eastern part). The green, purple, slight pinkish rounded spot along the Crocodile River channel are farm irrigations. (**b**) 30 m SRTM-DEM image showing topographic map of the reflected surface structural features. The topographic elevation is shown on the left-side by the colour scale, with each colour indicating the measure of elevation. (**c**) Map showing extracted lineaments of the Thabazimbi region and Kumba Fe-Mine. The green circle shows the NW–SE to NNW–SSE trending lineaments crosscutting the E–W-trending lineaments. The red ellipsoid shows the NE–SW trending lineaments crosscutting the NW–SE to NNW–SSE trending lineaments.

Figure 4.1c below is a map of linear features extracted from image 5-4-3 (**Figure 4.1a**). The map (**Figure 4.1c**) shows a systematic variation in trend directions and length of the extracted lineaments, which can be traced from hundreds of meters to several kilometers. The extracted linear features reflect either regional and/or localized tectonic trends, which clearly depend on the lithology. A total number of 116 geologically controlled lineaments were manually mapped. The minimum length of the mapped lineaments is calculated to be approximately 400 m, while the maximum length is ca. 20 km. The long, curvilinear lineaments cut through the Thabazimbi Range (Northern and Southern) into the Rooiberg Group. This indicates that these lineaments are of different generations as they cut through different stratigraphic position. The short and straight lineaments however, cut only the geology of the ranges. To better analyze and interpret the extracted lineaments of the Thabazimbi region and Kumba Fe-Mine as shown in **Figure 4.3c**, the lineaments are grouped in accordance with the ranges they cut.

4.1.1.1. **Mapped lineaments of the Thabazimbi Range:**

The geology of the Thabazimbi Range (Northern, Southern and Middle Range), as interpreted from the digitized 1:250000 scale geological map of the region, encompasses the 2.588 – 2.06 Ga Transvaal Supergroup rocks. From **Figure 4.1c**, the frequency rose diagram of the mapped lineaments of the Thabazimbi Range indicates a NNW–SSE as the first major predominant trend and a NW–SE as the second major predominant trend. This is consistent with the frequency rose diagram vector mean of 145˚ (**Figure 4.1c**). The WNW–ESE is the subdominant trend and a N–S and a NE–SW are minor trends. From the frequency rose diagram, the Thabazimbi Range lineaments appear to indicate an increment of 10˚ in trend direction, from the west-northwest to north-northwest. Tectonically the 10˚ increment of trend direction can be considered insignificant for any major tectonic interpretations. Therefore, the NNW, NW and NNW lineaments trend are grouped as a single set of NW–SE to NNW–SSE strike direction.

The statistics shown in the rose diagram for the Thabazimbi Range in **Figure 4.1c** indicates that most of the NW- to NNW–SSE-trending lineaments are long and curvilinear and, in some parts, crosscut through different stratigraphic units. As mentioned in the above paragraph, these lineaments crosscut the stratigraphic units of the Rooiberg Group and are also traceable in the Waterberg rocks as well (see, **Figure 4.1a** and **4.1b**). This indicates that the tectonic activity of the NW–SE to NNW–SSE-trending lineaments must be younger than the sedimentation of the upper Waterberg unconformity-bounded sequence (WUBS II). On average, 90% of the Thabazimbi Range lineaments are striking in the same direction (NW–SE to NNW–SSE). Further analysis indicates that 60 to 70% of the short and straight NW–SE to NNW–SSE lineaments overlap with the long, extensive and curvilinear NW–SE to NNW–SSE lineaments. This indicates that some of the short and straight lineaments trending in the NW–SE to NNW–SSE direction are of the same generation as the long, curvilinear NW–SE to NNW–SSE trending lineaments. Notably, the NW–SE to NNW–SSE trending lineaments are crosscut and displaced by the NE–SW lineaments in some parts (**Figure 4.1a** and **4.1b**). This indicates that the NE–SW trending lineaments are tectonically younger than the NW–SE to NNW–SSE lineaments. The crosscutting relationship between the N–S trending lineaments and the NW–SE and NE-trend lineaments is however, not clearly defined to reason any tectonic interpretations. Of structural importance is that the mapped lineaments of the Thabazimbi Range are not radially acentric (radiating from or converging to a common center) or concentrically positioned along the Northern and Southern ranges from east to west, which could suggest lineaments that developed around a dome or basin like structure.

4.1.1.2. **Mapped lineaments of the Rosseauspoort Range:**

Similar to the Thabazimbi Range, the Rosseauspoort Range is composed mainly by 2.588 – 2.06 Ga Transvaal Supergroup strata.

The frequency rose diagram of the mapped lineaments of the Rosseauspoort Range shown in **Figure 4.1c** indicates a predominant major trend of a E–W that is followed by a NW–SE and a subdominant WNW–ESE trends. The minor trend directions of NNW–SSE and NE–SW are indicated. Comparably, it is worth noting that the E–W lineaments trend direction is only apparent in the Rosseauspoort Range but not in the Thabazimbi Range. Nevertheless, the E–W trend is the predominant major direction of the Rosseauspoort Range lineaments. The NW- and WNW-trends observed in the Rosseauspoort Range are also present in the Thabazimbi Range. The crosscutting relationships between the different lineament trends reveal that the E–W direction is relatively oldest as it is crosscut by all other directions. The NE–SW trending lineaments crosscut the E–W and the NW–SE lineaments and are therefore relatively the youngest generation (**Figure 4.1c**). As the E – W trend is absent however in the Thabazimbi ranges and in the Rooiberg and Waterberg groups, the above age relationship of E – W being the oldest trend, can only be applied to the Rosseauspoort Range area. The E–W trending lineaments mapped in the Rosseauspoort Range suggest an extensional tectonic rather than compressional.

4.1.1.3. **Comparison between the mapped lineaments and the 1:250000 scale geological map faults:**

Figure 4.2a below, shows the lineaments of the Rosseauspoort and Thabazimbi Ranges mapped from the RGB composite image (**Figure 4.1a**) and the faults traced from the published 1:250000 scale geological map of the Thabazimbi region (**Figure 4.2b**). Some mapped lineaments (white dashed lines on **Figure 4.2a**) clearly overlap with the digital faults from the 1:250000 scale geological map (red dashed lines on **Figure 4.2a**). In some areas the lineaments mapped from RGB composite image (**Figure 4.1**) do not match with the faults (i.e. f_1, f_2, f_3, f_4 and f_5) extracted from the geological map (**Figure 4.2b**) and, vice versa, some of the faults traced from the geological map do not correspond with lineaments derived from RS.
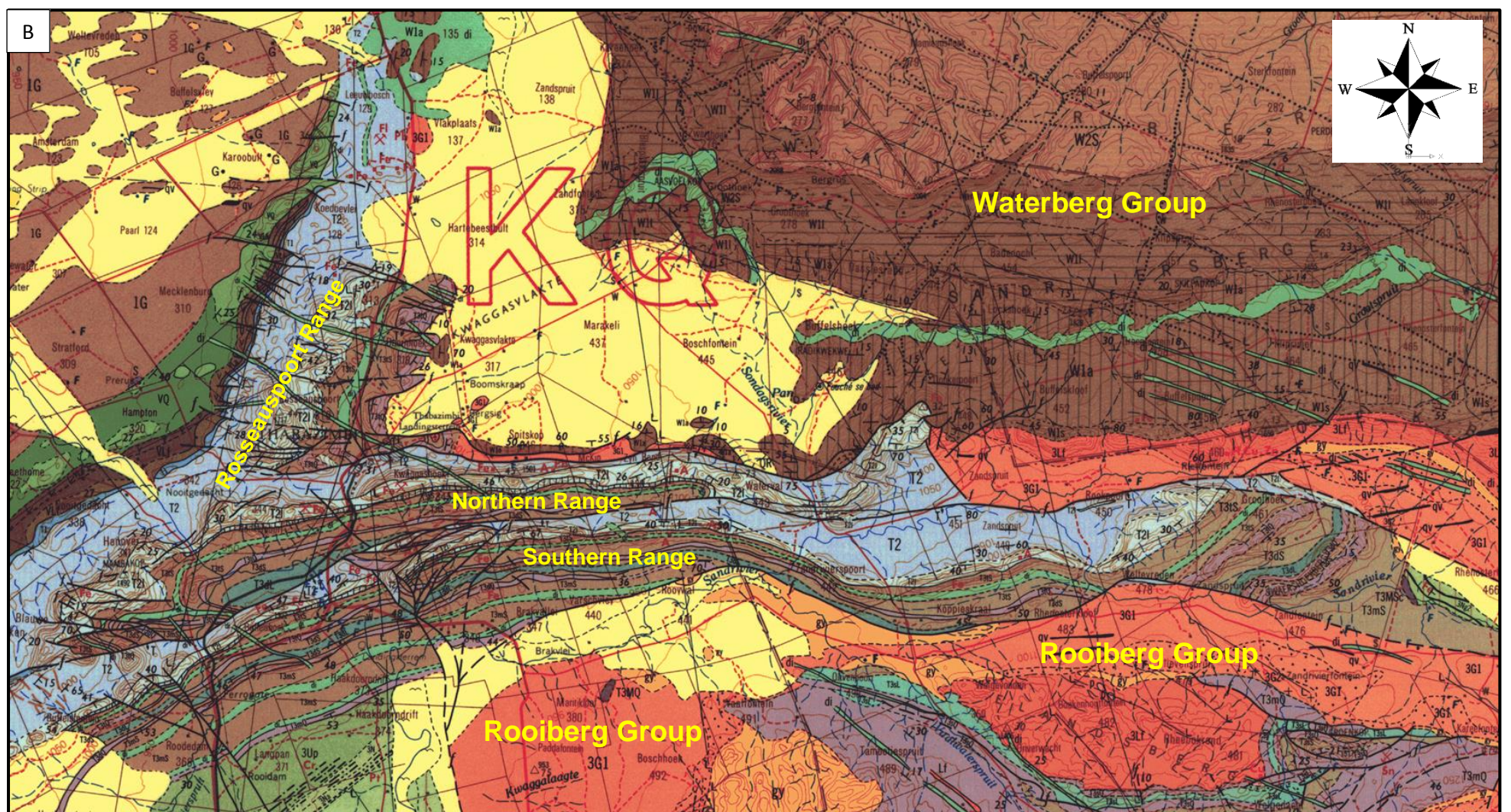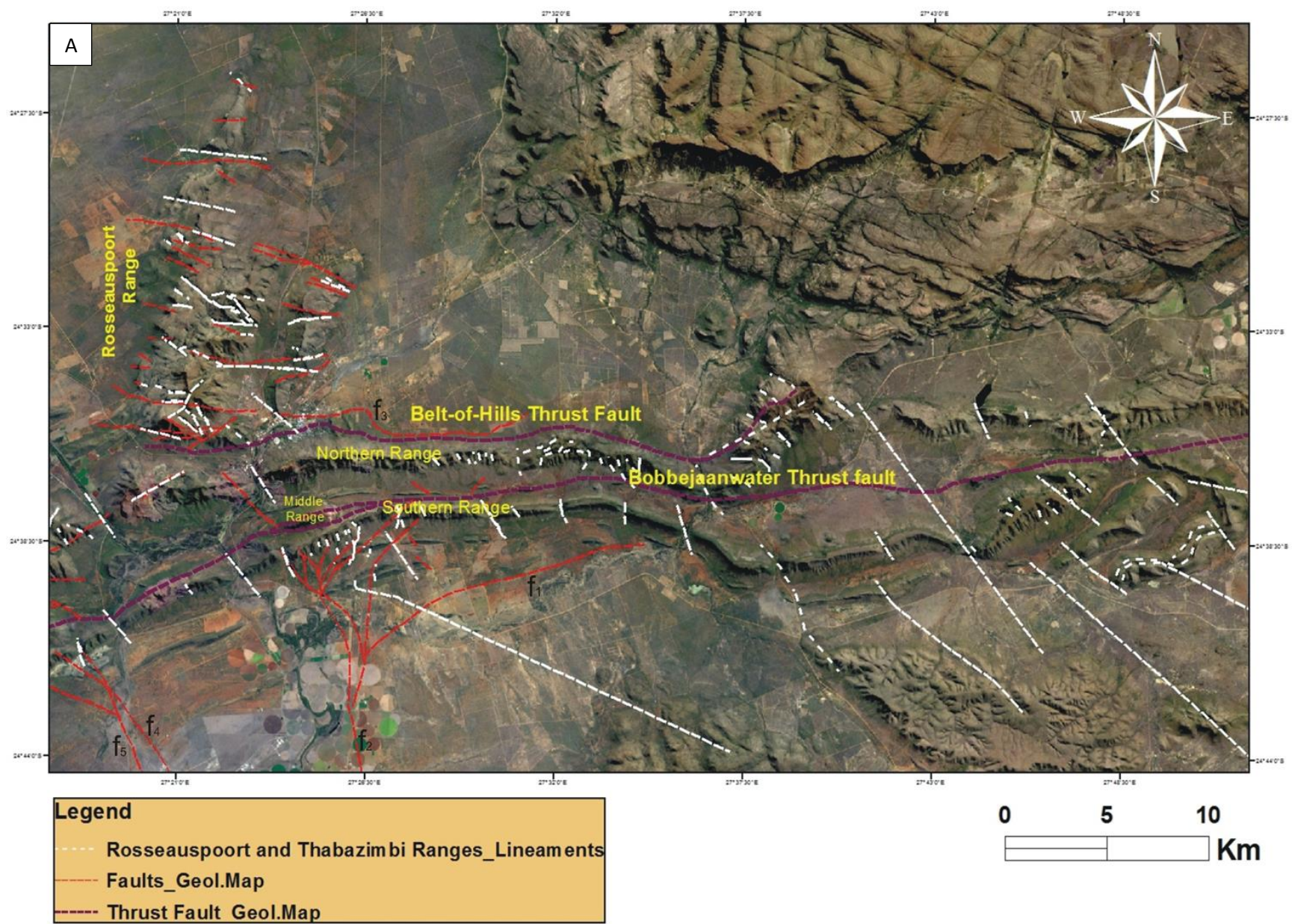
Figure 4.2: (**A**) RGB composite image 5-4-3 showing extracted lineaments of the Thabazimbi region and Kumba Fe-Mine (white dashed lines), traced faults from the 1: 250 000 scale geological map of the Thabazimbi region (red dashed lines) and projected thrusts fault lines (i.e. Belt-of-Hills Trust Fault and Bobbejaanwater Thrust Fault) traced from the 1: 250 000 scale geological map (magenta dashed line). (**B**) Zoomed in 1:250000 scale geological map of the Thabazimbi region scanned and georeferenced (Series 2426 Thabazimbi, 1974). For geological information on **Figure 4.2B**, refer to **Figure 3.2** in **chapter 3**.

There is further no apparent surface expression of geological and/or geomorphological structure features visible in the field or in the satellite images to support the existence of such faults as mapped at 250000 scale geological map of the region. This suggests that some of the faults from the geological map are either: 1.) exaggerated, 2.) poorly expressed on Landsat 8 OLI imagery or 3.) they were not recognized by RS measures, or 4.) are not existent. The last possibility is of course, very limited and field studies should always dominate interpretation over RS studies. But many of the areas, especially within the Bushveld igneous rocks domains, make no outcrop at all and there, the geological mapping (1:250000 scale geological map of Thabazimbi) may be based on illusive interpretations.

4.1.1.4. **A summary of lineaments mapped from the RGB composite**

From **Figure 4.1c**, it can be established that the Thabazimbi region and Kumba Fe-Mine consists of three significant sets of tectonic lineaments: E–W, NW–SE to NNW–SSE and NE–SW. Although the RS results proved the existence of few N–S trending lineaments, these are considered insignificant for tectonic interpretation of the Thabazimbi region. The NNW – SSE and WNW–ESE trending lineaments are grouped as a single set of NW–SE to NNW–SSE-trending lineaments for better interpretation of the tectonic framework of the region. From **Figure 4.1a** and **4.1b**, it can be deduced that the NW–SE to NNW–SSE trending lineaments which crosscut the Thabazimbi Range occur as well in the Rosseauspoort Range and in the Rooiberg Group strata (not shown on the image). This implies that the tectonic regime responsible for the NW–SE to NNW–SSE trending lineaments was most probably active after the deposition of the Rooiberg Group. Considering the ages of the exposed units of the Rooiberg Group, this indicates that the NW- to NNW–SSE trending lineaments were active after the formation of the Rashoop Granophyre Suite (RGS) and the granitic suite of the Bushveld Igneous Province.

Furthermore, the NW–SE to NNW–SSE trending lineaments are visible across the Waterberg rocks (northeast of the Thabazimbi Range, see **Figure 4.1**). This further suggests that the tectonic regime of the NW–SE to NNW–SSE trending lineaments must have been active even after the sedimentation of the upper Waterberg unconformity-bounded sequence (WUBS II). The E–W trending lineaments cross-cutting the Rosseauspoort Ranges are not occurring in the Thabazimbi Range. It is challenging to constrain the relative tectonic age of these lineaments considering that the Rosseauspoort Range and the Thabazimbi Range have the same stratigraphic units but different degree and trends of deformation. Based on the spatial alignment and surficial expression of these lineaments, it is reasoned that the E–W trending lineaments are most likely associated with fractures and faults which developed during extensional tectonics (see **chapter 5**, for further interpretation) and represent therefore, extensional fractures and normal faults formed as a result of sagging of the Transvaal strata due to cooling and thermal contraction of the Bushveld Igneous Complex (see **chapter 6**).

However, specific attention is given to the relationship between the E–W trending lineaments and the NW–SE to NNW–SSE and NE–SW trending lineaments. The tectonic regime responsible for the E–W trending lineaments was most probably active prior to the NW- to NNW–SSE trending lineaments and perhaps overprinted within the Thabazimbi Range during the intrusion and cooling. Seeing that the NW–SE to NNW–SSE trending lineaments crosscut the Rooiberg Group strata (southeast of Thabazimbi Range, see **Figure 4.2a** and **4.1a**) and are overprinted in the Waterberg Group, the tectonic regime responsible for E–W trending lineaments may possibly have been active prior to or concomitant to the Rashoop Granophyre Suite (RGS) and the granitic suite of the Bushveld Igneous Province. With respect to NE–SW-trending lineaments, these lineaments crosscut the NW–SE to NNW–SSE trending lineaments in some parts of the Thabazimbi Range and in the Rooiberg Group rocks (not shown herein). This indicates that the tectonic regime responsible for the NE–SW trending lineaments was most probably active after the NW–SE to NNW–SSE trending lineaments.

With the tectonic activity of the NW–SE to NNW–SSE trending lineaments determined to be active after the sedimentation of the upper Waterberg unconformity-bounded sequence (WUBS II). Therefore, the NE–SW trending lineaments must have been active after the deposition of the WUBS II as well. Of stratigraphic importance is that the NE–SW trending lineaments are also visible across the Waterberg sediments (northeastern part of the Thabazimbi Range, see **Figure 4.1a** and **4.1b**).

Figure 4.3 below shows the lineaments extracted from the Landsat 8 OLI imageries and those not yet documented on the geological map 1:250000 (Series 2426 Thabazimbi, 1974). This figure is here considered as the updated lineament map of the Thabazimbi region and Kumba Fe-Mine based on RS results (black dashed lines), digital faults traced from the geological map of the region (red dashed lines) and digital thrusts fault (i.e. BHTF and BTF) traced from the geological map of the region (magenta dashed line).
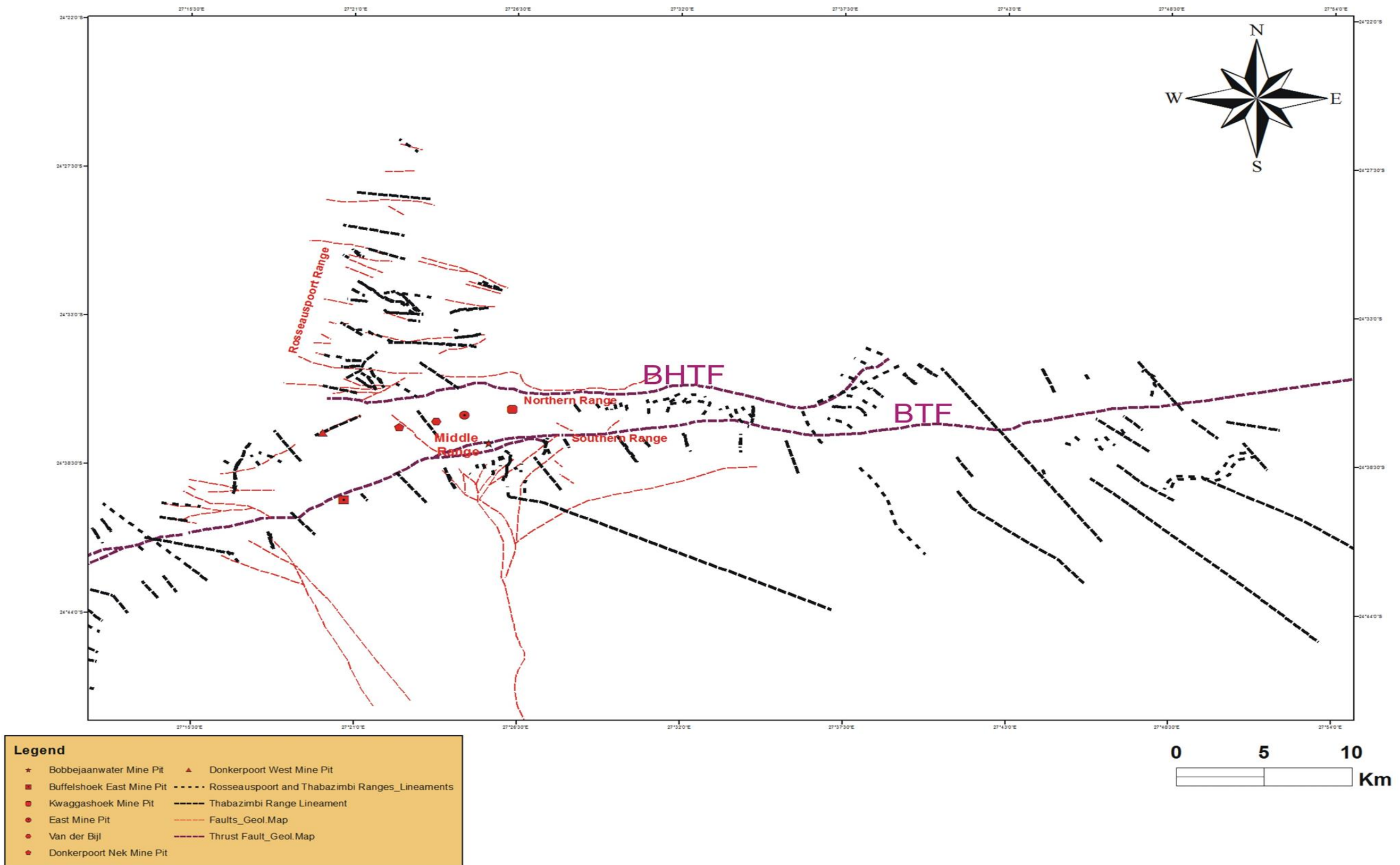
Figure 4.3: Tectonic lineament map showing extracted lineaments (black dashed line) of the Thabazimbi region and Kumba Fe-Mine and digital faults (red dashed lines) and thrusts (magenta dashed line) from the 1: 250 000 scale geological map of the Thabazimbi region. BHTF (Belt-of-Hill Thrust Fault) and BTF (Bobbejaanwater Thrust Fault).

4.1.2. Mapping of geological structure features from RGB composite image

From **Figure 4.4** below, the exposed strata of the Thabazimbi region are strongly faulted. This is revealed by a surficial expression that exposes a network of NW–SE to NNW–SSE trending lineaments in the eastern extremity of the Thabazimbi Range, interpreted as faults (yellow dashed lines in **Figure 4.4b**). The faults are distinguished by the visible displacement of the thrusted beds of the Thabazimbi Range, see **Figure 4.4b**. The fact that these faults crosscut the thrusted beds of the Transvaal Supergroup suggests that these faults have occurred during or later than the thrusting event. Thereby the observed NW–SE to NNW–SSE trending faults are consistent with the mapped NW–SE trending lineaments (**Figure 4.4**). Du Plessis (1990) and Basson and Koegelenberg (2017) have also documented strike-slip faults that crosscut the Northern range strata of the Thabazimbi Ranges. From **Figure 4.4b**, the gray values and surficial expression gives the impression that the NW–SE to NNW–SSE trending faults are sinistral (left-handed) in some areas and dextral (right-handed) in some areas.

By further examination of **Figure 4.4**, it is noticed that the image, in the eastern part, exhibits three mountain ridge morphologies (see label **2**, **3** and **4** in **Figure 4.4b**) that are made evident by land surface elevations and geomorphological valleys. From **Figure 4.4b**, the colour image gives the impression that the labelled mountain ridge 2 has a similar stratigraphic units as the Southern Range of the Thabazimbi Range. Furthermore, the surficial expression suggests that the labelled mountain ridge 2 extent as far as the labelled mountain ridge 1 (**Figure 4.4b**). Thus, labelled mountain ridge 1 and mountain ridge 2 are of one stratigraphic unit, which appears to be similar with the stratigraphic units of the Southern range of the Thabazimbi Range. With respect to labelled mountain ridge 3 and mountain ridge 4, the surficial expression appears to indicate that they are both of a similar stratigraphic units (**Figure 4.4b**). In contrast, these ridges appear to have different colour reflection and surficial expression to the labelled mountain ridge 1 and 2, suggesting a dissimilar stratigraphic units.
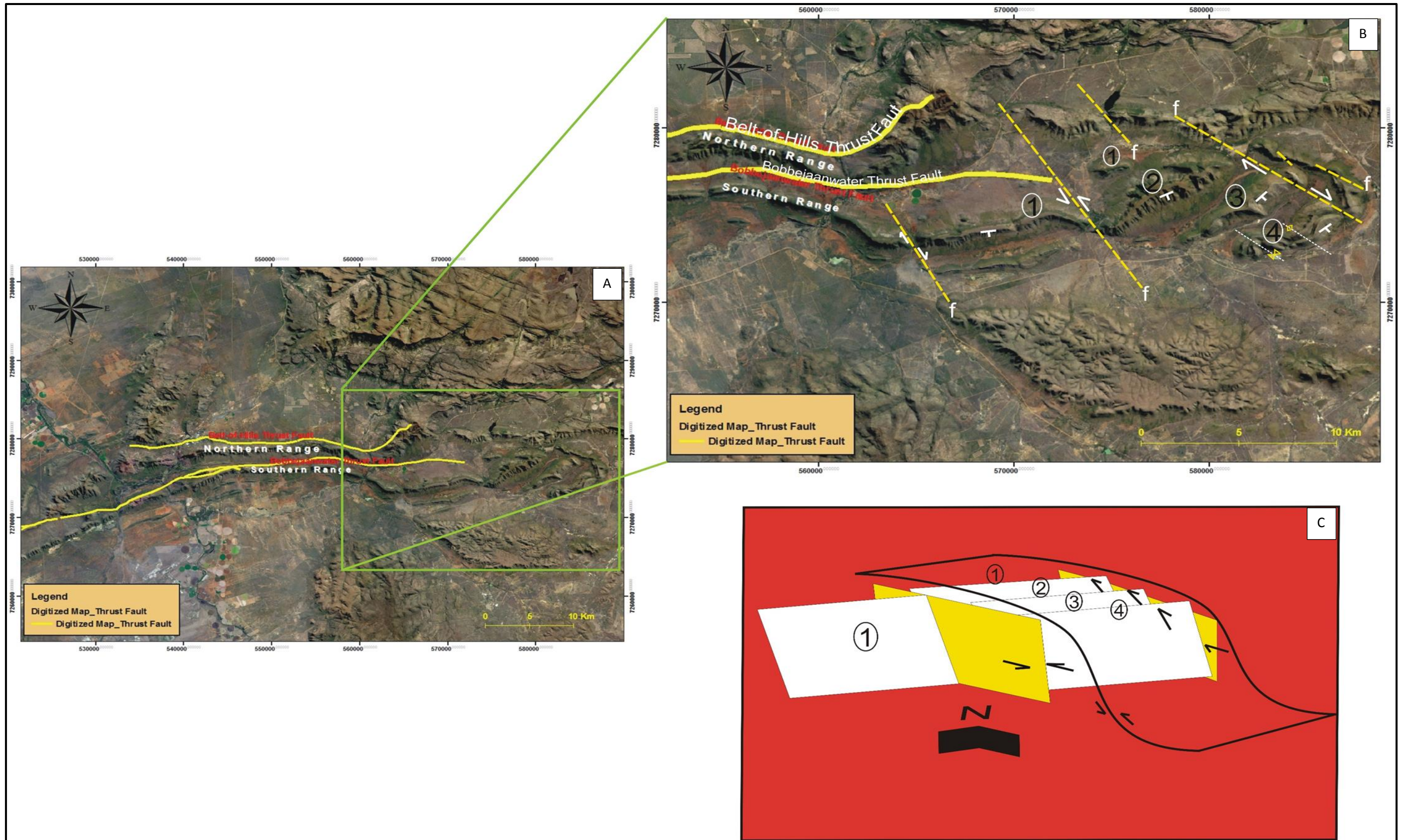
Figure 4.4: (**A**) RGB composite image 5-4-3 showing the Thabazimbi (Northern and Southern) Range. Belt-of-Hills Thrust Fault (BHTF) and Bobbejaanwater Thrust Fault (BTF) digitized from the geological map of the Thabazimbi are shown (yellow solid line) on the composite image. Belt-of-Hills Thrust Fault is in the north side of the Northern range. Bobbejaanwater Thrust Fault strikes E–W between the Northern and Southern Ranges. (**B**) Zoom in image showing the observed geological structure features, interpreted as thrust duplexes and left-lateral faults. The observed left-lateral faults cross-cut the duplexes (yellow dashed line). (**C**) Schematic drawing showing the duplexes observed.

The published 1:250000 scale geological map of the Thabazimbi region documents a recurrent Transvaal Supergroup lithological sequence across these ridges. In Figure 4.6b, the labelled mountain ridge 1 and 2 belongs to the Chuniespoort Group, the labelled mountain ridge 3 and 4 belong to the Pretoria Group. This agrees with the RS analysis revealing that the labelled mountain ridge 1 and 2 are of one stratigraphic unit, and different from the mountain ridge 3 and 4. The morphology, surficial expression and the observable flatirons of these ridges indicate that they are striking ENE or slightly NE and are sub-parallel to the Thabazimbi Range (Northern, Southern and Middle ranges). Furthermore, the observable flatirons indicate southwards dipping strata (**Figure 4.4b**). The surficial expression (i.e. repetition of stratigraphic units) and the morphology of these ridges are indicative of thrusting. Notably, this appears to be similar to what is described in the Thabazimbi Range (i.e. duplication and/or triplication of strata, Northern, Southern and Middle ranges by Netshiozwi, 2002). Of tectonic interest is that the mountain ridges occur adjacent to the Bobbejaanwater Thrust Fault (BTF), see **Figure 4.4**. These features are, therefore, suggestive of imbricated structures that form by the stacking of two or more thrust sheets with a northwards kinematic transport. The strata of the labelled mountain ridge 4 appears to be folded into anticline and syncline folds (**Figure 4.4b**). This is indicative of progressive folding that occurs in stepping thrusts with a dominant northwards kinematic transport. At inspection of **Figure 4.4b** the folded strata give the impression of folds being open, symmetric and upright. Further inspection shows that the three mountain ridges are bound in the East by the NW- to NNW-trending sinistral fault and in the West by the NW–SE to NNW–SSE trending dextral fault (**Figure 4.4b**).

4.1.2.1. **A summary of geological structure feature mapping**

Analysis of the mapped structural features of the Thabazimbi region and Kumba Fe-Mine using Landsat 8 OLI reveals extensive thrusting and faulting (see, **Figure 4.4**).

The faulting is unveiled by lateral offsetting of the thrusted beds of the Thabazimbi Range. The nature and character of this faulting suggests a NW–SE to NNW–SSE trending sinistral and dextral faults (plan view) (**Figure 4.4b**). Thrusting is best described by the E–W to ENE–WSW trending three mountain ridges that are sub-parallel to the BTF (**Figure 4.4b**). The three mountain ridges in the East of the mapping areas have a strong resemblance to surficial expression to the Northern, Southern and Middle ranges of the Thabazimbi Range. Tectonically, surficial expression and the morphology of the ridges suggest that these features may be imbricated thrusts that developed coeval to the E–W to ENE–WSW trending BTF (**Figure 4.4**). Thus, the three mountain ridges are suggestive of thrusted duplexes with dominant northwards kinematic transport (**Figure 4.4c**) that developed during imbricated thrusts system. The structural setting proposed by Boardman, (1948), Du Plessis and Clendenin, (1988), Good and De Wit, (1997), and Netshiozwi, (2002) all agree that the supracrustal rocks of the Thabazimbi region are tightly folded, thrusted and duplicated along the E–W trend, with a northerly vergency and southerly dips. Of tectonic significance is that the NW–SE to NNW–SSE trending sinistral and dextral fault (plan view) crosscut the thrusted beds of the Thabazimbi Range (**Figure 4.4b**). This implies that the age of the NW–SE to NNW–SSE trending sinistral and dextral faulting might be syn- to post thrusting.

4.2. **Fieldwork Results**

Structural field data were collected from three areas, 1, 2 and 3 as outlined in chapter 3 (**Figure 4.5**). Area 1 encompasses four locations (1, 2, 3, and 4, see **Figure 4.6**) of the Northern range. Examples of the tectonic structures observed in the four locations of area 1 are shown in **Figures 4.7**, **4.8** and **4.9**. Area 2 encompasses the Bobbejaanwater Mine Pit of the Middle range geology (see, **Figure 4.5**). The tectonic structures observed in area 2 are shown in **Figure 4.11**. Area 3 encompasses the lithological unit exposed between the Northern and Southern ranges (see, **Figure 4.5**).
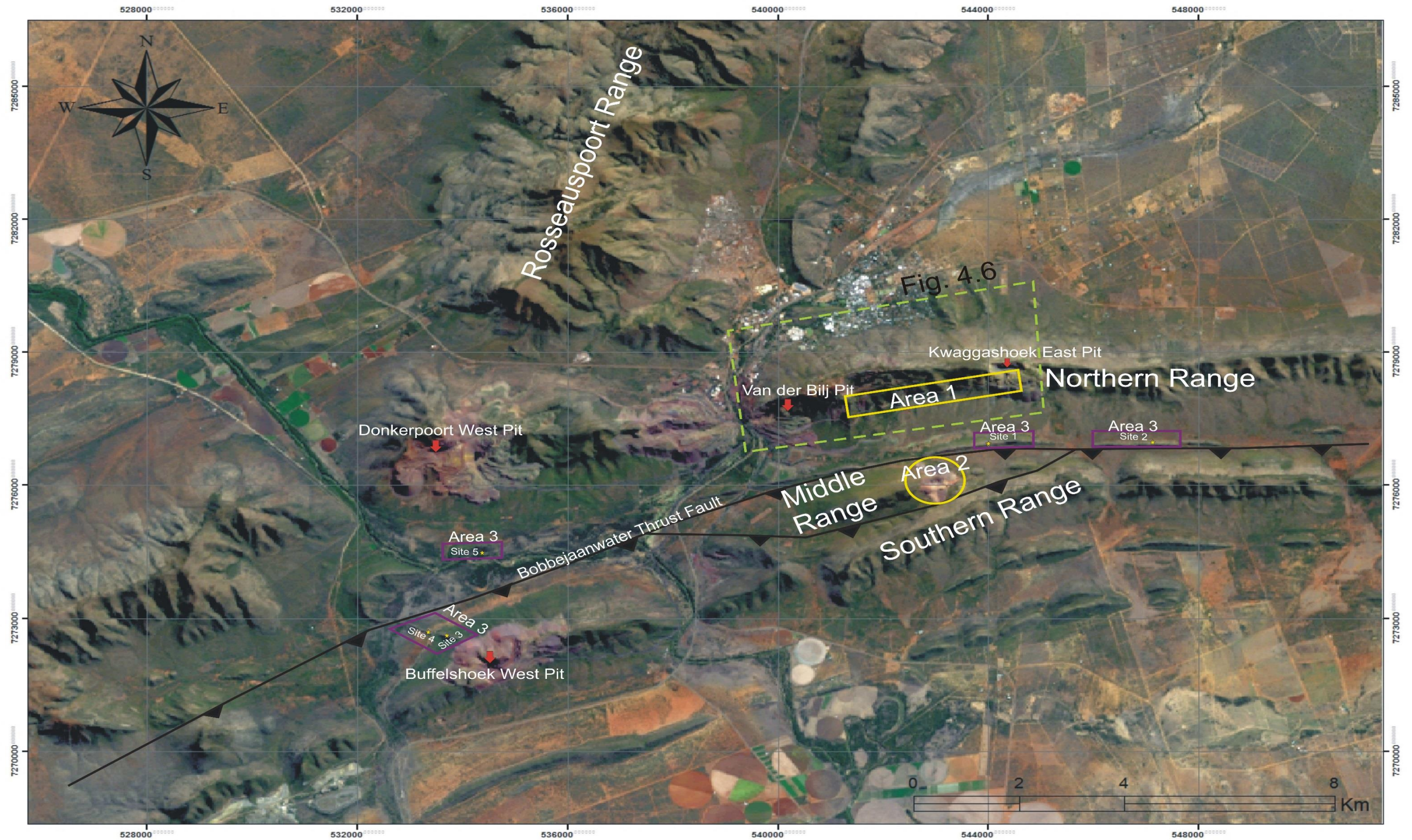
Figure 4.5: RGB composite image 3-4-5 of Landsat 8 OLI, showing areas where field structural investigation studies were done. Area 1 is represented by yellow rectangle on the map. The lime-green dashed rectangle enveloping Area 1 field study represent the limit–extension of the zoomed in google earth map that shows locations were structural data was collected in area 1 (see **Figure 4.6**). Area 2 is represented by yellow circle on the map. Area 3 is represented by purple rectangles, showing 5 sites where structural measurements were taken. The image is a Landsat 8 satellite data, with a Path_171 and Row_077.
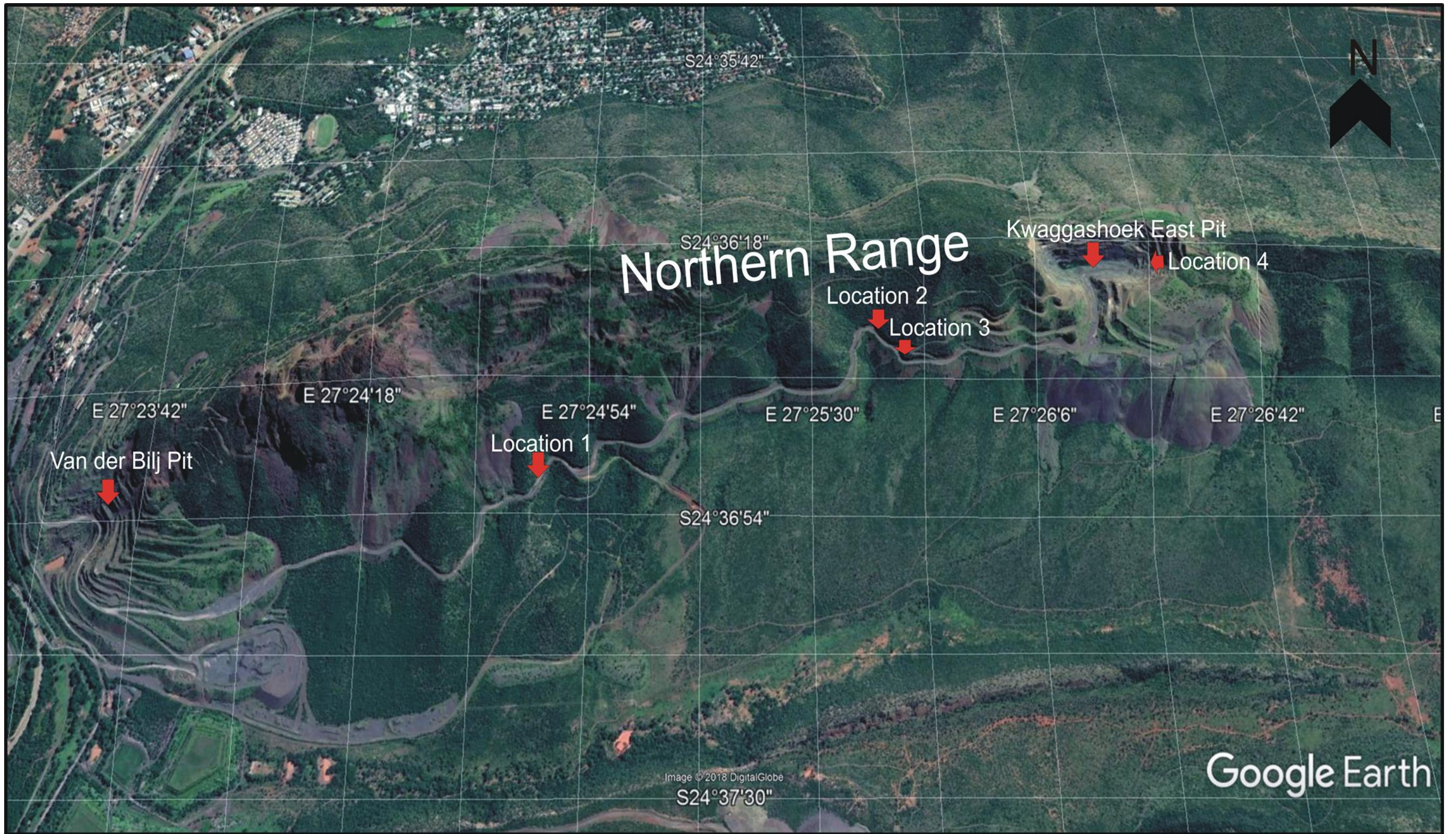
Figure 4.6: Google Earth Imagery (GEI) showing the zoomed in locations (Location 1 - 4) of Area 1 field study, where most tectonic structures were observed.

The structural measurements collected in area 3 are from five sites (**Figure 4.5**) and are further shown in detailed structural interpretation from **Figure 4.12**. This area was visited for verification of the synclinal fold indicated/interpreted by the published 1:250000 geological map of the Thabazimbi region and by Basson and Koegelengberg (2017).

4.2.1. Area 1 structural field investigation results:

Area 1 is an E–W striking, S - facing vertical section of road-cut outcrops, situated between the Van der Bijl Mine Pit and Kwaggashoek East Mine Pit. The area lies along the Thabazimbi Northern range (see **Figure 4.5**). Stratigraphically, the area contains mainly the Chuniespoort and Pretoria Group outcrops. Lithological outcrops identified within this area are the shale unit of the Pretoria Group and the banded iron formations (BIFs) and shale unit of the Penge Formation above the carbonates. The units host concordant sills and discordant dykes of varying thickness. Field structural investigations of Area 1 have revealed the presence of small-scale thrusts and folds and reverse faults.

4.2.1.1. Tectonic structures in Area 1

4.2.1.1.1. Thrusts

Parasitic thrusts are well-exposed along the E–W striking, S-facing vertical-section of road-cut outcrops, in the banded iron formation outcrop (see location 3, **Figure 4.8**). In the field, the thrust is evident by notable truncation of the banded iron layers and the cut-off of the step-up fault within the same lithological unit (thrust cut-offset) and the discontinuity of banded iron layers (see location 3, **Figure 4.8**). The thrusted BIF beds steepen from southwards directed dips to near vertical (~ 50˚ to 85˚ S). This is well displayed on the hanging-wall (HW) flat on footwall (FW) (termed the back-limb) and the HW ramp on FW (termed the front-limb).

The displacement between HW and FW of the thrust is clear and unambiguous in the steep ramping sections of the BIF sheets (see location 3, **Figure 4.8**). In the field, when the thrust fault is traced into the bedding plane that parallels the ramp-flat, it becomes less prominent and eventually disappears (see location 3, **Figure 4.8**). The parasitic thrusts are most pronounced in the BIF unit of the Penge Formation. Bending or kinking of the hanging-wall (HW) above the fault plane on the thrusted BIF beds can be observed, which forms an open, symmetric, upright, anticline (location 3, **Figure 4.8**). Such a feature is a classic case of a fault-bend fold caused by bending of a fault-block as it rides over a non-planar fault surface (Suppe, 1983). Largely, the parasitic thrusts indicate the probable presence of a major thrust that is characterized by E–W striking, SSE–NNW to S-dipping, with an NW–SE to N–S tectonic vergence. In support of the above interpretation, macro- to meso-scale ramp-flat geometries as described above were observed throughout the E–W striking, S-facing vertical-section of road-cut outcrops of Area 1 (see location 1 and 2, **Figure 4.7**). Close examination of the meso-scale ramp-flat geometries reveals thrust duplexes, which indicate NW–SE to N–S tectonic transport (**Figure 4.7** and **4.8**). These structural features support the field interpretation of thrusted beds, showing a consistent NW- to N-tectonic vergence.

4.2.1.1.1.1. Stereographic Projection of the structural data collected in Area 1

In **Figures 4.7 and 4.8**, identical lower hemisphere stereographic projections of the structural data collected in location 1, 2, 3 and 4 of area 1 are shown in a contoured projection of the poles to bedding and the hinge line data. The broad scatter around the π-girdle of the projection of the poles to bedding indicates folding for area 1 structural data (dip and dip-direction). From the computed π circle from Area 1 structural data, the fold axis is determined. This fold axis has a WSW-directed gentle plunge (14˚ => 248˚). To better understand the structural data collected from area 1, the limited field measurements of the hinge lines are plotted stereographically (**Figure 4.7** and **4.8**). The plot of the hinge line data clusters around the determined fold axis, WSW (**Figure 4.7** and **4.8**).
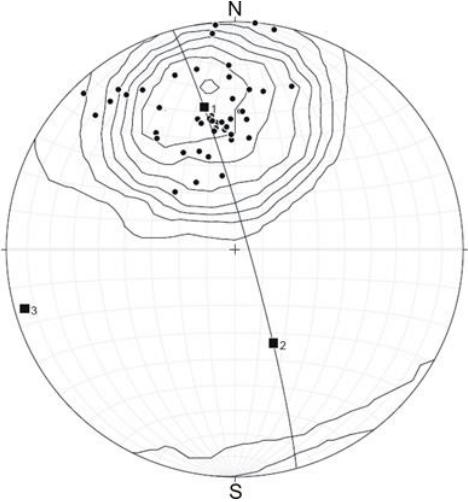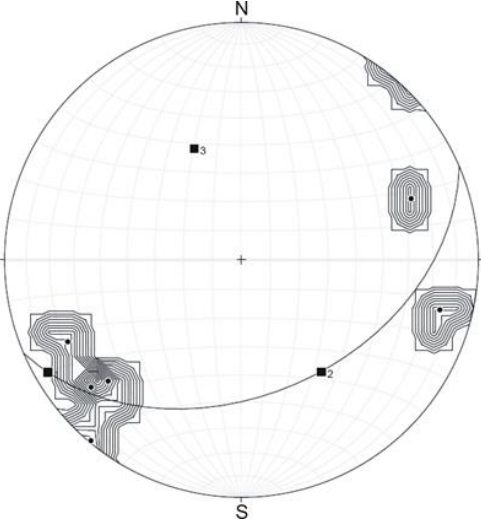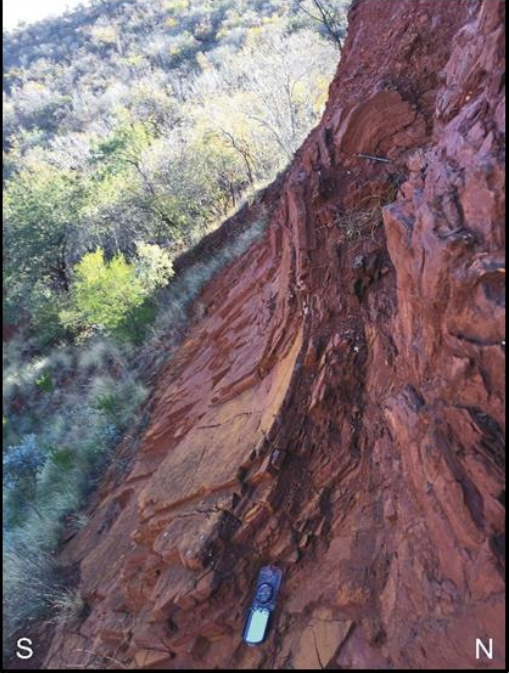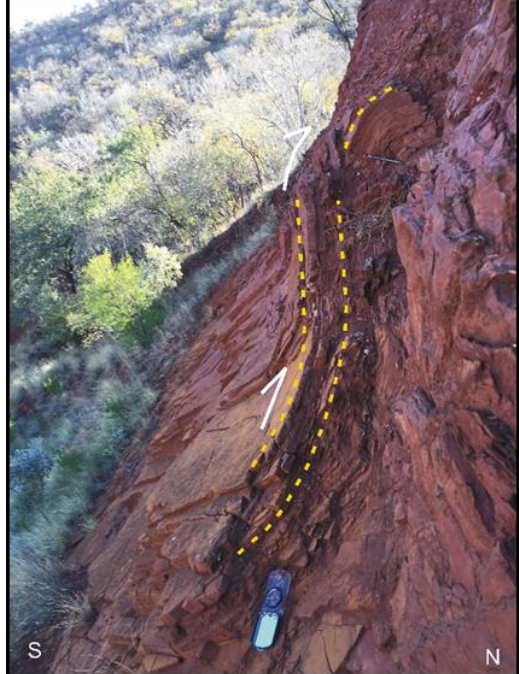
Area 1	Field photographic evidence	Schematic interpretation from the photograph	Lower hemisphere, equal area stereographic plot of surface data (pole to bedding),	Lower hemisphere, equal area stereographic plot of Hinge Line
			n = 45	n = 6
Location 1 **{24˚ 37' 002" S; 027˚ 24' 477" E}** - The photo was taken looking in the northeastern direction - Tectonic structure: ramp-flat				
Location 2 **{24˚ 36' 567" S; 027˚ 25' 554" E}** - The photo was taken looking towards the western direction - Tectonic structure: ramping				

Figure 4.7: Photographic field evidence showing tectonic structures observed in Area 1. (**Location 1**), Field photographic evidence of ramp-flat geometries and a schematic drawing showing the geometry of the tectonic movement along the ramp-flat observed in Location 1 of Area 1. (**Location 2**), Field photographic evidence of ramping observed along the road-cut outcrop of Area 1 and a schematic drawing showing the geometry of the ramps. Lower hemisphere, equal area stereographic plot of surface data, pole to bedding and hinge lines collected in the area are shown. The plots indicate σ_1 that gently plunge N, σ_2 gently west and σ_3 plunging steeply NW.
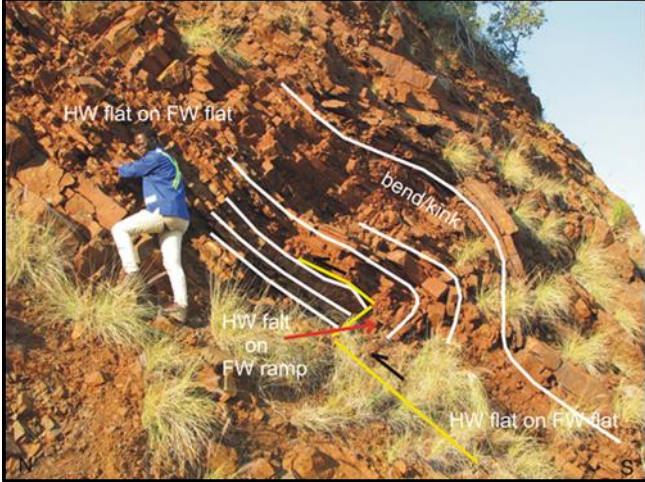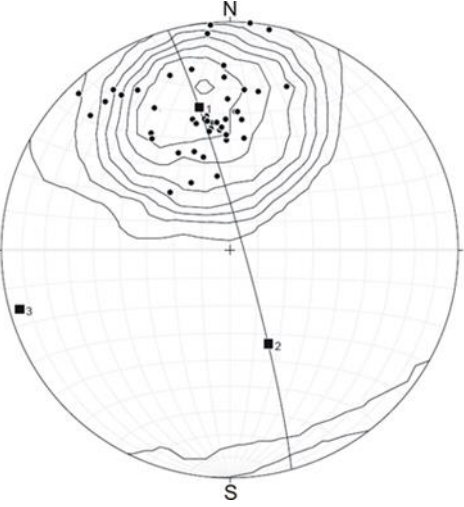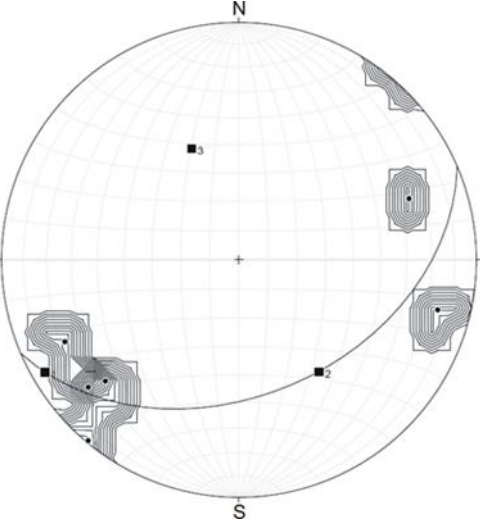
Area 1	Field photographic evidence	Schematic interpretation from the photograph	Lower hemisphere, equal area stereographic plot of surface data (pole to bedding),	Lower hemisphere, equal area stereographic plot of the Hinge Line
			n = 45 (same data as in **Figure 4.7**)	n = 6 (same data as in **Figure 4.7**)
Location 3 **{24˚ 36' 562" S; 027˚ 25' 775" E}** - The photo was taken looking in the eastern direction - Tectonic structure: parasitic thrust				
Location 4 **{24˚ 36' 777" S; 027˚ 24' 828" E}** - The photo was taken looking in the eastern direction - Tectonic structure: ramp-flat-ramp				

Figure 4.8: Photographic field evidence showing tectonic structures observed in Area 1. (**Location 3**) Photographic evidence of small scale thrust-bend-fold observed along the exposed outcrops of Area 1 and a schematic drawing showing thrust and ramping geometry (HW – Hanging-wall; FW – Footwall). (**Location 4**) Photographic evidence of ramping observed along the east-west striking, south facing vertical section, road-cut outcrop of Area 1 and a schematic drawing showing thrust and ramping geometry. Lower hemisphere, equal area stereographic plot of surface data, pole to bedding and hinge lines collected along the exposed outcrops of Area 1 are shown. The plot indicates σ_1 that gently plunge N, σ_2 gently west and σ_3 plunging steeply NW.

In the field, accurate axial surfaces of the folding could not be determined. However, the lower hemisphere stereographic projections of the structural data collected in area 1 (i.e. pole to bedding and hinge line) suggest a σ_1 that is moderately S-plunging, σ_2 that is gently WSW-plunging and σ_3 that is steeply N-plunging. This indicates a maximum compressive/shortening direction of NNW- to SSE, which clearly relates to the field structural interpretation of NW–SE to N–S tectonic vergence that is indicated by the ramp-flat-ramp geometries.

4.2.1.1.2. Faults

4.2.1.1.2.1. Dip-slip reverse

A reverse fault plane dipping steeply south at an angle of 60˚ - 80˚ is well-exposed in the Penge shale unit of area 1 field study (24˚ 36' 432" S; 027˚ 25' 470" E). In the field, this is exhibited by the limited expression of frictional grooves or fibrous lineations defining slickenside lineation. The slickenside lineations plunge at 55˚ (mean value) with a trend of 210˚ (**Figure 4.9A**). The fault is categorized as a dip-slip reverse fault (**Figure 4.9A**). The general shortening direction of the reverse fault was probably along layer parallel slip. Overall, the observed faulting is described as a steep to sub-vertical, S-dipping, reverse fault that strikes E–W. Furthermore, shearing, fault gouge, brecciation, and distinctive distortion of finely laminated bedding were also observed within the fault.

4.2.1.1.2.2. Sinistral reverse-slip fault

Along the E–W striking, S - facing vertical section of road-cut outcrops of area 1 field study, reverse fault plane dipping at an angle of 55˚ - 60˚S was observed (24˚ 37' 002" S; 027˚ 24' 477" E) in the shale unit of the Pretoria Group (**Figure 4.9**). Well-developed kinematic indicators were found in this outcrop. These include the shearing, micro-scale duplexes and most importantly, slickenside lineations, see **Figure 4.9B**.
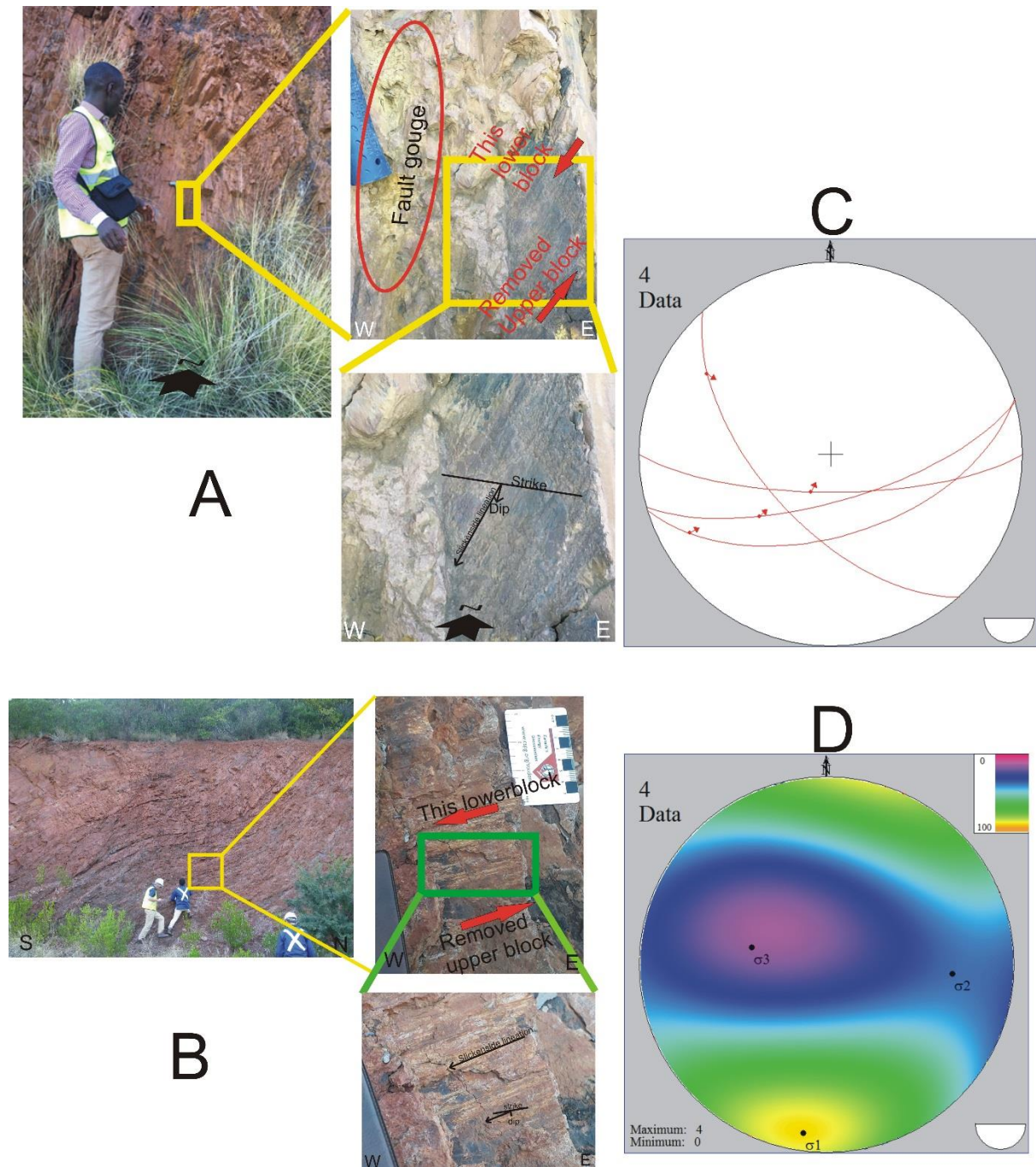
Figure 4.9: Field photographs showing two reverse faults observed in Area 1 field study. **(A)** Photographic image of the first fault showing slickenside lineations observed on a fault surface, indicating a dip-slip reverse fault. Also shown on (**A**) is the fault gouge. **(B)** Photograph of the second fault showing slickenside lineations observed on a fault surface, indicating a sinistral reverse-slip fault. **(C)** Shows a lower hemisphere stereographic projection of the two fault planes and slickensides lineations. The red arrows indicate the movement of the hanging-wall, which is upwards sense of movement. **(D)** Shows a paleostress analysis plot ($\sigma_{1,\,2}$ and σ_3) of fault A and B, observed in the Northern range.

The slickensides plunge nearly horizontally at 10˚ (mean value) towards an azimuth of 092˚. This indicates a strike-slip movement (**Figure 4.9B**). From the recorded slickenside lineations, the sense of the fault movement can be determined which suggest that the hanging wall moved upwards. The fault is therefore categorized as a sinistral reverse-slip fault.

4.2.1.1.2.3. **The paleostress analysis of the dip-slip and sinistral reverse faults**

The computed paleostress analysis of the faults in area 1 indicates a σ_1 that is gently plunging south, σ_2 that is gently plunging east and σ_3 that is plunging steeply north-west. Overall, the computed paleostress analysis of the faults in area 1 indicates a N–S directed shortening direction (**Figure 4.9D**). This shortening direction is consistent with the field structural observations of NW- to N-tectonic vergence that is indicated by the thrusts geometries (**Figure 4.7** and **4.8**) and RS interpretations of NW–SE to N–S tectonic vergence that is indicated by the thrust duplexes (**Figure 4.4**).

4.2.1.1.3. **Sill**

In area 1, a NE–SW striking mafic sill hosted in the Penge Iron Formation was observed (24˚ 36' 567" S; 027˚ 25' 773" E) (**Figure 4.10**). The mafic sill is about 12 m thick and is capped by loose blocks of deep-red BIF. Of structural significance is that the mafic sill is intruding the thrust ramp-flat geometries that are observed along the E–W striking, S-facing vertical-section road-cut outcrops of area 1, see **Figure 4.10(a)** and **4.10(b)**. In the field, the sill showed no indication of a structural alteration of primary features. This indicates that the ramping predated the intrusion of the mafic sill and thus the sill post-dates the thrusting and may have exploited the tectonic structure.
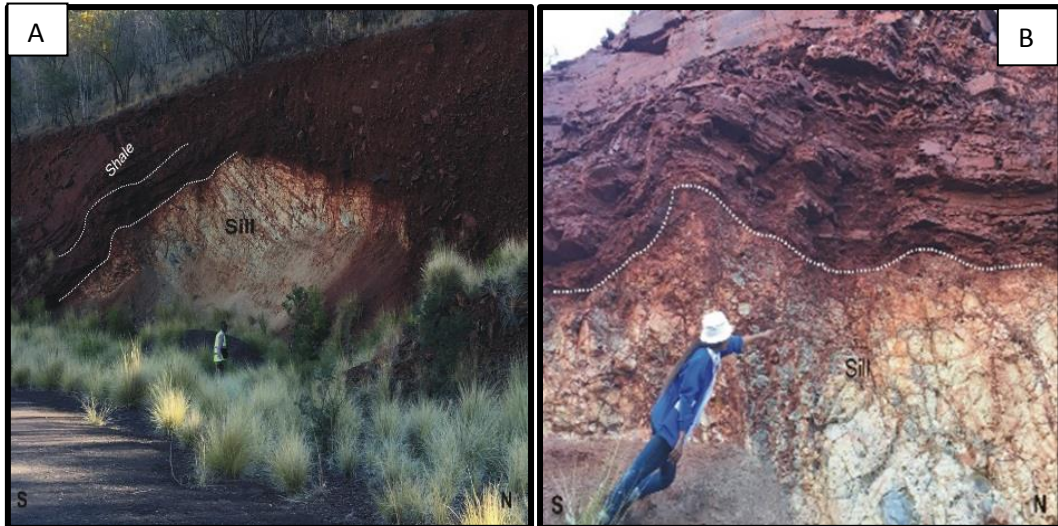
Figure 4.10: (**a**) and (**b**) shows a photographic field evidence of NE–SW mafic sill observed along Area 1 outcrops. The mafic sill in deep-red ferruginous shale and evidently intruding the ramp-flat geometries.

4.2.2. **Area 2 structural field investigation results:**

Area 2 (24° 37' 684" S; 027° 25' 523E) is located at the Bobbejaanwater Mine in the western perimeters of the Middle range of the Thabazimbi Ranges (**Figure 4.5**). Tectonically, the Middle range is sandwiched between the Bobbejaanwater Thrust Fault (BTF). The pit exposes the thick BIF strata of the Chuniespoort Group that are unconformably overlain by the Pretoria Group. The structural data collected in area 2 revealed the presence of normal faulting.

4.2.2.1. **Tectonic structures in area 2**

4.2.2.1.1. **Normal Fault**

Normal fault plane dipping at an angle of 70° - 75° towards 160° were noted in the NE site of the Bobbejaanwater Mine Pit (see **Figure 4.11**). Slickenside lineations plunging at an angle of 38° (mean value) towards a trend of 171° are recognizable on the fault planes (**Figure 4.11**).
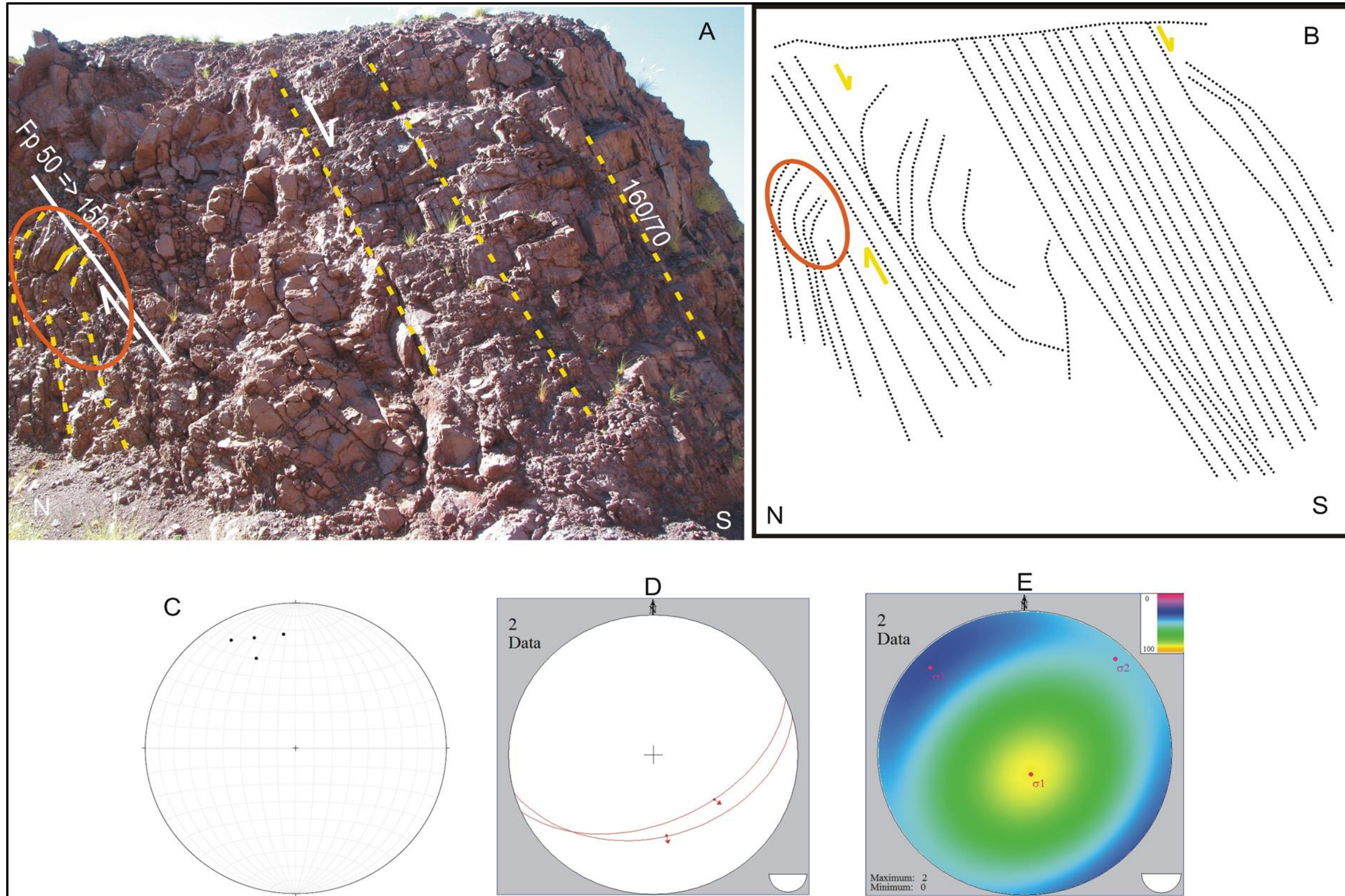
Figure 4.11: Field evidence of a normal fault observed in Area 2, the Bobbejaanwater pit. (**A**) The photographic image showing normal fault observed in the eastern site of the Bobbejaanwater pit. Red ellipse on the photograph indicates the drag folds that developed due to hanging-wall movements relative to the footwall. (**B**) Schematic sketch showing the BIF layers in relation to the fault. Red ellipse on the sketch indicates the drag folds that develop due to hanging-wall movements. (**C**) Shown are the lower hemisphere stereographic projection of the pole to bedding plane of the BIF strata. (**D**) Shows the lower hemisphere stereographic projection of the slickenside lineations plot, hanging-wall movement is indicating by the red arrow. (**E**) Shows the paleostress analysis plot ($\sigma_{1,2}$ and σ_3) of the Bobbejaanwater pit normal fault.

It was difficult to determine the sense of movement of the fault from these slickenside lineations, although drag folding indicates a downwards moving hanging wall (**Figure 4.11**). The fault is categorized as ENE–WSW striking normal fault, with BIF beds near the fault dipping steeply (~ 70˚), with a southeast to south directed dip-direction.

4.2.2.1.1.1. The paleostress analysis of the normal fault

The computed paleostress analysis of the normal fault indicates a sub-vertical σ_1, a σ_2 that is gently plunging north-east and a sub-horizontal σ_3 that trends north-west (**Figure 4.11**). This indicates a extensional tectonic that had a NW–SE/SE–NW directed direction and implies that after the NW–SE to N–S directed shortening that produced the thrusts and reverse faults (see, **Figure 4.7**, **4.8** and **4.9**), there must have been a NW–SE/SE–NW directed extension which produced the normal faulting. This indicates that the σ_1 of the compressional tectonic and σ_3 of extensional tectonic are in the same direction.

4.2.3. Area 3 structural field investigation results:

Area 3 consists of quartzite of the Pretoria Group, outcropping between the Northern and Southern Ranges. These outcrops can be seen on the satellite image (**Figure 4.12**), extending laterally from east to west, adjacent to the projected Bobbejanwater Thrust fault plane (see **Figure 4.5**). The published 1:250000 scale geological map of the Thabazimbi region and the previous works (i.e. Basson and Koegelenberg, 2017) suggest that these outcrops of site 3, 4, and 5 (see **Figure 4.12**) are folded into a synclinal fold (named Mambaskop syncline fold), between the Donkerspoort Pit and the Buffelshoek Pit (**Figure 4.12**). Kinematic interpretation of this structural feature is important for understanding of the geodynamic framework of the Thabzimbi region and Kumba Fe-Mine. In the field, the quartzite observed in site 1 (24˚ 37' 341" S; 027˚ 25' 700" E) and 2 (24˚ 37' 245" S; 027˚ 28' 307" E) dips variably to the south.
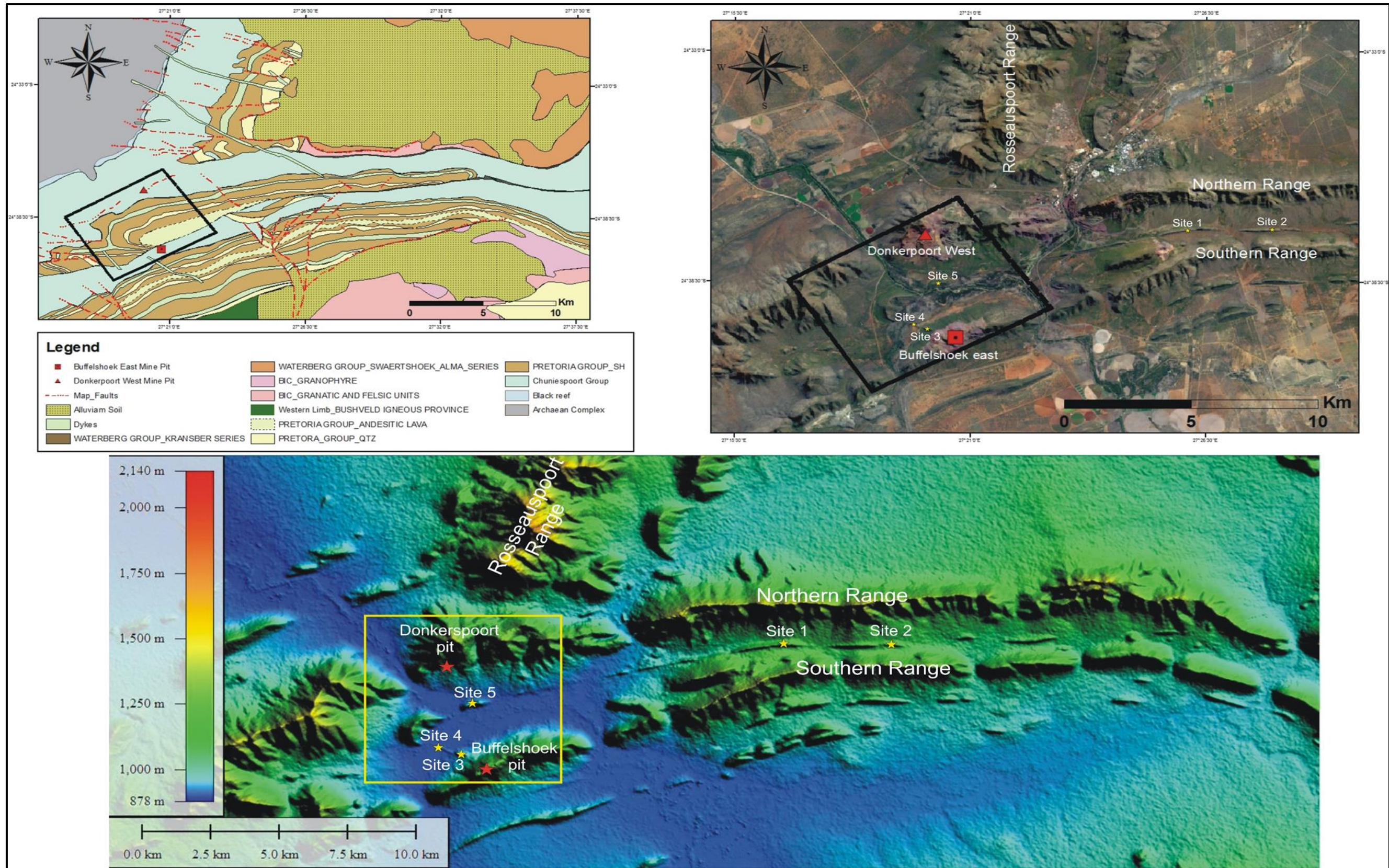
Figure 4.12: Shown is the digitized 1:250000 geological map of the Thabazimbi region in the upper left corner, the Landsat 8 image in the upper right corner and the SRTM-DEM image lower center of the figure. The black rectangle drawn in both the geological map and Landsat 8 and the yellow rectangle on the SRTM-DEM images shows the syncline fold. The yellow stars show site 1 – 5 of Area 3. Red triangle indicates the location of Donkerpoort West Mine Pit. Red square with black middle dot indicates the location of Buffelshoek Mine Pit.

This confirms the RS results showing flatirons indicating a southwards dipping strata. The strata at site 2 dip almost vertically (~85˚) southwards. Specific attention was paid to sites 3, 4, and 5 (**Figure 4.12**), as these outcrops can indicate whether the Pretoria Group quartzite is folded into a syncline. The outcrops in site 3 (24˚ 39' 661" S; 027˚ 20' 120" E) exhibit no bedding at all but exclusively a vein quartz breccia several 10s of meters to hundreds of meters thick, building the prominent topographic curved ridge in this area. This indicate hydrothermal reworking by fluids probably percolating from the fault. In the field, the area is characterized by loose angular clasts and cobbles to blocks, with not visible primary sedimentary structures (i.e. no internal bedding). In the field, this rock was interpreted as hydrothermal breccia, which might suggest faulting. The outcrops observed at sites 4 (24˚ 39' 432" S; 027˚ 19' 431" E) and 5 (24˚ 38' 522" S; 027˚ 20' 355" E) show mineralogical and textural similarity to site 3 outcrops, indicating brecciated quartzites and vein quartz with no visible internal bedding. Overall, the structural data collected from site 3, 4 and 5 suggests a hydrothermally entirely altered and reworked quartzites, probably by fluids percolating from the fault below (probably the Bobbejaanwater Thrust Fault). This feature is here interpreted as a fault breccia rather than a synclinal fold hinge, and in sharp contrast to the interpretation indicated by the 1:250000 scale geological map and by Basson and Koegelengberg (2017).

4.2.4. **A summary of field structural investigations**

Field structural investigations reveal thrusting, folding and faulting within the Thabazimbi region. Thrust faulting is evident by the presence of parasitic thrusts, thrust duplexes and flat-ramp-flat geometries (**Figure 4.7** and **4.8**). The Area 1, location 3, thrust (see, **Figure 4.7** and **4.8**) is described as an E–W striking, SSE–NNW to S-dipping, with a NW–SE to N–S tectonic vergence. Folding within the Thabazimbi region is evident by the bending or kinking of the hanging-wall above the thrust fault plane and the presence of parasitic folds (**Figure 4.8**).

The folding above the thrust fault plane (see, **Figure 4.7** and **4.8**) is characterized as open, symmetric, upright, anticline that has a NW–SE to N–S tectonic vergence. The bending or kinking above the thrust planes is a classic example of a fault-bend folds. The parasitic folds and the macro-scale to mesoscopic ramp-flat geometries observed in area 1, each shows a consistent NW–SE to N–S tectonic vergence as described for the area 1 location 3 thrust fault. Field structural measurements (E–W striking, S-dipping strata) are in support of the Remote Sensing results (i.e. flatirons) indicating southwards dipping strata for the Thabazimbi Northern, Southern and Middle Range. Stereographic projections of the structural measurements collected in area 1 (location 1 to 4) indicate fold axes with a WSW-directed gentle plunge and a maximum compressive/shortening direction (σ_1) of an NNW trend. This result is consistent with the field analysis suggesting a compressional deformation that has a NW–SE to N–S tectonic vergence. The timing for the thrusting event is constrained from the NE–SW striking mafic sill that incorporates the thrust ramp-flat geometries. The mafic sill shows no indications of a structural deformation of primary features and this suggests that the thrust ramp-flat predates the intrusion of the sill of unknown Proterozoic to possibly Mesozoic age.

Faulting within the Thabazimbi region is evident by fault planes which dip mostly southward and from the presence of slickenside lineations (see **Figure 4.9**). The fault, observed in area 1, is described as a steep to sub-vertical, S-dipping, dip-slip reverse fault that strike E–W. Another fault, observed in area 1, is characterized as a E–W trending, S-dipping sinistral strike-slip reverse fault (**Figure 4.9B**). A fault, observed in area 2, is categorized as E–W striking, near vertical, S-dipping normal fault. The paleostress analysis of the dip-slip reverse and the sinistral strike-slip reverse faults of area 1 indicates a N–S directed shortening direction (see, **Figure 4.9**). This is consistent with the field structural observations and analysis of the area 1, suggesting a compressional event that has a NW–SE to N–S tectonic vergence. On the other hand, the paleostress analysis of the normal fault identified in area 2 indicates a σ_3 that has a north-west directed trend (**Figure 4.11**).

This indicates an extensional event that has the same direction as the compressional event (see **Figure 4.9**). The observed sinistral movement of the strike-slip reverse fault (**Figure 4.9B**) supports the RS results (mapped geological structure features, see **Figure 4.4**) indicating a sinistral (left-lateral) movements for the NW–SE to NNW–SSE trending faults. The E–W trend direction for the reverse and normal faults supports the RS results (mapped lineaments, see **Figure 4.1c**) showing E–W trending lineaments along the Rosseauspoort and Thabazimbi Ranges. Field investigations of area 3 further indicate that the Thabazimbi region is faulted. This is revealed by the hydrothermal reworking of quartzites outcrops at site 3, 4 and 5 of area 3 (**Figure 4.5** and **4.12**), probably by fluids percolating from the Bobbejaanwater Thrust Fault (BTF).

Chapter 5

5. **Interpretations of results**

Analysis of the RS dataset and field structural investigations (described in **chapter 4**) were integrated with the results of previous work (i.e. Du Preez, 1944; Strauss, 1964; Du Plessis and Clendenin, 1988; Du Plessis and Walraven, 1990; Good and De Wit, 1997 and Basson and Koegelenberg, 2017) on the Thabazimbi region and Kumba Fe-Mine, to provide the basis for the interpretations presented here. Lineaments from the Rosseauspoort and Thabazimbi Ranges were mapped and analysed using Landsat 8 OLI (**Figure 4.1a**). The orientations of the mapped lineaments illustrated by rose diagrams, show three trend directions in the Thabazimbi region (**Figure 4.1c**); the NW–SE to NNW –SSE-trend, E–W-trend and the NE–SW lineament trends. Specific attention is given to the crosscutting relationship of the mapped lineaments. The NE–SW trending lineaments crosscut the E–W lineaments in the Rosseauspoort Range and the NW- to NNW–SSE trending lineaments in the Thabazimbi Ranges, while the NW–SE to NNW–SSE-trending lineaments crosscut the E–W lineaments of the Rousseauspoort Range (**Figure 4.1**).

This indicates that the tectonic regime responsible for the E–W trending lineaments was most probably active prior to the NW–SE to NNW–SSE and the NE–SW trending lineaments. It is, however, challenging to constrain the relative ages of the NW–SE to NNW–SSE and NE–SW trending lineaments. From **Figure 4.1c**, it can be deduced that both the NW–SE to NNW–SSE and NE–SW trending lineaments are laterally extensive and can be traced in the Rooiberg and Waterberg stratigraphic units. Therefore, these lineaments must post-date the Rashoop Granophyre Suite (RGS) and the granitic suite of the Bushveld Igneous Province and furthermore, be post- or syn- deposition of the upper Waterberg unconformity-bounded sequence (WUBS-II).

The NW–SE to NNW–SSE trend is congruent with the strike direction of the fault described in **Figure 4.4B**. Du Plessis, (1990) and Basson and Koegelenberg, (2017) detailed NE–SW and NNW–SSE trending, sinistral and dextral, oblique and/or strike-slip faults in the Thabazimbi Kumba Fe-Mines. Regionally, the NW–SE to NNW–SSE trend is paralleled to the strike of the Crocodile River fault, the Brits Graben fault and the Rustenburg Fault (Basson, 2019). Equally, Iannello (1966) documented dykes in the Thabazimbi region with similar orientation (i.e. an NW–SE to NNW–SSE and NE–SW) as the herein extracted lineaments. Dykes and sills in the Thabazimbi region and mines have previously been reported also by Netshiozwi (2002), Beukes et al. (2003), Rajesh et al. (2013), Smith and Beukes, (2016) and in the present work. The most acknowledged igneous dykes and sills occurring in this region and mine are attributed to ≥ 2.05 Ga Bushveld magmatic event (Du Preez, 1944; Willemse, 1959; Dreyer, 1982; Sharpe, 1985; Van Deventer, 1985; and Rajesh et al., 2013), to the 1.3 – 1.1 Ga Pilanesberg Complex, the 1.1 Ga Umkondo Igneous Province (Hanson et al., 2004) and/or 0.18 Ga dyke suite of the Karoo basalts. The tectonic activity and timing of the delineated NW–SE to NNW–SSE and NE–SW lineaments is here bracketed between post the deposition of the upper Waterberg unconformity-bounded sequence (WUBS-II) (≤1.87 Ga) and pre- to syn-Karoo basalts (≥ 0.18 Ga).

The reason for this broad range is that the trends are observed in most of the stratigraphic units including the Waterberg Group. However, it should be borne in mind that some of these lineaments (trending NW- to NNW–SSE and NE–SW) may be pre-existing trends of weakness within the Kaapvaal craton since the Neoarchaean (±2.58 Ga) and may have been reactivated over a protracted time of ± 2.55 – ± 0.18 Ga. The dykes, however, may have intruded well after the Bushveld magmatism and after deposition of the WUBS-II. It is nevertheless possible that several generations of dykes co-exist. Therefore, as many dykes as possible from different areas and intruding different stratigraphic and structural units should be dated for better understanding of the timing of deformation of the Thabazimbi region.

To better constrain the tectonic age of the E–W-trending lineaments, it is distinguished that this trend parallels the E–W to ENE–WSW Thabazimbi-Murchison Lineament (TML) trend. The TML has a recorded tectonic history of more than 2500 million years and has been reactivated several times in its long-lived tectonic history (Good and De Wit, 1997). With the E–W trending lineaments not observable across the Rooiberg and Waterberg group strata (**Figure 4.1**), this suggests that the tectonic activity of these lineaments might be synchronous to thrusting but most probably prior to the intrusion of the Rashoop Granophyre Suite (RGS) and the granitic suite of the Bushveld Igneous Province. Notably, the Transvaal strata exposed in Thabazimbi region are folded, faulted, thrusted and duplicated along the TML trend (Du Preez, 1944; Strauss, 1964; Du Plessis and Clendenin, 1988; Du Plessis and Walraven, 1990; Good and De Wit, 1997 and Basson and Koegelenberg, 2017). Based on the spatial alignment and surficial expression, the E–W trending lineaments are closely associated with extensional fractures and faults that developed during extension tectonics. The E–W trending lineaments are therefore, thought to be extensional fractures and normal faults that formed as a result of sagging of the Transvaal strata due to Bushveld magmatic event. This, therefore, suggests a tectonic period for the E–W trending lineaments that is bracketed around the cooling and sagging of the Bushveld intrusion.

Structural investigations in the Thabzimbi Kumba Fe-Mine reveal parasitic thrusts, reverse and normal faults and small-scale folding that have an E–W-trend (**Figure 4.7**, **4.8**, **4.9** and **4.11**). The parasitic thrusts and small-scale folding suggest the presence of major thrusts and folds in this region. The thrusting is characterized by a NW–SE to N–S direction of movement of the hanging wall. The presence of folding in this region is well demonstrated by the development of bending or kinking above the parasitic thrust fault plane, with northwards vergence. Similar structural features (i.e. N-verging bedding-parallel shear zones and thrusts, with associated folds) have been detailed in the Transvaal Supergroup south, south-west and west of the Thabazimbi Kumba Fe-Mine by McCarthy et al. (1986), Courtnage, (1995), Hartzer, (1995), Gibson et al. (1999), Alexandre et al. (2006) and Basson and Koegelenberg, (2017). Moreover, Good and De Wit (1997) describe a series of localized, NE–SW to ENE-plunging antiform-synform structures that develop at a similar stratigraphic position, the BIF unit of the Penge Formation, along the eastern extremity of the TML. The parasitic thrust, reverse fault and small-scale folding observed during field investigations are sub-parallel to the ENE–WSW trending Mohlapitsi Fold-and-Thrust Belt in the far-easternmost part of the TML (Good and De Wit, 1997).

The stereographic plot and paleostress analysis of the area 1 structural data suggests a deformational event that had a NW–SE to N–S directed principal shortening direction (see, **Figure 4.7**, **4.8** and **4.9**). The NW–SE directed principal shortening direction coincides with a NW–SE pre-Bushveld compressional shortening direction (i.e. determined by Hartzer, 1995 and Bumby et al., 1998) for the Transvaal basin. The N–S principal shortening direction coincides with the post Bushveld compressive shortening direction (i.e. determined by Du Preez, 1944; Strauss, 1964; Du Plessis and Clendenin, 1988; Du Plessis and Walraven, 1990 and Basson and Koegelenberg, 2017) for the Transvaal strata exposed in the Thabazimbi Kumba Fe-Mine.

Remarkably, a NW–SE and a N–S directed compressional shortening direction is proposed for similar stratigraphic sequence (Transvaal Supergroup, Kanye basin in Botswana) in the western extremity of the Thabazimbi Kumba Fe-mine, the Jwaneng area and Diamond Mine, which is along-strike of the Thabazimbi area (Creus et al., 2018). It is here proposed that the interpreted thrust duplexes in **Figure 4.4c** are most likely to be associated with the E–W-trending parasitic thrusts, reverse and normal faults observed during the field structural investigations (**Figure 4.7**, **4.8**, **4.9** and **4.11**) and those documented by previous works (i.e. Du Preez, 1944; Strauss, 1964; Du Plessis and Clendenin, 1988; Du Plessis and Walraven, 1990; Good and De Wit, 1997; and Basson and Koegelenberg, 2017). The precise timing to the E–W-trending thrust, and reverse fault activity can be best ascertained from the NE–SW mafic sill exposed at area 1 field study (see, **Figure 4.10**). The sill is not deformed, implying that the thrusting and folding must have predated the intrusion of the sill. The age of the sill is however unknown and can be anything from Neoarchaean to Mesozoic. However, recent work by Rajesh et al., (2013) documented post-Bushveld sills (ca. 2046 ± 3.4 Ma) in the Thabazimbi Kumba Fe-Mine. If the NE–SW mafic sill is identical to mafic sills documented by Rajesh et al., (2013), this suggests that the thrusting and folding described in **chapter 4** were likely formed pre- or syn-ca. 2.05 Ga Bushveld magmatic event and not post-ca 2.05 Ga Bushveld magmatic event as previously thought (Strauss, 1964; Du Plessis and Walraven, 1990; Netshiozwi, 2002; Basson and Koegelenberg, 2017).

Specific attention is given to the tectonic activity and timing of the normal fault observed in Area 2 (**Figure 4.11**). Notably, Netshiozwi (2002) and Basson and Koegelenberg, (2017) have described normal faults that strike E–W in the Thabazimbi Kumba Fe-mines. The paleostress analysis for the normal fault indicates a NW–SE to NNW – SSE directed σ_3 (see **Figure 4.11**), which implies an extensional event that has a NW- to NNW tectonic trend. This tectonic trend is paralleled to the trend direction of the compressional event, which produced the E–W striking reverse faults, thrusts and folding (**Figure 4.7**, **4.8** and **4.9**).

This is suggestive of either NW–SE to N–S directed compressional/shortening tectonics that precede a NW–SE to NNW–SSE trending extensional/relaxation tectonics or versa-versa, extensional/relaxation tectonics that shortly follows compressional/shortening tectonics. The nature and precise timing activity of the extensional event that caused the normal faulting in this region is here proposed to be most likely shortly after compressional event that produced E–W thrusts, folds and reverse faults (Altermann and Bumby pers. comm). Importantly, some authors (i.e. Dankert and Hein, 2010) have documented compressional/shortening tectonics that were followed shortly by extensional/relaxation tectonics (i.e. inversion tectonics) in the Transvaal Supergroup. This agrees with the interpreted tectonic timing activity of the E–W-trending lineaments mapped in the Rosseauspoort Range, which is thought to be most likely after thrusting and folding of the Transvaal strata exposed in the Thabazimbi region (i.e. around the Bushveld magmatic event).

Of structural importance is that the strata, thrusts, parasitic thrusts, and reverse and normal faults observed in the field are steeply dipping (~70˚) to the south. In general, most thrust faults have a dip angle ca. 45˚, whereas reverse faults and normal faults dip at ± 60˚ (Davis and Reynolds, 1996). Therefore, the dip angle of the thrusts, reverse and normal faults recorded in the field must be regarded as abnormally steep due to over-steepening of the Thabazimbi structures and strata by sagging of the Bushveld magmatic complex, parallel to the E–W to ENE–WSW trending TML (Bumby pers. comm). With the initial flatter dip angle of the Transvaal Supergroup strata (± < 30˚ to the south), the sagging and thus, over-steepening may have added an additional > 35˚ of tilt to the early dip angle, which resulted in steeply dipping thrusts, reverse and normal faults as observed to this day. This further advocate that the thrusting, folding, reverse and normal faulting must have occurred prior or at the same time as the Bushveld magmatic event.

6. **Discussions**

A remote sensing (RS) dataset merged with structural field investigation has been used to study the tectonic framework of the Thabazimbi region and Kumba Fe-Mine. Focus was given to (1) lineaments crosscutting the Rosseauspoort and Thabazimbi Ranges, (2) geological and structural features from both field structural investigations and RS, (3) the relative chronology of tectonic events and (4) relationship of lineaments and geological structural features to metallogenesis (Fe-ore formation) in this region. The data and interpretations clearly indicate that the tectonic framework of the Thabazimbi region developed through complex multiple stages of deformational events. Thrust-fold tectonics are evident in the region by triplication of the strata in the same stratigraphic sequence and include the ore deposits. These results are largely in accordance with the published 1:250000 scale geological map and previous works (Du Preez, 1944; Strauss, 1964; Du Plessis and Clendenin, 1988; Du Plessis and Walraven, 1990 and Basson and Koegelenberg, 2017) advocating that the supracrustal rocks of the Transvaal Supergroup exposed in the Thabazimbi region and Kumba Fe-Mine are thrusted parallel to the TML trend direction, E–W to ENE–WSW.

Thrust-fold tectonics are supported also by the development of folding and the occurrence of reverse faults/layer-parallel shortening as found in this region, as well demonstrated herein by the development of bending or kinking above thrust fault planes (see, **Figure 4.8**). However, the fold and thrust lines as marked on the Geological Map 1:250000, sheet Thabazimbi do not necessarily agree with lineaments and faults as mapped in this thesis. As described in **chapter 4** and interpreted in **chapter 5**, this thrust fault geometry is a classic example of a fault-bend fold that forms in thrust-fold belt (i.e. following Suppe, 1983; Dixon and Liu in McClay, 1992).

According to Suppe (1983), thrust fault planes do not run forever along a single bedding-plane decollement. The thrust normally steps up in the direction of slip to a higher decollement or to the land surface. If the rocks are layered, they may fold in response to step up/riding over a bend in a fault. As the thrust sheet rides over the bends in the fault plane it must fold. This mechanism was first studied by Rich (1934), Berger and Johnson, (1980) and Boyer and Elliott (1982), who applied the concept of fault-bend folding to the interpretation of folds in the Pine Mountain thrust sheet of the southern Appalachians. In the case of the Thabazimbi region the incompetent Fe-rich cherts will be most prone to tight isoclinal folding just like radiolarites do in Alpine thrust belt. In this model, the thrust develops while folding is concurrent with thrusting. The folding described above suggests a dominant NW – SE to N–S principal shortening direction for the thrust-and-fold event of the Thabazimbi region.

Evidence for the relative chronology of the Thabazimbi thrust-fold tectonics is vague. The timing of the Thabazimbi thrust-and-fold tectonics is probably pre- 2046 ± 3.4 Ma Bushveld Complex sills (U – Pb age after Rajesh at al., 2013), and thus pre- to syn- ≥ 2.05 Ga Bushveld magmatic event. However, the author of this thesis has no proof that the sill found intruding the BIF structure in area 1 is indeed of that age. It could equally well be of Karoo age. It is worth mentioning that the pre- to syn-Bushveld thrust-fold timing is in accordance with the (1) fold-thrust event discussed by Hartzer, (1995) in the rocks of the Transvaal Supergroup, ~ 30 km south of the Thabazimbi Kumba Fe-Mine, (2) the fold-thrust event recognized by Bumby et al., (1998) in the rooks of the Transvaal Supergroup, ~ 50 km southwest of the Thabazimbi Kumba Fe-Mine and (3) the pre-Bushveld fold-thrust age discussed by Alexandre et al., (2006) in the rooks of the Transvaal Supergroup, ~ 80 km south of the Thabazimbi Kumba Fe-Mine. Based on the RS and field structural investigation results, and with regards to Hartzer, (1995), Bumby et al., (1998) and Alexandre et al., (2006), this research proposes that post the Pretoria Group but, prior to the intrusion of the Bushveld Igneous Province into the Pretoria Group rocks, the Transvaal Supergroup strata could have been thrusted-and-folded along the northern margin of the Transvaal Basin.

The possibility that thrust-fold timing might be syn-Bushveld can best be explained by considering likely updoming or lateral displacement of wall rocks of the magma chamber that might develop during rapid intrusion of huge volumes of magma associated with the Rustenburg Layered Suite (RLS). It is envisaged that such updoming, concomitant unroofing, or the need for accommodation of space during magma intrusion may have resulted in the northwards-vergent thrusting, folding and gliding of the BIF and Pretoria Group slabs over each other along the northern margin of the RLS. Such deformation, verging away from the intrusion, is not observed in other areas around the circumference of the RLS, though BIF strata does not outcrop in other places around the edge of the intrusion.

This pre- to syn-Bushveld thrust-fold event could have resulted in the major E–W-trending, N vergent thrust belt (i.e. the Bobbejaanwater Thrust Fault and the Belt-of-Hill Thrust Fault) and the development of N-vergent folds, that are characterised by duplication and in parts, triplication of the stratigraphy of the region as observed from the RS imageries and documented by previous works (i.e. Du Preez, 1944; Du Plessis, 1990 and Basson and Koegelenberg, 2017). The Bobbejaanwater Thrust fault and the Belt-of-Hill Thrust fault may merge to a southwards dipping sole thrust system at depth. These two thrusts must have developed during one N–S shortening/compressional episode and not two autonomous N–S shortening/compressional event as previously discussed (i.e. by Du Preez, 1944). Although Du Preez (1944) reckoned that the Transvaal strata are under-thrust by the Waterberg rocks along the Belt-of-Hill Thrust fault and, also thrust over the Bushveld granitic rocks along this thrust plane, no field nor other evidence of such thrusting has been found.

The E–W trending lineaments found exclusively in the Rosseauspoort Range do not occur in the Thabazimbi Range (Northern, Southern and Middle ranges) (**Figure 4.1**) and are absent across the Rooiberg and Waterberg groups strata (**Figure 4.1a**). They only occur in the relatively undeformed Rousseauspoort Transvaal Supergroup rocks, away from the Western limb of the Bushveld Igneous Province and north of the Thabazimbi ranges and thrust.

Therefore, it is difficult to ascertain their age relative to the deformation of the thrust belt. However, these E–W trending lineaments and the normal fault (**Figure 4.11**) indicate extensional tectonic activity. It is here proposed that this extensional event followed or was coeval with the sagging of the Bushveld intrusion or later extensional events related to the Waterberg or later formed sedimentary basins, which is less probable because they are absent in rocks of that age. This implies an inversion from compressional to extensional tectonics in the Transvaal Supergroup strata. The NW–SE to NNW–SSE and NE–SW trending lineaments trend found across all stratigraphic units, the Transvaal Supergroup, Rooiberg and the Waterberg Group (**Figure 4.1**) indicate tectonic activity that post-dates deposition of the upper Waterberg unconformity-bounded sequence (WUBS-II) (≤1.87 Ga). The NE–SW trending lineaments crosscut the NW–SE to NNW–SSE lineaments, which indicate a relatively younger age to NW–SE to NNW–SSE trending lineaments. However, it is difficult to ascertain their relative timing. The tectonic activity and timing of these lineaments is, therefore, bracketed between post WUBS-II deposition (≤ 1.87 Ga) and pre- to syn-Karoo basalts (≥ 0.18 Ga).

Based on the discussion above, the tectonic history of the Thabazimbi region is here outlined by, but not limited to, the three deformational phases (D_1 through D_3) proposed. D_1 is here defined as a compressional deformation event that is characterised by the development of thrusts-and-folds that has an overall NW-to N–S kinematic vergence. This event is most exposed in the 2.558 – 2.06 Ga Transvaal Supergroup strata of the Thabazimbi region and Kumba Fe-Mine. D_1 is inferred to be a progressive deformational event that resulted from a rotation of the maximum principal stress orientation between NW–SE and a predominant N–S directed shortening. The rotation of the maximum principal stress orientations (i.e. from NW–SE to a more N–S or vice-versa) in the Thabazimbi region can be explained by the mechanism of how a lithological unit tends to behave differently during an increasing compressive stress (Davis and Reynolds, 1996). Also, the NW–SE component might be consequence of escape tectonics varying 45 degrees from the general N–S shortening direction.

This event generated ENE–WSW to E–W striking, low-angle thrusts that are accompanied by NE–SW to ENE–WSW trending, open, asymmetric, N-verging folding (F_1) and ENE–WSW to E–W striking, SE–NW to SSE–NNW dipping reverse faulting. The timing of compressional event defined here (D_1 in this study) is at variance with the compressional timing of the D_2 described by Du Preez, (1944); Strauss, (1964); Du Plessis and Clendenin, (1988); Du Plessis and Walraven, (1990); Good and De Wit, (1997); Netshiozwi, (2002) and Basson and Koegelenberg, (2017), for supracrustal rocks of the Thabazimbi region, who argued for a tectonic event that is bracketed around ca. ≤2.04 Ga to ≥1.9 Ga, which postdates the Bushveld magmatic event but precedes the deposition of lower Waterberg Group conglomerate. The data and interpretation herein suggest that the timing of the thrust-and-fold belt of the Thabazimbi region must have been after the deposition of the Pretoria Group but prior-to or synchronous to ≥ 2.06 Ga Bushveld magmatic event.

Pre-Bushveld thrust-and-fold tectonics is further supported by the high dip angle of the thrust, reverse and normal faults of the Thabazimbi region, which can be explained by the southwards tilting of the Transvaal Supergroup strata towards the center of the Bushveld Complex. The tilting must have taken place during the late phase of the Bushveld magmatic event, in which the molten mafic Rustenburg Layered Suite (RSL) was solidifying into the massive igneous rock unit known today. The huge magma volumes contracted and shrunk and gained density, imposing tremendous weight on the crust. During this time, the Transvaal strata in the Thabazimbi region sagged towards the centre of the BIC and gradually tilted southwards moderately dipping structures from ca. 30 – 40 degrees of southerly dip to 70 plus degrees of southerly dip. The Bushveld intrusion took about one million years to solidify into massive igneous rock (Zeh et al., 2015). This implies that the tilting and sagging of the thrusted-and-folded Transvaal strata in the Thabazimbi region must be bracketed to 2.05 – 2.04 Ga. It is herein proposed that the NW- to N–S directed compressional event (D_1) might have resulted in a sole thrust that formed the Bobbejaanwater Thrust Fault (BTF) and Belt-of-Hill Thrust Fault (BHTF).

The geological map of the Thabazimbi area (1:250000) indicates that the 2.054 Ga Bushveld granites and the Waterberg Group sediments (assigned to the 1st Waterberg Group unconformity-bounded sequence (WUBS-I)) are under-thrust by the Transvaal Supergroup strata along the BHTF plane. This would imply that the thrusting event must postdate Bushveld magmatic event and consequently, predate the WUBS-2. However, during field structural investigations Bushveld granites along this thrust plane were not found. Furthermore, the BTF and BHTF sit along the ENE-trending projected fault-line of the Thabazimbi-Murchison Lineament (TML), and these are regarded as relay thrusts that formed as a result of sporadic effects relating to reactivation of the TML (i.e. by Good and De Wit, 1997). The TML is a Neoarchaean tectonic fault of the Kaapvaal craton which has been reactivated several times in its long-lived history (Du Plessis, 1990; Good and De Wit, 1997).

On the other hand, the geochronological data presented by Dorland et al. (2006) for the lower sedimentary rocks of the Waterberg Group (WUBS-I) indicate an early age that is approximately contemporaneous with the Bushveld intrusion. It should be mentioned that the onset of deposition of the lower Waterberg unconformity-bounded sequence (WUBS-I) is a contested matter and might be far older that the chronicled age of ca. 2.054 Ga documented by Zeh et al. (2016). It is possible that the onset of deposition of the WUBS-I could have been synchronous with the extrusion of the Rooiberg Group ~2.06 Ga (Bumby, per. comm). This further supports the herein proposed D_1 timing. It is worth mentioning that the envisaged D_1 time frame is in agreement with the 2.06 Ga regional Rb/Sr mica ages from the Droogekloof Thrust that forms a south-easterly splay of the BHT and BWTF reported by Good and De Wit, (1997) and the bracketed (2.2 – 2.0 Ga) age of the Transvaal Supergroup compressional deformation, the Ukubambana event proposed by Drankert and Hein, (2010).

A later crustal extension event herein labeled D_2, following shortly after the compressional D_1, is indicated by the ENE–WSW to E–W striking, steeply S dipping normal fault observed in the Bobbejaanwater pit.

This event is further supported by the mapped E–W trending lineaments of the Rosseauspoort Range, interpreted as extensional fractures (**Chapter 5**). The E–W trending lineaments and the normal faults formed as a result of sagging of the Transvaal strata due to Bushveld magmatic event. This extensional event must have occurred during or post the tilting, in which the Transvaal strata of the Thabazimbi region was sagged into the BIC and gradually tilted into steeply southwards dipping direction. It is here proposed that D_2 occurred during cooling-sagging of the Bushveld intrusion (2.05 Ga – 2.04 Ga). The timing of the herein proposed extension event (D_2) (**Table 6.1**) of the Thabazimbi region disagrees with tentative models by Du Preez, (1944); Strauss, (1964); Du Plessis and Clendenin, (1988); Du Plessis and Walraven, (1990); Netshiozwi (2002) and Basson and Koegelenberg, (2017), where early extensional event (labelled D_1 by those workers) was proposed (**Table 6.2**).

Table 6.1. Sequence of event as herein proposed.

Time	Event	Comments	
Syn-BIC ≤ 2.05 Ga	D_2	Extensional tectonics, sagging of BIC, steepening of S-dipping structures	E–W striking Normal faults E–W-trending lineaments
2.0 5 Ga Bushveld Magmatic Event			
Pre- to syn BIC ≥ 2.06 Ga	D_1	Compressional tectonics	Thrust-fold belt Reverse faults/ layer parallel faults

Table 6.2. Sequence of event as proposed by Du Preez, (1944); Strauss, (1964); Du Plessis and Clendenin, (1988); Du Plessis and Walraven, (1990); Netshiozwi (2002) and Basson and Koegelenberg, (2017).

Time	Event	Comments	
Syn- to post BIC ≤ 2.05 Ga	D_2	Compressional tectonics	Thrust-fold belt
2.0 5 Ga Bushveld Magmatic Event			
Pre- to syn BIC ≥ 2.05 Ga	D_1	Extensional tectonics	E–W striking Normal faults

According to Netshozwi (2002), the extensional event (which is labelled D_1 by Du Preez, (1944); Strauss, (1964); Du Plessis and Clendenin, (1988); Du Plessis and Walraven, (1990); Netshiozwi (2002) and Basson and Koegelenberg, (2017)), which resulted in E–W-trending normal faults, introduced hydrothermal fluids and subsequent haematite mineralization before the fold and thrust compressional event (labelled D_2). Contrary to these authors, the author of this thesis proposes that the extensional event (that resulted in E–W-trending lineaments and normal faults), herein labelled D_2, must have rather followed shortly after compressional event (that produced thrust-and-folds) (**Table 6.1**). It is herein thought that the Thabazimbi Fe-enrichment (BIF-hosted high-grade (>60 weight percent (wt%) Fe) haematite iron ore) may have likely occurred during D_2 that produced E–W-trending lineaments and normal faulting. Basic principles that control haematite iron ore mineralization are structural discontinuities that form during deformation and hydrothermal fluids (Robb, 2005). D_2 produced structural discontinuities (i.e. E–W striking normal faults) needed for hydrothermal fluid to pervasively move through a stratigraphic units of the Thabazimbi region.

The 2.05 Ga Bushveld magmatism is the only high temperature source favourable for hydrothermal fluid (i.e. Fe-rich fluid expulsion and movement) that can enrich the Fe content of the Thabazimbi region. This is supported by the 2.05 Ga Fe-mineralisation age determined by De Kock et al. (2008) using a palaeomagnetic approach, suggesting that the Fe-enrichment occurred during the Bushveld magmatic event. Furthermore, the syn-to late-tectonic Fe mineralization expressed by the pseudomorphs of hematite in metamorphic muscovite and microplaty hematite formed from grunerite and ankerite (Netshiozwi, 2002; Gutzmer et al, 2005), suggests that Fe-enrichment was through hydrothermal fluids that percolated during faulting. D_2 extension (syn- to post-Bushveld) that subsequently follows a compression event (D_1, a pre- to syn-Bushveld) are thus, herein proposed.

D_3 is here inferred to be a deformational event that resulted in NW–SE to NNW–SSE and NE–SW tectonic lineaments trend. However, the NE–SW lineaments crosscut the NW–SE to NNW–SSE lineaments, suggesting that the NW–SE to NNW–SSE trending lineaments are older than the NE–SW trending lineaments. This therefore suggests a D_3 that has a D_{3a} and a D_{3b}. It is difficult to constrain the time of D_{3a} and a D_{3b}, as these lineaments are observed crosscutting the stratigraphic units of the Rooiberg (the granophyre and the granitic rocks of the Bushveld magmatic event, ≤ 2.055 Ga) and ≤1.87 Ga Waterberg Group (upper Waterberg unconformity-bounded sequence, WUBS-II). This event suggests a new stress field that was active after deposition of the WUBS-II. Importantly, the NW–SE to NNW–SSE direction is considered as parallel to a pre-existing trend of weakness within the Kaapvaal craton since the ±2.58 Ga Neoarchaean (Bumby et al., 1998). This therefore implies that the NW–SE to NNW–SSE direction is a major tectonic trend within the Kaapvaal craton that may have a recorded tectonic history of more than 2500 million years. Such a major tectonic trend might be influenced by regional stresses and therefore, be reactivated several times over the long-lived tectonic history of it. This trend coincides with the strike direction of the Crocodile River Fault, Brits Graben Faults and The Rustenburg Fault.

Furthermore, the NW–SE to NNW–SSE-trend parallels the broad trend orientation of the East Cape dyke set or swarm east of the Crocodile River and Brits Graben Faults (northeast of the Pilanesberg Dyke Swarm) (Basson, 2019). The NE–SW trend coincides with the orientations of different generations of dyke swarms crosscutting the Bushveld Igneous Province of the Kaapvaal craton (Basson, 2019). The tectonic ages of the NW–SE to NNW–SSE and NE–SW trending lineaments is therefore, here bracketed between post ≤1.87 Ga Waterberg Group (WUBS-II) and pre- to syn-Karoo basalts (≥ 0.18 Ga).

Chapter 7

7. Conclusions

Remote sensing (RS) techniques (Landsat 8 Operational Land Imager (OLI)) and structural field study has enabled the tectonic framework of the Thabazimbi region and Kumba Fe-Mine to be constrained in considerable detail. The timing of events proposed in this thesis have opened a new perspective for the deformations observed in the Thabazimbi region. The below section summarises the proposed events which have occurred in the Thabazimbi region:

I. D_1, a pre-Bushveld compressional deformation event that is characterised by the development of thrusts-and-folds and reverse faults that has an overall NW–SE to N–S kinematic vergence. This event is most exposed in the 2.558 – 2.06 Ga Transvaal Supergroup strata of the Thabazimbi region. The timing of the thrust-and-fold belt of the Thabazimbi region must have been after the deposition of the Pretoria Group but prior-to or synchronous to ≥ 2.06 Ga Bushveld magmatic event

II. D_2, a later crustal extension event that follows immediately after D_1. D_2 is characterised by the development of E–W striking normal faults and E–W-trending lineaments. This event occurred during or after the tilting, in which the Transvaal strata of the Thabazimbi region was sagged into the BIC and gradually tilted into steeply southwards dipping direction. Accordingly, D_2 occurred during cooling and sagging by the Bushveld Igneous Province (2.05 Ga – 2.04 Ga). The Fe-enrichment (BIF-hosted high-grade (>60 weight percent (wt%) Fe) haematite iron ore) of the Thabazimbi region must have occurred during this time.

III. D_3 is characterised by the development of NW–SE to NNW–SSE and NE–SW tectonic lineaments trend. These lineaments are observed crosscutting the stratigraphic units of the Rooiberg (the granophyre and the granitic rocks of the Bushveld magmatic event, ≤ 2.055 Ga) and ≤1.87 Ga Waterberg Group (upper Waterberg unconformity-bounded sequence, WUBS-II). The NW–SE to NNW–SSE and NE–SW lineament trends are pre-existing trends of weakness within the Kaapvaal craton and may have been reactivated over a protracted time of ± 2.55 Ga. D_3 is therefore, bracketed between post the WUBS-II (≤ 1.87 Ga) and pre- to syn-Karoo basalts (≥ 0.18 Ga).

References

Abdullah, A., Nassr, S., Ghaleeb, A., 2013. Landsat ETM-7 for Lineament Mapping using Automatic Extraction Technique in the SW part of Taiz area, Yemen. Global Journal of Human Soccial Science Geography, Geo-Sciences, Environmental and Disaster management 13(2), 35-38.

Alexandre, P., Andreoli, M.A.G., Jamison, A., Gibson, R.L., 2006. $^{40}Ar/^{39}Ar$ age constraints on low-grade metamorphism and cleavage development in the Transvaal Supergroup (central Kaapvaal craton, South Africa): implications for the tectonic setting of the Bushveld Igneous Complex. South African Journal of Geology 109, 393-410.

Ali, S.A., Pirasteh, S., 2004. Geological applications of Landsat Enhanced Thematic Mapper (ETM) data and Geographic Information System (GIS): mapping and structural interpretation in south-west Iran, Zagro Structural Belt. International Journal of Remote Sensing 25(21), 4715-4727.

Altermann, W., Hälbich, I.W., 1990. Thrusting, folding and stratigraphy of the Ghaap Group along the southwestern margin of the Kaapvaal Craton. South Africa. Journal of Geology 93, 556-616.

Altermann, W., Nelson, D.R., 1998. Sedimentation rates, basin analysis and regional correlations of three Neoarchaean and Palaeoproterozoic sub-basins of the Kaapvaal craton as inferred from precise U-Pb zircon age from volcaniclastic sediments. Sedimentary Geology 120, 225-256.

Barker, O.B, Brandl, G., Callaghan, C.C., Eriksson, P.G., Neut (van der), M., 2006. The soutpansberg and Waterberg Groups and the Blouberg Formation. In Johnson, M.R., Anhaeusser, C.R. and Thomas, R.J. (Eds). The Geology of South Africa. Geological Society of South Africa, Council for Geoscience, Pretoria, 301-318.

Basson, I.J., Koegelenberg, C., 2017. Structural controls on Fe mineralization at Thabazimbi Mine, South Africa. Ore Geology Reviews 80, 1056-1071.

Basson, I.J. 2019. Cumulative deformation and original geometry of the Bushveld Complex. Tectonophysics 750, 177-202.

Bekker, A., Slack, J.F., Planavsky, N., Krapež, B., Hofmann, A., Konhauser, K., Rouxel, O.J., 2010. Iron Formation: The sedimentary Product of a Complex Interplay among mantle, Tectonic, Oceanic, and Biospheric Processes. Society of Economic Geology 105, 457-608.

Beukes, N.J., 1980. Suggestion towards a classification of and nomenclature for iron-formation. Transaction of the Geological Society of South Africa 83, 285-290.

Beukes, N.J., Gutzmer, J., Mukhopadhyay, J., 2002. The Geology and Genesis of High-Grade Hematite Iron Ore Deposits. Iron Ore Conference, Perth, WA, 23-29.

Beukes, N.J., Gutzmer, J., Mukhopadhyay, J., 2003. The geology and genesis of high-grade hematite iron ore deposits. Applied Earth Science (Trans. Inst. Min. Metall. B) 112, B18-25.

Beukes, N.J., Tsikos, H., Moore, J.M., Harris, C., 2003. Deposition, Diagenesis, and secondary enrichment of metals in the Paleoproterozoic Hotazel iron formation. Kalahari manganese field, South Africa. Economic Geology 98, 1449-1462.

Beukes, N., Mukhopandhyay, J., Gutzmer, J., 2008. Genesis of High-grade Iron Ores of the Archean iron Ore group around Noamundi, India. Society of Economic Geology 103, 365-395.

Boadman, L.C., (1948). The geology of iron ore and other minerals of the Thabazimbi area, Unpublished PH.D. Thesis, University of Pretoria.

Bumby, A.J., Eriksson, P.G., Van der Merwe, R., 1998. Compressive deformation in the floor rocks to the Bushveld Complex (South Africa): evidence from the Rustenburg Fault Zone. Journal of African Earth Science 27, 307-330.

Bumby, A.J., 2000. The geology of the Blouberg Formation, Waterberg and Soutpansberg Group in the area of Blouberg mountains, Northern Province, South Africa. PhD. Thesis, University of Pretoria, pg 1-295.

Bumby, A.J., Eriksson, P.G., Catuneanu, O., Nelson, D.R., Rigby, M.J., 2012. Meso-Archaean and Palaeo-Proterozoic sedimentary sequence stratigraphy of the Kaapvaal Craton. Marine and Petroleum Geology 33, 92-116.

Bumby, A.J. 2016. Personal communication. University of Pretoria, Department of Geology

Catuneanu, O., Eriksson, P.G., 1999. The sequence stratigraphic concept and the Precambrian rock record: an example from the 2.7-2.1 Ga Transvaal Supergroup, Kaapvaal craton. Precambrian research 97, 215-251.

Cawthorn, R.G., Walraven, F., 1998. Emplacement and crystallization time for the Bushveld Complex. Journal of Petrology 39(9), 1669-1687.

Cawthorn, R.G., Webb, S.J., 2001. Connectivity between the western and eastern limbs of the Bushveld Complex. Tectonophysics 330, 195-209.

Clarke, B., Uken, R., Reinhardt, J., 2009. Structural and compositional constraints on the emplacement of the Bushveld Complex, South Africa. Lithos 111, 21-36.

Courtnage, P.M., 1995. Post-Transvaal Deformation between the Johannesburg Dome and the Bushveld Complex. Unpublished MSc Thesis, University of the Witwatersrand, Johannesburg, 217 pp.

Creus, P.K., Basson, I.J., Stoch, B., Mogorosi, O., Gabanakgosi, K., Ramsden, F., 2018. Structural analysis and implicit 3D modelling of Jwaneng Mine: Insights into deformation of the Transvaal Supergroup in SE Botswana. Journal of African Earth Science 137, 9-21.

Dalstra, H., Harding, T., Riggs, T., Taylor, D., 2003. Banded iron formation hosted high-grade hematite deposits, a coherent group. Applied Earth Science 112, 68-72.

Dalstra, H., Harding, T., Riggs, T., Taylor, D., 2003. Banded iron formation hosted high-grade hematite deposits, a coherent group. Applied Earth Science (Trans. Inst. Min. Metall. B) 112, B68-72.

Dalstra, H., Guedes, S., 2004. Giant hydrothermal hematite deposits with Mg-Fe metasomatism: a comparison of the carajÁs, Hamersley, and other iron ores. Economic Geology 99, 1793-1800.

Dankert, B.T., Hein, K.A.A. 2010. Evaluating the structural character and tectonic history of the Witwatersrand basin. Precambrian Research 177, 1-22. Hard hematite deposits – A Paleomagnetic approach. Society of Economic Geologists 15, 49-71.

Davis, G.H., Reynolds, S.T., 1996. Structural geology of rocks and regions second edition. John Wiley and Sons Inc. 760 pp.

De Kock, M.O., Evans, D.A.D., Gutzmer, J., Beukes, N.J., Dorland, H.C., 2008. Origin and timing of Banded Iron Formation-hosted high-grade

De Villiers J.E., 1944. The origin of the iron and manganese deposits in the Postmasburg and Thabazimbi Areas. Transactions of the Geological Society of South Africa XLV11, 123-157.

De Wit, M.J., Jones, M.G., Buchanan, D.L., 1992. The geology and tectonic evolution of the Pietersburg greenstone belt, South Africa. Precambrian research 55, 123-153.

Department of the Interior U.S. Geological Survey, 2016. Landsat 8 (L8) Data Users handbook, Version 2.0. Land Satellites data System, LSDS-1574, 98 pp.

Di Tommaso, I., Rubinstein, N., 2007. Hydrothermal alteration mapping using Aster data in the infiernillo porphyry deposit, Argentina. Ore Geology Reviews 32, 275-290.

Dorland, H.C., Beukes, N.J., Gutzmer, J. 2006. Precise SHRIMP U-Pb zircon age contraints on the lower Waterberg and Soutpansberg Groups, South Africa. South African Journal of Geology 109, 139-156.

Du Plessis, C.P., Clendenin, C.W., 1988. The Bobbejaanwater Fault System south Thabazimbi, western Transvaal. South African Journal of Geology 91, 97-105.

Du Plessis, C.P., Walraven, F., 1990. The tectonic setting of the Bushveld Complex in South Africa Part 1. Structural deformation and distribution. Tectonophysics 179, 305-319.

Du Plessis, C.P., 1990. Tectonics along the Thabazimbi-Murchison Lineament. Unpublished Ph.D Thesis. University of the Witwatersrand, Johannesburg, 307 pp.

Du Preez, J.W., 1944. The structural geology of the area east of Thabazimbi and genesis of the associated ore. MSc. Thesis, Annals of the University of Stellenbosch, v. 22A

Ducart, D.F., Silva, C.L.B.T., Assis, L.M., 2016. Mapping iron oxides with Landsat-8/OLI and EO-1/Hyperion imagery from the Serra Norte iron deposits in the Carajás Mineral Province, Brazil. Brazilian Journal of Geology 46(3), 331-349.

Eriksson, P.G., Schreiber, Van Der Neut, M., 1991. A review of the sedimentology of the Early Proterozoic Pretoria Group, Transvaal Sequence, South Africa: implications for tectonic setting, Journal of African Earth Sciences, 13-1, 107-119.

Eriksson, P. G., Schreiber, U. M. Van Der Neut, M., Labuschagne, H., Van Der Schyff, W., and Potgieter, G., 1993. Alternative marine and fluvial models for the non-fossiliferous quartzitic sandstones of the Early Proterozoic Daspoort Formation, Transvaal Sequence of South Africa, Journal of African Earth Sciences, 16-3, 355-366.

Eriksson, P. G., Schweitzer, J. K., Bosch, P. J. A., Schreiber, U. M., Van Deventer, J. L., Hatton, C. J., 1993. The Transvaal Sequence: an overview, Journal of African Earth Sciences, 16-1/2, 25-51.

Eriksson, P.G., Hatting, P.J., Altermann, W., 1995. An overview of the geology of the Transvaal Sequence and Bushveld Complex, South Africa. Mineral Deposita 30, 98-111.

Eriksson, P.G., Reczko, B.F.F., Callaghan, C.C., 1997. The economic mineral potential of the mid-Proterozoic Waterberg Group, northwestern Kaapvaal craton, South Africa. Mineralium Deposita 32, 401-409.

Eriksson, P.G., Altermann, W., 1998. An overview of the geology of the Transvaal Supergroup dolomites (South Africa). Environmental Geology 36, 176-188.

Eriksson, P.G., Altermann, W., Catuneanu, O., Van der Merwe, R., Bumby, A. J., 2001. Major influences on the evolution of the 2.67-2.1 Ga Transvaal basin, Kaapvaal craton. Sedimentary Geology 142-142, 205-231.

Eriksson, P.G., Altermann, W., Catuneanu, O., Van der Merwe, R., Bumby, A.J., 2001. Major influences on the evolution of the 2.67-2.1 Ga Transvaal basin, Kaapvaal craton. Sedimentary Geology 141-142, 205-231.

Frauenstein, F., Veizer, J., Beukes, N., Van Niekerk, H.S., Coetzee, L.L., 2009. Transvaal Supergroup carbonates: implications for Paleoproteroic $\delta^{18}O$ and $\delta^{13}C$ records. Precambrian Research 175, 149-160.

Friese, A.E.W., Alchin, D.J., 2007. New insights into the formation, structural development and preservation of iron ore deposits in the northern Cape Province, South Africa. Iron Ore Conference, Perth, WA, pp. 85-97.

Gannouni, S., Gabtni, H., 2015. Structural Interpretation of Lineaments by Satellite Image Processing (Landsat TM) in the Region of Zahret Medien (Northern Tunisia). Journal of Geographic Information System 7, 119-127.

Gibson, R.L., Courtnage, P.M., Charlesworth, E.G., 1999. Bedding-parallel shearing and related deformation in the lower Transvaal Supergroup north of the Johannesburg Dome, South Africa. South African Journal of Geology 102, 99-108.

Gleason, J.D., Gutzmer, J., Kesler, E., Zwingmann, H., 2011. 2.05 Ga Isotopic Ages for Transvaal Mississippi Valley-Type Deposits: Evidence for Large-Scale Hydrothermal Circulation around the Bushveld Igneous Complex, South Africa. The Journal of Geology 119, 69-80.

Good, N., De Wit, M.J., 1997. The Thabazimbi-Murchison Lineament of the Kaapvaal Craton, South Africa: 2700 Ma of episodic deformation. Journal of the Geological Society, London 154, 93-97.

Gutzmer, J., Beukes, N.J., de Kock, M.O., Netshiozwi, S.T., 2005. Origin of High-grade iron ores at the Thabazimbi deposit, South Africa. Australasian Institute of Mining and Metallurgy, Iron Ore 2005 conference, Fremantle, Western Australia September 19-21 (2005), Proceedingsp 57-65.

Hagemann, S.H., Rosière, C.A., Lobato, L., Baars, F., Zucchetti, M., Figueiredo e Silva, R. C., 2006. Controversy in genetic models for Proterozoic high-grade, banded iron formation (BIF)-related iron deposits – unifying or discrete model(s). Applied Earth Science (Trans. Inst. Min. Metall. B) 112, B147-151.

Hälbich, I.W., Lamprecht, D., Altermann, W., Horstmann, U.E., 1992. A carbonate-banded iron formation transition in the Early Protorezoicum of South Africa. Journal of African Earth Science 15 (2), 217-236.

Hanson, R.E., Crowley, J.L., Bowring, S.A., Ramezani, J., Gose, W.A., Dalziel, I.W.D., Pan-cake, J.A., Seidel, E.K., Blenkinsop, T.G., Mukwakwami, J., 2004. Coeval large-scale magmatism in the Kalahari and Laurentian cratons during Rodinia assembly. Science 304, 1126-1129.

Hartzer, F.J., 1995. Transvaal Supergroup inliers: geology, tectonic development and relationship with the Bushveld complex, South Africa. Journal of African Earth Science 21, 521-547.

Heddi, M., Eastaff, D.J., Petch, J., 1999. Relationships between tectonic and geomorphological linear features in the Guadix-Baza basin, Southern Spain. Earth Surface Processes and Landforms 24, 931-942.

Iannello, P., 1969. The Bushveld granites around Rooiberg, Transvaal, South Africa. Government Printers Copyright Concession No. 4516 of the 6/5/, 630-655.

Kamel, S.R., Almasian, M., Pourkermani, M., Dana, S., 2015. Structural and Fault Analysis of Haji Abad with Interpretation of Landsat 8 satellite Image. Open Journal of Geology 5, 470-488.

Karnieli, A., Meiseis, A., Fisher, L., Arkin, Y., 1996. Automatic extraction and evaluation of geological linear features from digital remote sensing data using a hough transform. American Society for Photogrammetric Engineering and Remote Sensing 62(5), 525-531.

Kesler, S.E., Reich, M., Jean, M., 2007. Geochemistry of fluid inclusion brines from Earth's oldest Mississippi Valley-type (MVT) deposits, Transvaal Supergroup, South Africa. Chemical Geology 237, 274-288.

Kinnaird, J.A., 2005. The Bushveld Large igneous province. http://www.largeigneousprovinces.org (June 2016).

Klemm, D., 2000. The formation of Palaeoproterozoic banded iron formations and their associated Fe and Mn deposits, with reference to the Griqualand West Deposits, South Africa. Journal of African Earth Sciences 30, 1-24.

Kusky, T.M., Ramadan, T.M., 2002. Structural controls on Neoproterozoic mineralization in the South Eastern Desert, Egypt: an integrated field, Landsat TM, and SIR-C/X SAR approach. Journal of African Earth Sciences 35, 107-121.

Laake, A., 2011. Integration of Satellite Imagery, Geology and Geophysical Data. In Dar I.A., (Eds). Earth and Environmental Sciences, 467-492.

Li, N., Frei, M., Altermann, W., 2011. Textural and knowledge-based lithological classification of remote sensing data in Southwestern Prieska sub-basin, Transvaal Supergroup, South Africa. Journal of African Earth Science 60, 237-246.

Maier, W.D., Barnes, S.J., Groves, D.I., 2013. TheBushveld Complex, South Africa: formation of platinum-palladium, chrome-and vanadium-rich layers via hydrodynamic sorting of a mobilezed cumulate slurry in a large, relatively slowly cooling, subsiding magma chamber. Miner Deposita 48, 1-56.

Maier, W.D., Groves, D.I., 2013. The Bushveld Complex, South Africa: formation of platinum-palladium, chrome- and vanadium-rich layers via hydrodynamic sorting of a mobilized cumulate slurry in a large, relatively slowly cooling, subsiding magma chamber. Mineral Deposita 48, 1-56.

Marghany, M., Hashim, M., 2010. Lineament Mapping Using Multispectral remote Sensing Satellite Data. Research Journal of Applied Science 5(2), 126-130.

Martin, D.McB., Clendenin, C.W., Krapez, B., McNaughton N.J., 1998. Tectonic and geochronological constraints on late Archaean and Paleoproterozoic stratigraphic correlation within and between the Kaapvaal and Pilbara Cratons. Journal of the Geological Society, London 155, 311-322.

Martini, J.E.J., Eriksson, P.G., Snyman, C.P., 1995. The Early Proterozoic Mississippi Valley-type Pb-Zn-F deposits of the Campbellrand and Malmani Subgroups, South Africa. Mineral Deposita 30, 135-145.

Masoud, A., Koike, K., 2006. Tectonic architecture through Landsat-7 ETM+/SRTM DEM-derived lineaments and relationship to the hydrogeologic setting in Siwa region, NW Egypt. Journal of African Earth Sciences 45, 467-477.

Mather, P.M., and Koch, M., 2011. Computer Processing of Remotely-Sensed Image An Introduction, Fourth Edition. John Wile and Sons, Ltd, UK, 427 pp.

Meinster, B., 1972. The geology of the area around Gatkop, East of Thabazimbi. Open Report, Council for Geosciences, Pretoria, 15 pp.

McCarthy, T.S., Charlesworth, E.G., Stanistreet, I.G., 1986. Post-Transvaal structural features of the northern portion of the Witwatersrand Basin. Transactions of the Geological Society of South Africa 86, 311-323.

McClay, K.R. 1992. Thrust Tectonics. Chapman and Hall, 2-6 Boundary Row, London SE1 8HN. 433 pp.

McCourt, S., 1995. The crustal architecture of the Kaapvaal crustal block South Africa, between 3.5 and 2.0 Ga, A synopsis. Mineral Deposita 30, 89-97.

Mekonnen, S.Z., 2008. Geological and mineral potential mapping by geoscience data integration. MSc Thesis, International institute for geo-information science and earth observation enschede, The Netherlands, 86 pp.

Möller, V., Klemd, R., Jachimski, M., Barton Jr, J.M., 2014. Hydrothermal controls on iron and lead mineralization on the farms Leeuwbosch and Cornwall, Thabazimbi District, South Africa. Ore Geology 63, 40-63.

Nama, E.E., 2004. Technical note: Lineament detection on Mount Cameroon during the 1999 volcanic eruption using Landsat ETM. International Journal of Remote Sensing 25(3), 501-510.

Netshiozwi, S.T., 2002. Origin of high-grade hematite ores at Thabazimbi Mine, Limpopo Province, South Africa. Unpublished Magister Scientae Dissertation, University of Johannesburg, 109 pp.

Papadaki, E.S., Mertikas, S.P., Sarris, A., 2011. Identification of Lineaments with Possible Structural Origin Using Aster Images and DEM Derived Products In Western Crete, Greece. EARSel eProceedings 10(1), 9-26.

Price, J.C., 1994. How Unique are spectral signatures. Remote sensing and Environment 49, 181-186.

Rajesh, H.M., Chisonga, B.C., Shindo, K., Beukes, N.J., Armstrong, R.A., 2013. Petrographic, geochemical and SHRIMP U-Pb titanite age characterization of the Thabazimbi mafic sills: Extended time frame and a unifying Petrogenetic model for the Bushveld Large Igneous Province. Precambrian research 230, 79-102.

Reczko, B.F.F., Oberholzer, J.D., Res, M., Eriksson, P.G., Schreiber, U.M., 1995. A re-evaluation of the volcanism of the Palaeoproterozoic Pretoria Group (Kaapvaal craton) and a hypothesis on basin development. Journal of African Earth Sciences 21(4), 505-519.

Reynolds, M., 2004. Oxford junior atlas for South Africa. Oxford University press Southern Sfrica (Pty) Ltd, Cape Town. pp.64.

Robb, L., 2005. Introduction to Ore-Forming Processes. Blackwell Science Ltd. 368 pp.

Sabins, F.F., 1999. Remote sensing for mineral exploration. Ore Geology Review 14, 157-183.

Schreiber, U. M., Eriksson, P. G., and Snyman, C. P., 1991. A provenance study of the sandstones of the Pretoria Group, Transvaal Sequence, South Africa: petrography, geochemistry, and palaeocurrent directions, 94-4, 288-298.

Schreiber, U.M., 1990. A palaeonvironmental study of the Pretoria Group in the eastern Transvaal. Unpublished Ph.D thesis, University of Pretoria, South Africa. 308 pp.

Schreiber, U.M., Eriksson, P.G., Van der Neut, M., Snyman, C.P., 1992. Sedimentary petrography of the early Proterozoic Pretoria Group, Transvaal Sequence, South Africa: implications for tectonic setting. Sedimentology Geology 80, 89-103.

Sharpe, M.R., Hulbert, L.J., 1985. Ultramafic sills beneath the eastern Bushveld Complex: mobilized suspensions of early lower zone cumulates in a parental magma with boninitic affinities. Economic Geology 80, 849-871.

Smith, A.J.B., Beukes, N.J., 2016. Palaeoproterozoic banded iron formation-hosted high-grade hematite iron ore deposits of the Transvaal Supergroup, South Africa. Episodes 39(2), 269-284.

Solomon, S., Ghebreab, W., 2006. Lineament characterization and their tectonic significance using Landsat TM data and field studies in the central highlands of Eritrea. Journal of African Earth Sciences 46, 371-378.

Sonbil, A.R., El-Shafei, M., Bishta, A.Z., 2016. Using remote sensing techniques and field-based structural analysis to explore new gold and associated mineral sites around Al-Hajar mine, Asir terrane, Arabian Shield. Journal of African Earth Sciences117, 285-302.

Strauss, C.A., 1964. The iron ore deposits in the Thabazimbi Area, Transvaal. Geology of some ore deposits of southern Africa 2, 383-392.

Sumner, D. Y., Beukes, N.J., 2006. Sequence Stratigraphic Development of the Neoarchean Transvaal carbonate platform, Kaapvaal Craton, South Africa. South Africa Journal of Geology 109, 11-22.

Suppe, J. 1983. Geometry and kinematics of fault-bend folding. American Journal of Science 283, 684-721.

Suzen, M.L., Toprak, V., 1998. Filtering of satellite images in geological lineament analyses: an application to fault zone in Central Turkey. International Journal of Remote Sensing 19(6), 1101-1114.

Taylor, D., Dalstra, h.J., Harding, A.E., Broadeent, G.C., Barley, M.E., 2001. Genesis of High-Grade Hematite Orebodies of the Hamersley Province, Western Australia. Economic geology 96, 837-873.

Thorne, W. S., Hagemann, S., Sepe, D., Dalstra, H.J., Banks, D. A., 2014. Structural control, hydrothermal alteration zonation, and fluid chemistry of the concealed, high-grade 4EE iron orebody at the Paraburdoo 4E Deposit, Hamersley Province, Western Australia. Economic Geology 109, 1829-1862.

Trendall, A., 2012. Iron Formation: The sedimentary Product of a Complex Interplay among mantle, Tectonic, Oceanic, and Biospheric Processes – A discussion. Society of Economic Geology 107, 377-380.

Trendall, A.F., 1968. Three Great basin of Precambrian Banded Iron Formation Deposition: A Systematic Comparison. Geological Society of America Bulletin 79, 1527-1544.

Van Deventer, J.L., Eriksson, P.G., Snyman, C.P., 1986. The Thabazimbi iron ore deposits, north-western Transvaal. Mineral Deposits of Southern Africa 1-2, 923-929.

Van Deventer, J.L., Eriksson, P.G., Snyman, C.P., 1986. The Thabazimbi iron ore deposits, north-western Transvaal. In Anhaeusser, C.R., Maske, S.S. (Eds). Mineral Deposits of South Africa. Geological Society of South Africa, Council for Geoscience, Johannesburg, pp. 923-929.

Van Schalkwyk, J.F., Beukes, N.J., 1986. The Sishen iron ore deposit. In Anhaeusser, C.R., Maske, S.S. (Eds). Mineral Deposits of South Africa. Geological Society of South Africa, Council for Geoscience, Johannesburg, pp. 157-182.

Viola, G., Kounov, A., Andreoli, M.A.G., Mattila, J., 2012. Brittle tectonic evolution along the western margin of South Africa: More than 500 Myr of continued reactivation. Tectonophysics 514-517, 93-114.

Wagener, P.A., 1921. Report on the Crocodile River iron deposits: Pretoria. Geol. Surv.S.Afr. Memo 17, 65.

Walraven, F., 1997. Geochronology of the Rooiberg Group, Transvaal Supergroup, South Africa. University of Witwatersrand. Econ Geol Res Unit Info Circular 316:21.

Walraven, F., Hatting, E., 1993. Geochronology of the Nebo granite, Bushveld Complex. South African Journal of Geology 96, 31-41.

Walraven, F., Martini, J., 1995. Zircon Pb-evaporation age determination of the Oak Tree Formation, Chuniespoort Group, Transvaal Sequence: implications for Transvaal-Griqualand West basin correlation. South African Journal of Geology 98, 58-67.

Wright, P.M., Lirah, H., Ramsey, D.R., 1990. Interpretation of Landsat Thematic Mapper Satellite Imagery at Los Azufres Geothermal Field, Michoacan, Mexico. Geothermal resources Council Transactions 14(2), 1553-1559.

Zeh, A., Ovtcharova, M., Wilson, A.H., Schaltegger, U., 2015. The Bushveld Complex was emplaced and cooled in less than one million years – results of zirconology, and geotectonic implications. Earth and Planetary Science Letters 418, 103-114.

Zeh, A., Wilson, A.H., Ovtcharova, M., 2016. Source and age of upper Transvaal Supergroup, South Africa: Age-Hf isotope record of zircons in Magaliesberg quartzite and Dullstroom lava, and Implications for Paleoproterozoic (2.5-2.0 Ga) continent reconstruction. Precambrian research 278, 1-21.